

Comparison of the performance of active suspension systems on handling

Shilp Dixit
DC 2015.080 0872256

Master's Thesis

Supervision: dr.ir. T.P.J. (Tom) van der Sande
dr.ir. I.J.M. (Igo) Besselink
prof.dr. H. (Henk) Nijmeijer

MSc. Automotive Technology
Eindhoven University of Technology
Department of Mechanical Engineering
Dynamics and Control Group
Eindhoven

September 11, 2015

*To my grandparents,
Mahalakshmi Dixit & Hari Vallabh Dixit
Sulochana Dwivedi & Dr. Pranshankar Dwivedi*

Abstract

THIS research project focuses on the development of active suspension controllers to enhance the handling characteristics of a vehicle. An additional important goal of this thesis is to investigate if a high bandwidth controller can provide substantial gains to balance out the additional power consumption.

A survey of the prominent literature from the academic and industrial circles shows that vehicle handling is a complex topic that cannot be defined or measured from one quantity. Yaw-rate, r_z and vehicle side-slip angle, β are identified as two important measures to describe the lateral and yaw dynamics of the vehicle. The yaw-rate provides insight into the steering response during transient maneuvers and also helps define the yaw stability limits of the vehicle. Furthermore, the vehicle side-slip angle provides crucial information regarding the lateral stability limits of the vehicle. In this thesis active suspension controllers are designed to improve the handling characteristics of the vehicle by enhancing the yaw and lateral stability of the vehicle.

An analysis of the multi-body vehicle model [1] is used to study the influence of actuator forces on the yaw-rate and vehicle side-slip angle and also understand how the handling balance of the vehicle can be influenced. This understanding is used to propose a vehicle model that provides a state space representation from inputs; tire forces to output; yaw-rate and vehicle side-slip angle. This model is then used to design a slow active suspension controller and a fully active suspension controller. The controllers are designed such that they depict the same behavior at low frequencies such that a comparison study can highlight the differences in performance arising due to the control bandwidth.

The controllers designed are implemented in a closed loop environment and the system performance is evaluated for improvements in lateral and yaw stability. The relative gains obtained over an uncontrolled vehicle are highlighted and also a performance comparison between the system dynamics and actuator dynamics of the two suspension controllers is performed.

Contents

| | |
|---|-----------|
| Abstract | v |
| Preface | x |
| Nomenclature | xi |
| 1 Introduction | 2 |
| 1.1 Vehicle handling | 3 |
| 1.2 Role of a suspension system | 5 |
| 1.3 Objectives | 6 |
| 1.4 Contributions | 6 |
| 1.5 Thesis Outline | 7 |
| 2 Literature Review | 9 |
| 2.1 Vehicle comfort and handling: a constant compromise | 9 |
| 2.2 Evaluating vehicle handling | 11 |
| 2.3 Active suspension design | 13 |
| 2.3.1 Active suspension: State-of-the-art | 15 |
| 2.4 Conclusion | 16 |
| 3 Analysis of a Multi-body Vehicle Model | 18 |
| 3.1 Introduction | 18 |
| 3.2 Reference Vehicle | 18 |
| 3.2.1 Multi-body Model | 19 |
| 3.3 Static Analysis | 20 |
| 3.3.1 Suspension travel | 20 |
| 3.3.2 Vertical force transfer | 22 |
| 3.3.3 Suspension modal analysis and coupling | 23 |
| 3.4 Dynamic Analysis | 26 |
| 3.4.1 Exploring vehicle's stability limits | 26 |
| 3.4.2 Lateral load transfer | 28 |
| 3.4.3 Steady-state yaw-velocity gain | 28 |
| 3.4.4 Handling diagram | 30 |
| 3.4.5 Vehicle side-slip angle | 32 |
| 3.5 Conclusion | 33 |

| | | |
|----------|---|-----------|
| 4 | Vehicle Model | 35 |
| 4.1 | Introduction | 35 |
| 4.2 | Proposed Vehicle Model | 35 |
| 4.2.1 | Tire Modeling | 36 |
| 4.2.2 | Vehicle body dynamics | 38 |
| 4.3 | Model Validation | 40 |
| 4.3.1 | Ramp-steer maneuver at $V_x = 13.3$ m/s | 40 |
| 4.3.2 | Ramp-steer maneuver at $V_x = 27.7$ m/s | 42 |
| 4.3.3 | Double step-steer | 44 |
| 4.3.4 | Key takeaways | 45 |
| 4.4 | Conclusion | 47 |
| 5 | Controller Design | 48 |
| 5.1 | Introduction | 48 |
| 5.2 | Vehicle Model | 48 |
| 5.2.1 | Input Transformation | 50 |
| 5.3 | Controller bandwidth selection | 51 |
| 5.4 | Slow active suspension control | 53 |
| 5.5 | Fully active suspension control | 54 |
| 5.6 | Key observations: open-loop dynamics | 54 |
| 5.7 | Closed-loop implementation of active suspension | 56 |
| 5.7.1 | Closed-loop behavior | 56 |
| 5.7.2 | Calculate lateral tire force requirement | 58 |
| 5.8 | Conclusion | 60 |
| 6 | Results Analysis | 61 |
| 6.1 | Introduction | 61 |
| 6.2 | Simulation Environment | 61 |
| 6.3 | Extreme Maneuvers | 62 |
| 6.3.1 | Yaw stability test | 62 |
| 6.3.2 | Lateral stability test | 65 |
| 6.3.3 | Key takeaways: active suspension for improving vehicle safety | 67 |
| 6.4 | Enthusiastic Driving | 68 |
| 6.5 | Exploring actuator limits | 71 |
| 6.6 | Slow active control versus fully active control | 73 |
| 6.7 | Summary | 74 |
| 7 | Conclusion and Future Work | 76 |
| 7.1 | Summary | 76 |
| 7.2 | Conclusions | 77 |
| 7.3 | Recommendations | 78 |
| A | Vehicle Parameters | 80 |
| B | Multi-body Model Layout | 81 |
| C | Suspension travel and bump-stops | 82 |
| D | Suspension Modes | 83 |

| | |
|---------------------|-----------|
| Bibliography | 84 |
| Vita | 88 |

Preface

THIS thesis is submitted in partial fulfilment of the requirements for obtaining the degree of Master of Science in Automotive Technology at Technical University Eindhoven. It contains work done from January to September 2015.

I would like to thank Prof. dr. Henk Nijmeijer for his guidance and support during the entire thesis. I am also very thankful to dr. ir. Igo Besselink and dr. ir. Tom van der Sande for lots of inspiration, ideas and comments through all phases of the research project.

A huge thank you to my fellow members in the famous AES lab for the fun and enjoyable working atmosphere during the project. Special thanks to all my friends back home who chipped in with their suggestions to improve my work.

Eindhoven, Netherlands
Thursday 17th September, 2015

Shilp Dixit

Nomenclature

| Symbol | Definition | Unit |
|---------------|--|---------------------|
| α | Tire side-slip angle | [°] |
| α_1 | Front axle side-slip angle | [°] |
| α_2 | Rear axle side-slip angle | [°] |
| β | Vehicle side-slip angle | [°] |
| δ | Steering angle of front wheel | [°] |
| δ_{sw} | Steering wheel angle | [°] |
| κ | Spring stiffness ratio | [-] |
| η_1 | Efficiency of force transfer from front actuator to front tire | [-] |
| η_2 | Efficiency of force transfer from rear actuator to rear tire | [-] |
| φ | Roll angle | [°] |
| θ | Pitch angle | [°] |
| ψ | Yaw angle | [°] |
| ω | cut-off frequency of second order low pass filter | [rad/s] |
| ζ | damping ratio of second order low pass filter | [-] |
| ΔF | Lateral load transfer | [N] |
| a_1 | Distance from COG to front axle | [m] |
| a_2 | Distance from COG to rear axle | [m] |
| a_y | Lateral acceleration | [m/s ²] |
| C_1 | Front cornering stiffness | [N/rad] |
| $C_1(s)$ | Yaw-rate controller transfer function | [-] |
| C_2 | Rear cornering stiffness | [N/rad] |
| $C_2(s)$ | Side-slip controller transfer function | [-] |
| c_{ϕ_1} | Front roll stiffness | [N m/rad] |
| c_{ϕ_2} | Rear roll stiffness | [N m/rad] |
| D | Feedthrough matrix | [-] |
| F_{ac_i} | Actuator force | [N] |
| $F_{y,net}$ | Net lateral tire force | [N] |
| F_y | Lateral tire force | [N] |
| F_z | Vertical tire force | [N] |
| $G(s)$ | Transfer function of lateral dynamics of vehicle | [-] |
| $G_{dc}(s)$ | Transfer function of lateral dynamics of vehicle in decoupled form | [-] |
| g | Acceleration due to gravity | [m/s ²] |
| h' | Perpendicular distance of COG from roll-axis | [m] |
| h | Height of axle roll centre from the ground | [m] |
| ii | Global loop counter | [-] |
| I_{xx} | Moment of inertia along x-axis | [kgm ²] |
| I_{yy} | Moment of inertia along y-axis | [kgm ²] |
| I_{zz} | Moment of inertia along z-axis | [kgm ²] |

| Symbol | Definition | Unit |
|------------|---|-------|
| i_s | Steering ratio | [-] |
| K | Transfer function of a controller | [-] |
| K_P | Proportional gain | [-] |
| K_V | Derivative gain | [-] |
| k_{s1} | Spring stiffness front | [N/m] |
| k_{s2} | Spring stiffness rear | [N/m] |
| l_s | Suspension spring length | [m] |
| l | Wheelbase | [m] |
| m | Mass of vehicle | [kg] |
| P_I | Suspension optimization performance index | [-] |
| r_1 | Weighting factor for spring compression | [-] |
| r_2 | Weighting factor for tire compression | [-] |
| r_3 | Weighting factor sprung mass acceleration | [-] |
| r_z | Yaw-rate | [°/s] |
| s_1 | Half of front track-width | [m] |
| s_2 | Half of rear track-width | [m] |
| T_s | Total simulation time | [s] |
| T_{step} | Time at which step input is applied | [s] |
| T_u | Static input coupling matrix | [-] |
| T_z | Torque acting about vehicle's z-axis | [N m] |
| u | Input vector | [-] |
| V_x | Longitudinal velocity | [m/s] |
| V_y | Lateral velocity | [m/s] |
| V | Vehicle velocity | [m/s] |
| x | State vector | [-] |
| x_q | Quarter car state vector | [-] |
| y | Output vector | [-] |
| z_r | Road input | [m] |
| z_s | Sprung mass position | [m] |
| z_u | Unsprung mass position | [m] |

| Acronym | Definition |
|---------|--|
| 1G | 1 st generation |
| 2I2O | 2 input 2 output |
| 3D | Three dimensional |
| 4I2O | 4 input 2 output |
| ABC | Active body control |
| ARB | Anti-roll bar |
| COG | Center of gravity |
| DOF | Degree of Freedom |
| fa | fully active |
| FL | Front left |
| FR | Front right |
| GAS | Globally Asymptotically Stable |
| GES | Globally Exponentially Stable |
| ISO | International Organization for Standardization |

| Acronym | Definition |
|---------|--|
| max | Maximum |
| min | Minimum |
| MF | Magic formula |
| MIMO | Multi-input multi-output |
| MMM | Milliken Moment Method |
| MPC | Model predictive control |
| MR | Magneto-Rheological |
| PSD | Power spectral density |
| RL | Rear left |
| rms | Root mean square |
| RR | Rear right |
| sa | slow active |
| SISO | Single-input single-output |
| SSC2 | Side slip control 2, second generation side slip control designed by Ferrari |
| temp | Temporary |

CHAPTER 1

Introduction

The last thing that we find in making a book is to know what we must put first.

Blaise Pascal

THE automobile has dominated the personal transportation industry since the closing decades of the nineteenth century. The car has evolved greatly over the ages but the role of the vehicle suspension system has remained largely unchanged. The tires, suspension springs and shock absorbers form the main components of a vehicle's suspension system and are responsible for transmitting the power from the powertrain to the road, support braking systems, contributing to a steering system and providing specific responses to the driver and road inputs. In addition to providing a medium for point-to-point transportation, the role of a modern day car has expanded to many facets. The car has to provide an enjoyable driving experience, have a comfortable and absorbent ride, achieve certain performance measures and so on. As a result the days of generic cars belong in the past and the latter part of the 20th century and the current century has paved way for highly specialized cars that cater to every kind of customer. The customer base for a contemporary vehicle available in the market can be divided into two broad categories: the passionate driver and the passenger. The driver expects the car to be responsive to each input and provide good feedback from the tires and steering wheel i.e. vehicle handling. On the other hand, the passenger of the vehicle wishes for a comfortable vehicle that greatly reduces the jerks and accelerations of the vehicle body when driven over uneven surfaces i.e. ride-comfort. The suspension system of the vehicle plays a pivotal role in determining the inherently complex ride-comfort and handling behavior of a vehicle. The complex multi-body system with varying degrees of stiffness and damping [2] formed by the the tires, suspension springs and shock-absorbers comprises of a vehicle's suspension system. The relative orientation of these mechanical linkages give rise to a variety of different systems each tailored to provide a specific response to driver and road inputs.

There have been great advancements in suspension system technology and significant strides have been taken in the development of increasingly sophisticated tire and active suspension spring and damper systems. Every major car manufacturer has at some point or another dabbled around with cutting edge suspension spring and damper control techniques in a bid to improve the ride comfort and vehicle handling behavior

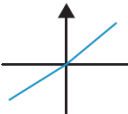
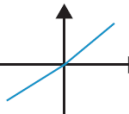
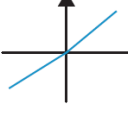



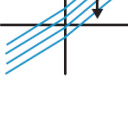
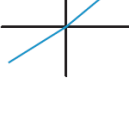
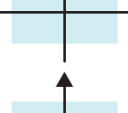
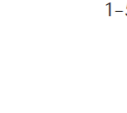

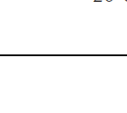
| System class | Control range (spring) | Control range (damper) | Control bandwidth | Power request | Control variable |
|---------------|---|---|-------------------|---------------|---------------------|
| Passive |  |  | - | - | - |
| Adaptive |  |  | 1–5 Hz | 10–20 W | c (damping ratio) |
| Semi-active |  |  | 30–40 Hz | 10–20 W | c (damping ratio) |
| Load leveling |  |  | 0.1–1 Hz | 100–200 W | W (static load) |
| Slow active |  |  | 1–5 Hz | 1–5 kW | F (force) |
| Fully active |  |  | 20–30 Hz | 5–10 kW | F (force) |

Figure 1.1: Classification of electronically controlled suspension [3]

and a classification of the different electronically controlled suspension types has been provided in Figure 1.1. The main objective of this graduation thesis is to investigate the influence of active suspensions on vehicle handling and study the effect of the control bandwidth on the actuator performance of an active suspension system. To fulfill this goal, a slow active suspension controller and a fully active suspension controller will be developed to show that electronic suspension actuation can help improve vehicle handling.

The perception of vehicle handling and ways of measuring it are discussed in Section 1.1. The influence of vehicle suspension on vehicle handling will be touched upon in Section 1.2. The objectives of this thesis are listed in Section 1.3 and an outline of the report is given in Section 1.5.

1.1 Vehicle handling

Over the last century driving has become a very organic and personal experience for a vast majority of people. Thus, it is natural for each individual to associate and define the experience distinctly. A vehicle with sharp and quick responses might be fun for one person and oversensitive for another. Similarly, a car with soft suspension might be comfortable for a certain person but seem to wallow about for another person. To account for the multitude of handling preferences, car manufacturers use multiple measures

as shown in Figure 1.2 to categorize and compare the handling characteristics of vehicles.

There exist certain vehicle states that can be used to quantify the handling characteristics of the vehicle during transient and steady-state cornering maneuvers. Some of the vehicle states that will be used throughout this thesis to study both, steady-state and transient handling characteristics are mentioned below.

Yaw-rate (r_z)

The yaw-rate measures the rate of change of the heading (yaw) angle of the vehicle [4].

$$r_z = \frac{d\psi}{dt} = \dot{\psi} \quad (1.1)$$

During transient conditions such as corner entry, the yaw-rate is an appropriate measure for the steering response of the vehicle where higher values of yaw-rate signify increased steering response. The measure, steady yaw-velocity gain (r_z/δ) is also a standard measure used to classify the handling balance of the vehicle during steady state cornering. Thus, yaw-rate will be used as an important metric throughout this thesis to evaluate the transient as well as steady-state handling characteristics of the vehicle.

Vehicle side-slip angle (β)

The angle between the orientation of the vehicle and the direction of travel at the COG is called the vehicle side-slip angle (β) and it is calculated using the equation given below.

$$\beta = \tan^{-1} \left(\frac{V_y}{V_x} \right) \quad (1.2)$$

The vehicle side-slip angle is an important visual and sensory cue used by drivers to assess the lateral stability of the vehicle during steady state cornering situations. The maximum value of a side-slip that a vehicle can attain before loss of lateral stability depends on the tires compounds, tire forces and road surface.

Lateral acceleration (a_y)

The lateral acceleration (a_y) of the vehicle is also used to study the lateral stability of the vehicle. The lateral acceleration of the vehicle can be computed using the equation below:

$$a_y = \frac{dV_y}{dt} + r_z V_x \quad (1.3)$$

The lateral acceleration developed during a cornering maneuver is another relevant tactile feedback the driver uses to perceive the lateral dynamics of the vehicle. Passenger cars are generally known to generate a peak lateral acceleration of $\approx 0.8g$ before losing traction whereas the professional race cars can generate lateral acceleration upwards of $1g$. In normal driving conditions there exists a tight connection between yaw-rate, lateral acceleration and vehicle side-slip angle. (1.3) can be rearranged to derive the relation stated below:

$$\dot{\beta} + r_z = \frac{a_y}{V_x} \quad (1.4)$$

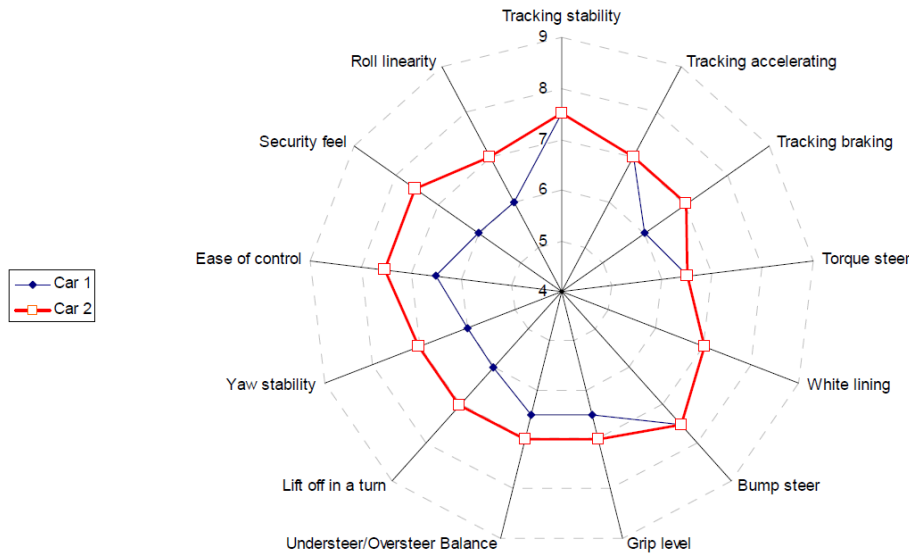


Figure 1.2: Tangible and intangible vehicle handling criterion: typical handling spider graph [5]

The multitude of measures used to characterize a vehicle's handling behavior were illustrated in this section. Some of the key vehicle states that can be used as quantitative measures of handling behavior were identified. The yaw-rate of the vehicle has been used throughout this thesis to evaluate the steering response of the vehicle during transient maneuvers and also assess yaw stability during steady-state conditions. In addition to the yaw stability of the vehicle, the side-slip angle has been used as a measure for the lateral stability of the vehicle.

Note: Vehicle side-slip angle can be notoriously difficult to measure in a real world scenario. However, it can be measured with reasonable accuracy when the vehicle is generating high lateral acceleration. Keeping this in mind one can use side-slip angle to define the stable boundaries for the vehicle.

1.2 Role of a suspension system

The tires, suspension springs and suspension dampers play a significant role in the transient as well as steady-state handling characteristics of the vehicle. The suspension compliance, damper characteristics, springs and anti-roll bar stiffness are some of the suspension parameters that affect the handling characteristics of the vehicle. One can observe from Figure 1.1 the different classes of electronically controlled suspension control the suspension spring stiffness and the damper characteristics. The development of slow active and the fully active suspension controller fall within the scope of this graduation thesis.

Dynamically controlling the spring and damper characteristics of a suspension alters many kinematic and dynamic aspects of the vehicle such as: lateral and longitudinal load transfer, vehicle roll stiffness distribution, vehicle weight distribution, individual tire compression and individual tire loads. The handling characteristics of any vehicle is

inherently associated with these factors and thus the class of active suspensions have the potential to improve the lateral and yaw dynamics of the vehicle. A review of the existing literature on active suspension design has shown significant gains in improving the handling of the vehicle by minimizing the dynamic tire loads. Also as expected the fully active suspension is able to provide better results when compared to a slow active suspension. However, there is a dearth of research performed on influence of an active suspension on the transient and steady state handling characteristics of a vehicle. Moreover, there is not much insight available in existing literature that documents the correlation between control bandwidth and improvements achieved by using an active suspension.

1.3 Objectives

The rationale presented in Sections 1.1 and 1.2 instigates the need for a study on the impact of active suspension on the lateral and yaw dynamics of a vehicle. The main research objective of this graduation thesis can be stated as:

Design a slow active suspension controller and a fully active suspension controller to improve a vehicle's handling characteristics and investigate the relation between control bandwidth and achievable handling enhancements.

The different aspects of development stages aid in sub-dividing the primary research question into smaller objectives with individual results and outcomes which are enlisted as follows:

- Perform a thorough literature survey on past research in the field of semi-active and active suspension setup and its impact on the ride and handling behavior of a vehicle. Based on the findings from the review process provide substantiated arguments for the research work.
- Develop a vehicle model that can accurately capture and replicate the required dynamics of a vehicle and validate the designed model with the BMW SimMechanics™ 1G model.
- Design a slow active suspension and a full active suspension controller to influence the handling behavior of the vehicle model.
- Implement the active suspension controllers on a validated vehicle model and investigate the capability of the active suspension at improving the transient and steady-state handling of the vehicle model.
- Compare the performance of the two different active suspension controllers to determine the relation between controller bandwidth and achieved handling improvements.

1.4 Contributions

A short summary of the contributions resulting from this thesis are given below:

- *Two-track vehicle model:* A two-track vehicle model that captures the lateral and yaw dynamics of a vehicle is developed. The model incorporates lateral load transfer during cornering and uses Magic Formula based tire models for improved accuracy at extreme handling simulations.
- *Dynamic inversion of Magic Formula:* The Magic Formula based tire model uses the vertical tire force and tire side-slip angle to determine the lateral force. In this thesis a algorithmic method of inverting the Magic Formula was developed. This algorithm takes the tire side-slip angle and requested lateral force to output the appropriate tire force.
- *Active suspension control for handling:* Two active suspension controllers for improving the lateral and yaw dynamics of the vehicle are designed. The two controllers are designed such that they exhibit identical low frequency behavior such that a performance comparison between the two will highlight the potential benefits arising due to high frequency gains.

1.5 Thesis Outline

This masters thesis report discuss the impact of an active suspension on the handling characteristics of a vehicle. The research work and findings are documented in the subsequent chapters. This section provides an outline of the contents of the report.

Key takeaways from relevant research work pertaining to the topic of vehicle handling and active-suspension design is cataloged in Chapter 2. The insight from this chapter affirms the hypothesis from Sections 1.1 and 1.2 and serves as the foundation stone for the rest of the thesis. The observations and analysis performed from the scientific papers and journal publications are used to create and chart out the strategy for this research project.

The influence of actuator forces on the handling characteristics of a BMW 318i are studied in Chapter 3. A multi-body vehicle model is used as the reference model describing the vehicle and the open-loop handling dynamics are analyzed in Chapter 3 and the potential of an active suspension is scrutinized in detail by performing open-loop tests. The findings of this chapter are also utilized in obtaining the limits of the actuator, calculating the efficiency of force transfer and understanding the coupling behavior of various suspension components.

A mathematical model to describe the lateral and yaw dynamics of the BMW 318i is designed in Chapter 4 and the performance of the model is validated against the standard BMW SimMechanics™ 1G model. The mathematical model captures the tire behavior via the Magic Formula representation and depicts the lateral and yaw dynamics of the vehicle using a state-space representation. This mathematical model is developed with the intention of enabling active-suspension controller design that can control the lateral and yaw dynamics of the vehicle.

Active-suspension controllers are designed in Chapter 5. The suspension controllers are designed to control the yaw-rate (r_z) and vehicle side-slip angle (β) and closed loop

controller implementation is discussed in the chapter. The problem of implementing a frequency method based linear controller to a non-linear model are also looked in detail in the chapter and the provided solution is also explained further.

The results of the research work are presented in Chapter 6. The improvements in the transient and steady-state handling of the vehicle due to active suspension is shown along with a comparison of the performance of the two active suspension controllers. The relation between control bandwidth and potential handling improvements is also presented and discussed in this chapter.

Chapter 7 summarizes and highlights the major findings and developments from the thesis and lists the essential conclusions that can be drawn. The primary contributions from this graduation thesis are provided. Additionally, the chapter also discusses the possible directions to develop the concept further.

CHAPTER 2

Literature Review

To read without reflecting is like eating without digesting.

Edmund Burke

THIS chapter serves as a record for the relevant and important work pertaining to this thesis. The publications pertinent to the field of vehicle handling and active suspension design are reviewed. Section 2.1 touches upon the age old problem of finding the right compromise between ride-comfort and vehicle handling. Lateral and yaw dynamics are critical aspects of vehicle handling studies. In Section 2.2 some of the methodologies used by researchers to study lateral and yaw-dynamics of the vehicle are discussed. Section 2.3 documents the major findings in the field of active suspension controller design and focuses primarily on active suspension design for improving the vehicle handling behavior.

2.1 Vehicle comfort and handling: a constant compromise

A majority of today's vehicle suspensions use hydraulic dampers and steel coil springs to absorb the road bumps, minimize the car's body movements and keep the tires in contact with the road surface. The main objectives for achieving a good ride are to reduce the accelerations of the occupants and the payload when driving over uneven surfaces and keep the tires in good contact with the ground for controllability and traction. On the other hand vehicle handling deals with the responses of the vehicle to driver commands, road disturbances and weather conditions.

A typical 2 DOF quarter car model representation of a vehicle is shown in Figure 2.1. The equations of motion for such a model can be represented in a state-space format as:

$$x_q = [z_s \quad \dot{z}_s \quad z_u \quad \dot{z}_u]^T \quad (2.1)$$

$$\dot{x}_q = \begin{bmatrix} 0 & 1 & 0 & 0 \\ -\frac{k_s}{m_s} & -\frac{d_s}{m_s} & \frac{k_s}{m_s} & \frac{d_s}{m_s} \\ 0 & 0 & 0 & 1 \\ \frac{k_s}{m_u} & \frac{d_s}{m_u} & -\frac{k_s+k_t}{m_u} & -\frac{d_s}{m_u} \end{bmatrix} x_q + \begin{bmatrix} 0 & 0 \\ 0 & -\frac{1}{m_s} \\ 0 & 0 \\ \frac{k_t}{m_u} & \frac{1}{m_u} \end{bmatrix} \begin{bmatrix} z_r \\ F_{ac} \end{bmatrix} \quad (2.2)$$

Vertical acceleration of sprung mass, (\ddot{z}_s) and suspension stroke, $(z_s - z_u)$ are two very important measures to evaluate the ride-comfort of a vehicle [6][7][8][9][1]. On the other hand, tire deflection, $(z_u - z_r)$ is typically used to quantify vehicle handling [10][11][12]. Minimizing the acceleration of sprung mass and decreasing suspension stroke help improve the ride-comfort of the vehicle whereas minimizing the tire deflection improves the handling of the vehicle.

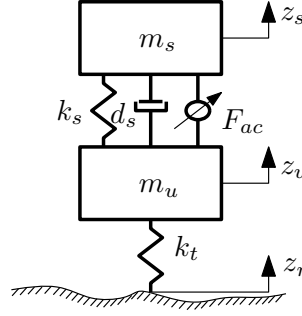


Figure 2.1: 2 DOF quarter car model

An active suspension can be designed to minimize both the ride-comfort and handling measures. The actuator force of such a suspension can be computed by creating a performance index, (P_I) for the control effort. This performance index can be written in the form of an optimization problem:

$$\begin{aligned} & \underset{\ddot{z}_s, (z_s - z_u), (z_u - z_r)}{\text{minimize}} \quad P_I = [r_1(z_s - z_u)^2 + r_2(z_u - z_r)^2 + r_3\ddot{z}_s^2] \quad (2.3) \\ & \text{subject to (2.2)} \\ & \text{where } r_1, r_2, r_3 \text{ are weighting factors} \end{aligned}$$

A schematic illustration to the solution of the optimization problem in (2.3) can be observed in Figures 2.2a and 2.2b. One can examine that there exist certain portions in the graph that cannot be reached for any set of weighting factors. Thus, all possible solutions to the minimization problem lie on the optimal set or beyond it and it is not possible to minimize all three performance indices simultaneously, Figures 2.2a and 2.2b (solid line).

Key Takeaways

It is evident from the discussion in Section 2.1 that there exists a constant compromise between designing for ride-comfort and vehicle handling and a suspension needs to attain the fine balance between ride-comfort and handling. One can also conclude that the 2 DOF quarter car model can account for most of the important measures used to quantify ride-comfort but fails to provide sufficient insight on vehicle handling. Lateral and yaw dynamics form a major part of vehicle handling and hence any study that focuses on vehicle handling needs to look beyond the 2 DOF quarter car model as a mathematical framework to define vehicle handling.

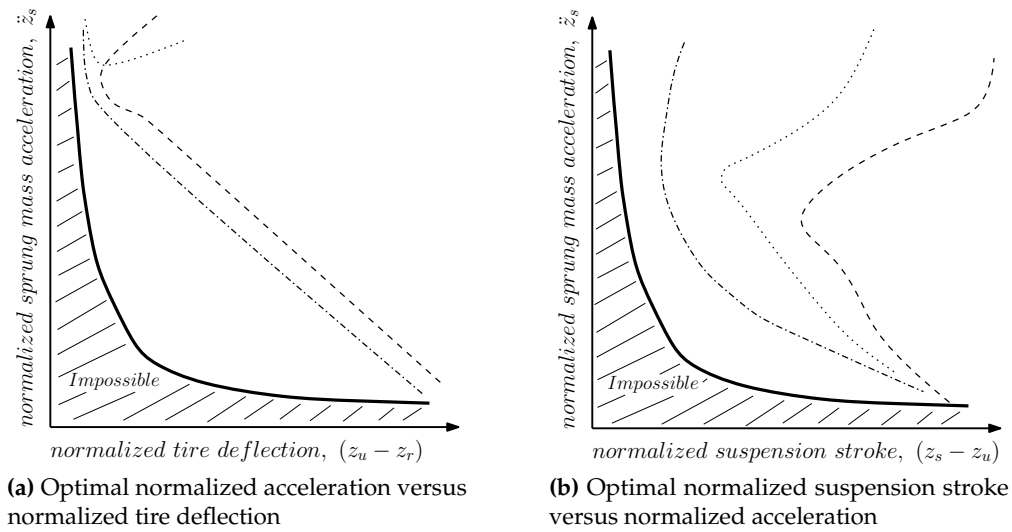


Figure 2.2: Schematic plots for results of optimization problem in (2.3) [10][11]. **Note:** Each dotted line indicates a solution set for a distinct set of weighting filters, (r_i) . **Note:** Lower normalized value indicates improved comfort or improved handling.

2.2 Evaluating vehicle handling

The definition of ride-comfort has been extensively described and documented as explained in Section 2.1. On the other hand, vehicle handling is a subjective topic and cannot be described by a single equation or definition. Researchers affiliated to the industry and academic realms have been working on arriving at an exhaustive set of parameters that can be used to evaluate vehicle handling.

The vehicle dynamics team at Lotus Engineering describes vehicle handling by the lateral dynamic responses of the vehicle to driver commands and external disturbances [2]. The engineers state that lateral dynamic responses depend on a range of factors such as front and rear tire performance, lateral and longitudinal load transfer, vehicle roll stiffness distribution, front and rear roll center positions and vehicle weight and weight distribution. The factors mentioned by the engineers are suspension parameters and thus one can conclude that dynamically controlling the suspension parameters can influence the lateral dynamics of the vehicle.

Manning et al. [13] review a selection of 68 papers in the field of lateral handling control and focuses on three control objectives: yaw-rate control, side-slip control and combined yaw-rate and side-slip control. The authors propose that the yaw-rate control objective addresses the issue of improving steering feel and side-slip control related more to the vehicle stability and is important near the limit of vehicle handling. The bulk of the work deals with critical review of the control approaches followed by researchers in the aforementioned fields of vehicle handling and the efficacy of these methods to improve vehicle handling.

The work of Bobier [14] focuses on vehicle handling by studying the phase-plane trajectories of the yaw-rate and side-slip angle. A non-linear two track planar vehicle model is defined to study these signals and the concept of stable envelope control is used to design an active steering controller. The research work also deals with the relation between the suspension geometry and vehicle handling characteristics.

Horiuchi et al. [15] determined that in general the driver focuses on the yaw angle and yaw-rate rather than lateral position especially when driving a car steered by its front wheels. The authors state that vehicle heading angle and yaw-rate provides crucial visual cues to the driver during a cornering maneuver. These visual indications are used by the driver to adjust the steering and throttle during cornering and also judge the yaw-stability of the vehicle. These findings suggest the yaw-rate is an invaluable measure for determining the steering response of the vehicle and also estimate the yaw stability criterion.

Badiru [16] studied the requirements for steering feel of a vehicle. In this paper, the author discusses the importance of steering feel and states that steering feel is fundamentally related to vehicle handling. The author further provides objective metrics to categorize steering feel and conducts real world driving tests to determine driver preferences. The drivers perform J-turn maneuvers and the results obtained depict a large correlation between perception of lateral acceleration and yaw-rate. Additionally, the author reports that the test drivers regarded lateral acceleration gain, vehicle side-slip and roll rate as the most important metrics during steady-state turning.

The work by Ono et al. [17] deals with the vehicle instability caused by rear tire side-force saturation. They develop a two track nonlinear model of the vehicle to study the yaw-rate (r_z) and vehicle side-slip angle (β) dynamics. The research primarily focuses on the equivalent cornering characteristics of a tire on different road surfaces and methods to obtain larger steady state-rate without vehicle spin.

Hoffman et al. [18] study the stability of vehicle dynamics through phase plane analysis of a two DOF bicycle model. The vehicle is initialized in a particular state and the open-loop trajectory is plotted on a phase plane of the states, r_z and β . The authors provide physical interpretations of vehicle controllability and suggest either $\beta - r_z$ phase plane or $\dot{\beta} - \beta$ phase plane as effective approaches to analyze the system dynamics. The research work deals with comparison of phase-plane analysis of a 2 DOF nonlinear bicycle model and Milliken MMM diagram of traction boundary [19].

Williams et al. [20] study the influence of roll-moment distribution and its effect on the handling dynamics of a vehicle. The authors state that an understeering vehicle is perceived as sluggish and over-steering vehicle is twitchy. The authors use a nonlinear bicycle model to describe the vehicle dynamics and use the concept of under-steer gradient to define vehicle handling characteristics. A nonlinear controller is designed via feedback linearization of the vehicle states, yaw-rate and lateral velocity. The authors report that the controller is implemented on a full sized passenger sedan and shows large improvements in the step-steer response of the vehicle.

Ross et al. [21] analyze the handling characteristics of an automobile in the nonlinear region of tire characteristics. A two DOF nonlinear bicycle model is used to define the dynamics of the vehicle in the horizontal plane and the handling characteristics of the automobile is studied based on bifurcation analysis of the tire side-slip angles and handling diagram theory. The vehicle under-steering and over-steering behavior is studied in detail by considering various vehicle parameters configurations due to steering angle (δ), vehicle side-slip angle (β) and axle side-slip angles (α_i).

Key Takeaways

Some of the prominent research papers reviewed in Section 2.2 reaffirm the belief that vehicle handling cannot be evaluated just on the basis of tire compression. In addition to studying tire forces it must also be accompanied by evaluating the steady-state and transient behavior of a vehicle. Interestingly, yaw-rate and lateral stability are the two most frequently recurring measures that are mentioned in the publications that that explore the topic of vehicle handling.

Throughout this thesis, yaw-rate, (r_z) is used as the measure for steering response during transient driving maneuvers. Moreover, if the yaw-rate increases too fast in proportion to the steering wheel angle the driver loses control of the vehicle's heading which results in loss of yaw stability. Hence, yaw-rate will also be used to evaluate the yaw stability of the vehicle. During a cornering maneuver, if the tires lose traction there is a loss of lateral stability which results in the vehicle sliding further away from the corner. The vehicle side-slip angle (β) will be used throughout this thesis to monitor and ensure the lateral stability of the vehicle. The review carried out in Section 2.2 bolsters these decisions and also provides appropriate scientific context.

The review of the work done by the authors also throws light on another aspect of vehicle handling analysis; the vehicle model. The researchers rely either on a test vehicle or vehicle models that can describe the yaw and lateral dynamics of the vehicle. This insight will be a valuable tool during the latter parts of the thesis when a need for an accurate vehicle model will arise.

2.3 Active suspension design

Active suspension design has been a topic of extensive research and there is an abundance of literature available on the topic. This section discusses a few prominent publications dealing with active suspension controllers for improving vehicle handling. There exists no standard model and control technique to design an active suspension and the publications prove this by the sheer variety of vehicle models and control techniques employed to delve deeper into a certain dynamic behavior.

Koch et al. [22] explore the potential of a low bandwidth active suspension to tackle the joint problem of improving ride-comfort and vehicle handling. The authors use normalized root mean square (rms) chassis acceleration to measure ride comfort and normalized rms tire deflection to measure handling and vehicle safety. A quarter car model is used to develop two different controllers, a low bandwidth active suspension and a high bandwidth active suspension. The performance of both the controllers is

tested on highway measurement data and the authors document the effect of the controller bandwidth and influence of damping on ride comfort and safety.

The work of Wang et al. [23] documents an active suspension design based on a full vehicle model. The author claims that the active suspension is successfully able to improve vehicle ride and steady-state handling. The authors propose that the energy of the weighted vehicle body accelerations are good measures for ride-comfort and understeer gradient as the metric to measure vehicle handling. A full vehicle model is used to describe the vertical dynamics of the vehicle and a single track bicycle model is used to describe the steady-state handling characteristics of the vehicle. The authors analyze the nonlinear relationship between lateral and normal force of a tire and use it to define the understeer gradient of the vehicle. Additionally, the lateral force on the front and rear axle that arises due to roll moment distribution is included in the lateral and yaw dynamics of the bicycle model. Ride comfort is quantified by the energy of weighted sprung mass accelerations and the understeer gradient as the handling performance index. An \mathcal{H}_∞ controller is designed for the active suspension to minimize vehicle handling and ride comfort performance indices. The authors report an improvement in frequency response measurements of the body accelerations thereby improving ride-comfort. Additionally, the authors also claim improvements in vehicle handling due to improved disturbance rejection from external roll moments.

An active suspension control of vehicle based on a full vehicle model is designed by Ikenaga et al. [24]. The authors propose a multi-loop control design with the inner loop that reject terrain disturbances and an outer loop that stabilizes heave, pitch and roll responses of the sprung mass. A linear full vehicle model is used and an input decoupling transformation is used to decouple the control loops mentioned above. The inner loop controller is implemented using a feedback system whereas the outer control loop is realized via skyhook control. This multi-loop system was simulated for three different frequencies for input terrain disturbances and it was shown that motions of the sprung mass above and below the wheel frequency could be mitigated by using active filtering of spring and damping coefficients through inner control loops (ride controller) plus skyhook damping of heave, pitch and roll velocities through outer control loops (attitude controller). Performance improvement in ride-comfort due to the active suspension control was demonstrated in simulations.

Sande [1] tackles the two-fold problem of influencing the ride-comfort and handling of a vehicle by a semi-active suspension. The author shows via simulations that adjusting the damping characteristics of the vehicle has an influence on the vehicle handling in the transient state. This insight is used to design to reduce the overshoot in the lateral acceleration during extreme maneuvers. The author depicts that controlling the lateral acceleration overshoot improves vehicle handling as it maximizes the potential for steering corrections. The results are substantiated by simulations on limit of handling step steering maneuvers

Chen et al. [25] present a robust MPC scheme for an active suspension with the aim of isolating road disturbance from the sprung mass acceleration to improve ride-comfort and suppressing wheel hop to improve vehicle handling. The authors state that the con-

trol scheme implemented provides \mathcal{H}_∞ level performance for the given control problem and the system is implemented on a quarter car model. Through simulation results a significant improvement in the ride comfort and vehicle handling is reported.

An \mathcal{H}_∞ control theory based active suspension is developed by Yamashita et al. [26] and implemented on a full vehicle model. The authors use heave mode suspension displacement as a measure for ride comfort and suspension displacement as a measure for vehicle handling. A quarter car model is used for the controller design which is then implemented on a full vehicle model for straight driving and lane change maneuvers. The PSD of the closed loop system decreases by 35.6% in the frequency range of 1 to 8 Hz and body roll is seen to decrease by 42.3% when the vehicle is subjected to a lateral acceleration (a_y) of 4 m/s^2 .

Bodie et al. [27] discuss the design of a new suspension control system that enhances vehicle stability and handling in fast evasive maneuvers close to the limit of adhesion. The authors state that the yaw-rate (r_z) of a vehicle is proportional to the steering input (δ_{sw}) and vehicle handling behavior should remain close to that experienced in the linear range of tire operation. The effect of variations in magneto-rheological (MR) damper settings on vehicle handling responses is analyzed via simulations and by comparing the two extreme cases of the damper setting, the degree to which the damper settings can influence vehicle yaw response was determined. A new vehicle control system was proposed, which uses electronically controllable magneto-rheological (MR) dampers to distribute damping force between the front and rear axles to correct for errors between the actual and desired yaw rates.

The work of Williams et al. [28] is based on studying the influence of roll moment distribution on handling dynamics of automobiles. The authors state that an over-steering vehicle is perceived as twitchy and an under-steering vehicle as sluggish. They use simulation data to show that loss in lateral force due to weight transfer exceeds the gains obtained by addition of normal force from the other side. To represent this phenomenon a tire model which requires normal force and slip angle to generate side force and a higher order dependence of side force on normal force to capture the effect of roll moment is incorporated with a bicycle model of the vehicle. The vehicle handling is defined using the under-steer gradient and the given control problem is solved by using a nonlinear input-output linearization method. The designed controller was implemented on a full sized vehicle and marked differences in steering response and perceived vehicle lateral stability were reported when compared to a reference vehicle.

2.3.1 Active suspension: State-of-the-art

In addition to the theoretical work presented in research publication it is also interesting to study the cutting edge implementation of the active suspension systems in production vehicles. In this section a couple of such production examples are introduced in an attempt to bridge the gap between academic concepts and industrial applications.

Traditional methods for active control for vehicle dynamics has seen engineers and researchers measure lateral acceleration (a_y), yaw angle (ψ), steering wheel angle (δ_{sw}) to estimate the vehicle state and then control it by regulating the throttle, brake torque

and differentials to alter the trajectory of the vehicle. The side-slip control 2 (SSC2) [29] developed by Ferrari for its road cars also actively controls the suspension damping and the anti-roll bar damping to optimize the contact patch between the tire and the road. This integrated chassis, powertrain and suspension control setup allows the engineers to tweak the handling behavior of the vehicle from safe understeer all the way up to controllable oversteer.

On a similar vein, the Active Body Control (ABC) developed by Mercedes-Benz [30][31] uses five sensors to measure the vehicle lateral, pitch and heave motions of the vehicle and cabin to actively control the suspension travel with the goal of negating cabin roll movements and maximizing ride comfort. Additionally, the current generation ABC systems also integrates crosswind stabilization into the active suspension system to provide an additional safety net to the driver during extreme weather conditions.

Key Takeaways

From the review in Section 2.3 it can be clearly observed that a significant fraction of active suspension research classifies vehicle handling as the road holding ability of the tires. Contrary to the views taken by the researchers in Section 2.2, there is a dearth of literature that documents the impact of active suspension systems on the lateral and yaw dynamics of a vehicle. Out of the papers that do study combine the facets of active suspension, lateral and yaw dynamics of the vehicle the approach shares the technique of using a single track vehicle model to control the yaw-rate of the vehicle. However, such an approach provides no insight on the influence of active suspension systems of the transient and steady-state handling of a vehicle. Furthermore, the researchers either use linear expressions or simplified polynomials to model the tires in a vehicle. This severely limits the accuracy while simulating maneuvers which generate high lateral acceleration.

To summarize, it is a logical conclusion to conduct research on active suspension control design that focuses on the lateral and yaw dynamics of the vehicle. The suspension controller that intends to control the yaw and lateral dynamics of the vehicle should also be based on a vehicle model that accurately captures the tire and vehicle dynamics during different driving simulations.

2.4 Conclusion

The current chapter documents some of the dominant and pioneering research work that has been carried out in the domain of vehicle dynamics and active suspension control design. The arguments presented in Section 2.1 demonstrated the deficiencies of the quarter car model at depicting the complete handling characteristics of the vehicle. It allowed for a decision to lead this thesis towards the study of yaw and lateral dynamics of the vehicle. The review of decisive publications in Section 2.2 helped understand the vehicle states that can be used to identify and study the yaw and lateral dynamics of the vehicle. The decision to utilize yaw-rate as the measure for steering response and yaw-stability was rationalized from the insight gained in this section. Similarly, the reasons for narrowing down to vehicle side-slip angle as the measure for lateral stability of the vehicle was also treated in this section. The findings from Section 2.2 also gave rise to a need for a vehicle model that accurately captures the tire and vehicle dynamics

during cornering maneuvers. The methods and results followed by researchers for active suspension design were discussed in Section 2.3. The limited results related to enhancements in yaw and lateral dynamics due to active suspension further laid proof for the need of such an exercise. Lastly, there were no significant results that demonstrated the relation between active suspension control bandwidth and achievable performance gains. The lack of such studies has resulted in investigating the influence of control bandwidth on the performance of an active suspension system one of the cornerstones of this thesis.

CHAPTER 3

Analysis of a Multi-body Vehicle Model

If we knew what it was we were doing, it would not be called research, would it?

Albert Einstein

3.1 Introduction

THIS chapter is dedicated to understanding the influence of actuator forces on the yaw and lateral dynamics of a vehicle in an open-loop setup. This exercise is undertaken to ascertain whether active suspension gives enough control to markedly affect vehicle handling. The system analysis that is carried out in this chapter can be broadly classified into two categories: static vehicle analysis and dynamic driving tests. The first set of simulation tests are carried out to understand the coupling between the suspension bump stops, anti-roll bars and how they influence some of the properties of the suspension. The second set of tests are carried out to study the open loop dynamics of the vehicle during various driving maneuvers. A multi-body model of a BMW 318i developed in SimMechanics™ 1G will be used to understand the interaction between the various components also gain insight into the system dynamics [32]. This exercise is carried out so that the knowledge gained from the simulation studies will provide guidelines for the subsequent model simplification and controller design exercises.

3.2 Reference Vehicle

The reference vehicle used throughout this thesis is a 2001 BMW 318i [1], see Figure 3.1. The BMW is a rear wheel drive four door saloon car equipped with an in-line four cylinder engine and an automatic transmission. The front suspension of the BMW 318i is of the McPherson type and a central-link setup at the rear is used. Additionally, a stabi-link connects the left and right suspension with a stabilizer bar to reduce vehicle body roll. Such a mechanical connection exists both on the front as well as the rear suspension. Throughout this thesis the sign convention for all measurement performed are based on the ISO8855 [4]. The tires on the BMW are Vredestein Sportac3 195/65 R15

91V. The mechanical properties of these tires have been determined and available as *.tir* property files.



Figure 3.1: BMW 318i reference vehicle [1]

3.2.1 Multi-body Model

A multi-body model of the vehicle has been developed using Simulink® SimMechanics™ 1G [1][32]. The chassis is modeled as a single rigid mass to which four suspension units are connected. Each suspension is modeled in detail with all physical links as they are present in the real car. The left and right suspension systems at the front and rear are connected by means of an anti-roll bar. Furthermore, the steering system dynamics are taken into account. Finally, the tires mentioned in Section 3.2 are modeled with the TNO Delft-Tyre package which represents the forces created by the tire by means of the Magic Formula [33]. Extensive verification and validation exercises have already been undertaken on the model and the accuracy of the model has been established for various driving maneuvers [32].

Model Inputs

The multi-body model can be operated by inputs to simulate distinct and realistic driving maneuvers. The variables that can be used as input signals are enlisted below:

- Longitudinal velocity, V_x can be imparted to the vehicle model via drive/brake torque or by a PI cruise control based on a velocity profile.
- The lateral motion of the vehicle can be directed by providing a steering wheel angle, δ_{sw} input.
- To successfully perform open-loop tests by force actuation in the suspension system of the multi-body model described in Section 3.2.1 and Appendix B actuators were setup up along the spring axis of each suspension to mimic a hydraulic or linear motor setup. These forces on these actuators, F_{ac_i} can be provided as a function of time to compress or extend the individual suspension springs.

Note: A negative actuator force, F_{ac_i} means the suspension spring is extended whereas a positive actuator force, F_{ac_i} means that the suspension spring is compressed.

3.3 Static Analysis

In this section simulation tests are performed to understand how the various interconnections between the different suspension components interact and influence one another during actuation with the suspension actuators.

3.3.1 Suspension travel

The springs of a suspension system do not have the ability to compress or extend infinitely. There comes a point in their travel when they hit the mechanical and physical ends of their movement known as bump-stops, see Appendix C. When the spring is forced to expand or compress beyond these points there is a marked difference in the spring stiffness. In this section, the limits of suspension actuators are determined such that the actuation does not breach the bump-stop limits.

To gain a better understanding of the actuator force limits, a stationary vehicle with no steering angle is actuated with step force inputs on an individual wheel. Since the front and the rear suspension systems have different suspension parameters, it is expected that the front and rear actuators will have distinct actuator limits. The front suspension hits the upper and lower bump stop when the particular unit is actuated with a force of $F_{ac,FL} = \pm 2250$ N, see Figure 3.2. In addition to the behavior of the front left spring length one can also observe the slight extension of the front right spring which is due to the front anti-roll bar. On the other hand, the rear suspension did not breach the bump stop limits even when the actuator force $F_{ac,RR} = \pm 3750$ N, see Figure 3.3. An interesting observation is the change in the spring length for the remaining three units which are not actuated. The front left and front right spring produce opposing deflections which hints at roll moment being generated at the front axle when one of the rear suspension is actuated. However, the rear left and rear right spring deflection is identical. This phenomenon can be attributed to the low stiffness of the rear anti-roll bar and this hypothesis will be confirmed in upcoming sections. Furthermore, one can observe the small oscillations that are present in all the springs after the step input is applied at $T_{step} = 2$ s. These oscillations are damped in approximately 1 s as the system attains a new equilibrium position.

Influence of anti-roll bar

The front and rear anti-roll bars were removed from the multi-body model and the simulation test from Figure 3.3 was repeated to understand the influence of the anti-roll bar on the other suspension components. By observing the spring travel length on the rear suspension one can inspect the drastic change in the spring length on removal of the anti-roll bars. The rear left suspension is extended much less whereas the (actuated) rear right corner hits the upper bump-stop limit. Thus, along with the coupling between the bump-stops and anti-roll bars in a vehicle suspension is a major another source of nonlinear behavior that should either be accounted for while designing an active-suspension or replaced by actively controlled anti-roll bars.

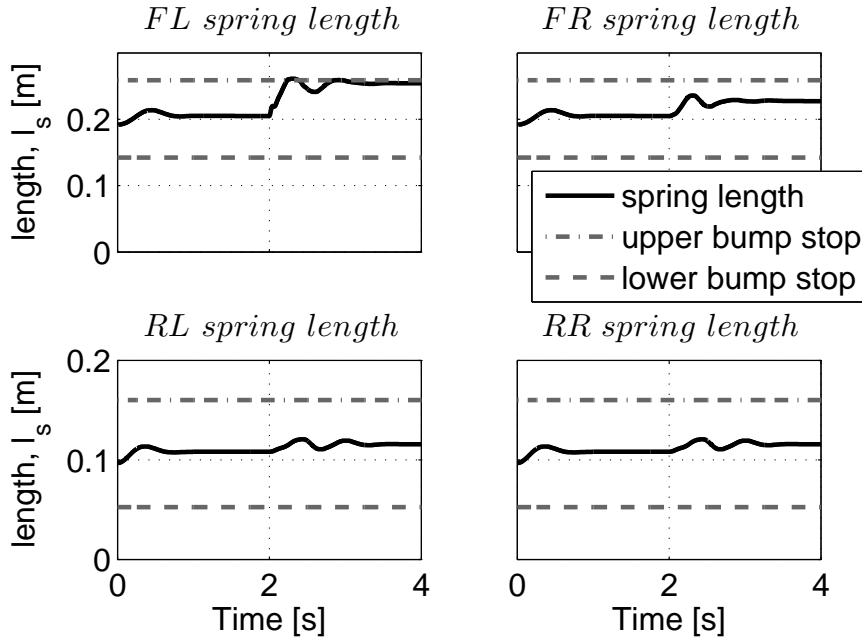


Figure 3.2: Suspension spring travel for front left actuation with $F_{ac,FL} = -2250$ N for input ($\delta_{sw} = 0^\circ$, $V_x = 0$ m/s, $T_{step} = 2$ s); front suspension (top row), rear suspension (bottom row).

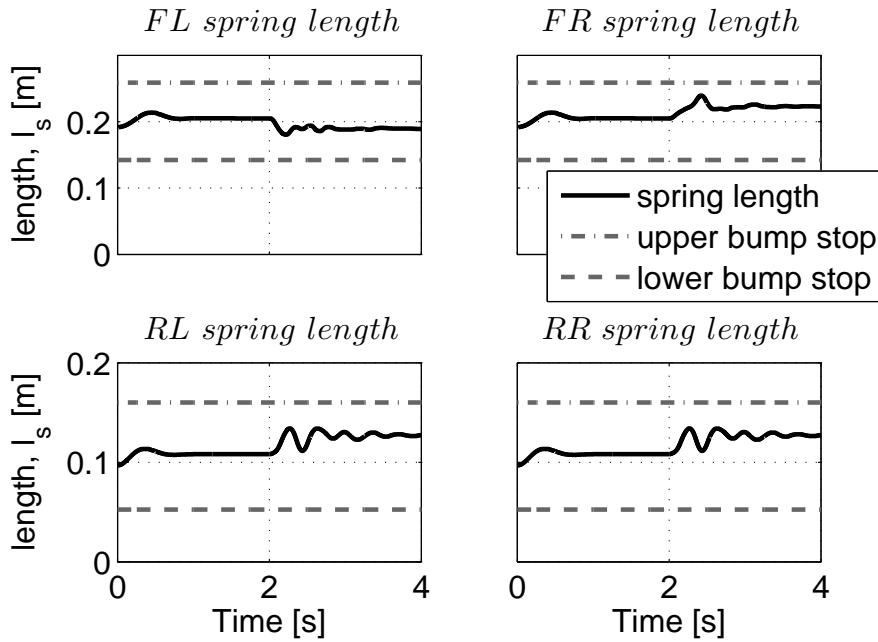


Figure 3.3: Suspension spring travel for rear right actuation with $F_{ac,RR} = -3750$ N for input ($\delta_{sw} = 0^\circ$, $V_x = 0$ m/s, $T_{step} = 2$ s); front suspension (top row), rear suspension (bottom row).

Key Takeaways

The simulations performed in Section 3.3.1 have helped in deriving the actuator limits for the front and rear suspension. Since, the front suspension bump-stop limits are breached at $F_{ac,i} = \pm 2250$ N the limits of the front actuator are set to $|F_{ac,i}| = 2000$ N. On the other hand, in the presence of an anti-roll bar the rear bump-stop limits are not breached even at $F_{ac,i} = \pm 3750$ N and hence the rear actuator limit is set to $|F_{ac,i}| = 3750$ N.

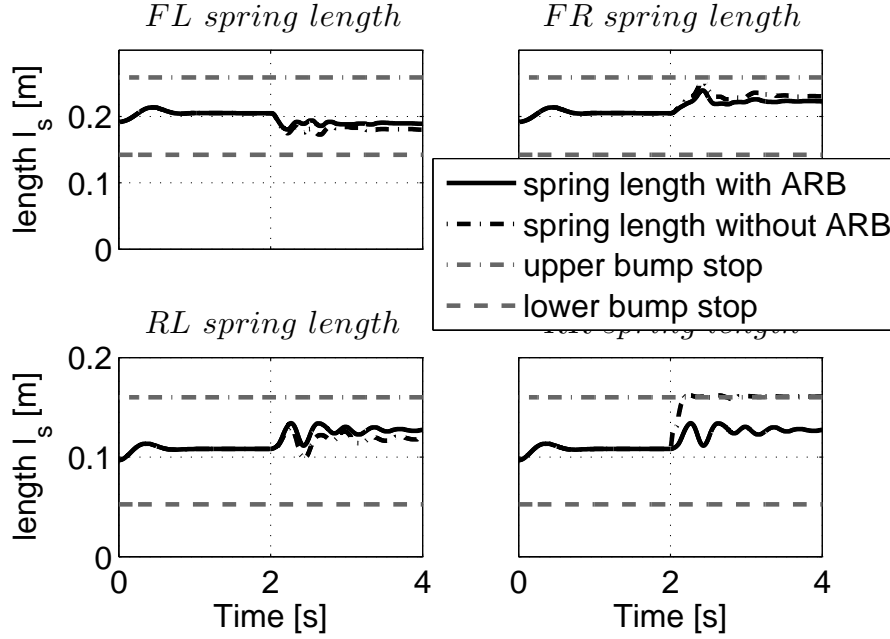


Figure 3.4: Comparison of suspension spring travel for rear right actuation with $F_{ac,RR} = -3750$ N for input ($\delta_{sw} = 0^\circ$, $V_x = 0$ m/s, $T_{step} = 2$ s); front suspension (top row), rear suspension (bottom row).

3.3.2 Vertical force transfer

In its simplest form, the tire is equated to a spring acting between the unsprung mass (suspension system) and the ground. As mentioned in Section 3.2.1, the reference vehicle model uses a Magic Formula tire model at each corner. The lateral force, $F_{y,i}$ developed by the tire is primarily a function of the vertical load, $F_{z,i}$ and the side-slip angle, α_i . Since the active suspension is designed to vary the vertical force in the suspension strut, it is imperative to calculate how efficiently this vertical force is transferred to the tire.

Once again simulations were carried out by actuating a single suspension unit and observing the corresponding change in vertical tire force. The simulation results for the front and rear suspension can be examined in Figure 3.5 (black stems). The low efficiency of transfer of the actuator force to vertical tire force is an elemental observation. The efficiency for the front and the rear suspension remains constant within the bump-stop limits, beyond which efficiency drops as additional force is spent in countering the increased stiffness in the suspension springs.

The front and rear anti-roll bars were removed and the results of the simulation can be observed in Figure 3.5 (grey stems). The absence of the stiff front anti-roll bar allows the front left and front right suspensions to move independently resulting in a higher efficiency of vertical force transfer. In absence of the anti-roll bars, the efficiency of the front suspension falls beyond 1500 N as the increased suspension travel causes the bump-stop limits to be breached much earlier in the range of actuator force. The opposite observation can be made by observing the stem plots for the rear suspension.

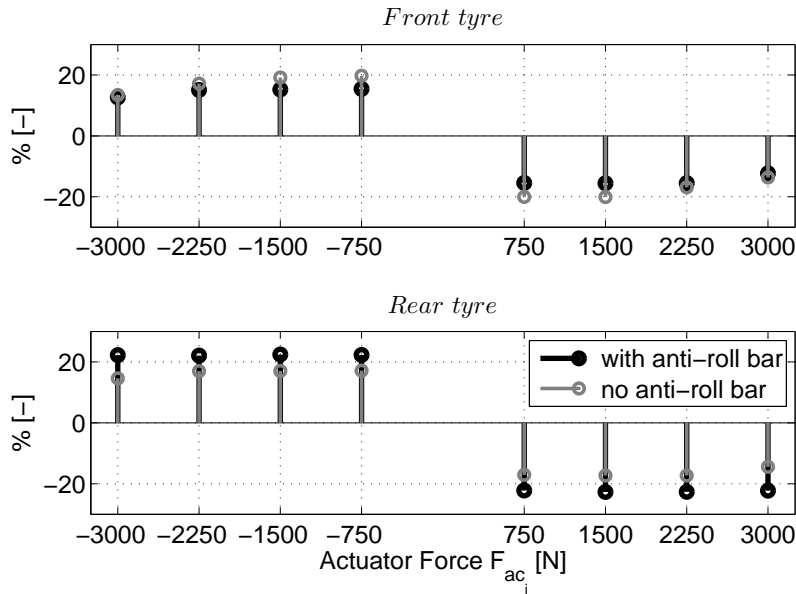


Figure 3.5: Comparison of percentage change in vertical tire force due to suspension actuation for input ($\delta_{sw} = 0^\circ$, $V_x = 0$ m/s); front suspension (top), rear suspension (bottom).

Key Takeaways

The lateral forces generated by the tires play a crucial role in defining the yaw and lateral dynamics of the vehicle. The lateral force generated by tire depends mainly on the vertical tire force and the tire side-slip angle. An active suspension is designed to control the vertical tire force thereby controlling the lateral force that a tire can develop. The simulations performed in Section 3.3.2 help in determining the efficiency of the suspension actuator in varying the vertical tire forces. The simulations show that within the range of the bump-stops the front actuator has an efficiency of 17.5% and the rear actuator has an efficiency of 20%.

3.3.3 Suspension modal analysis and coupling

The effect of a single suspension unit actuation on vertical tire load and suspension spring lengths was covered in Sections 3.3.1 to 3.3.2. In addition to the behavior mentioned in these sections, the suspension units of a vehicle is very intricately coupled with each

other. Any change at one end brings cascades into the other suspension units as well. Thus, extending or compressing one of the suspension springs causes the remaining suspension springs (3 in our case) to compress or extend as well. A proof for this behavior was observed in Section 3.3.1. This in turns cascades into a change in the vertical tire force at each end. Additionally, the movement of the spring also causes the vehicle cabin to change its orientation depending on the strength of the coupling between the suspension units.

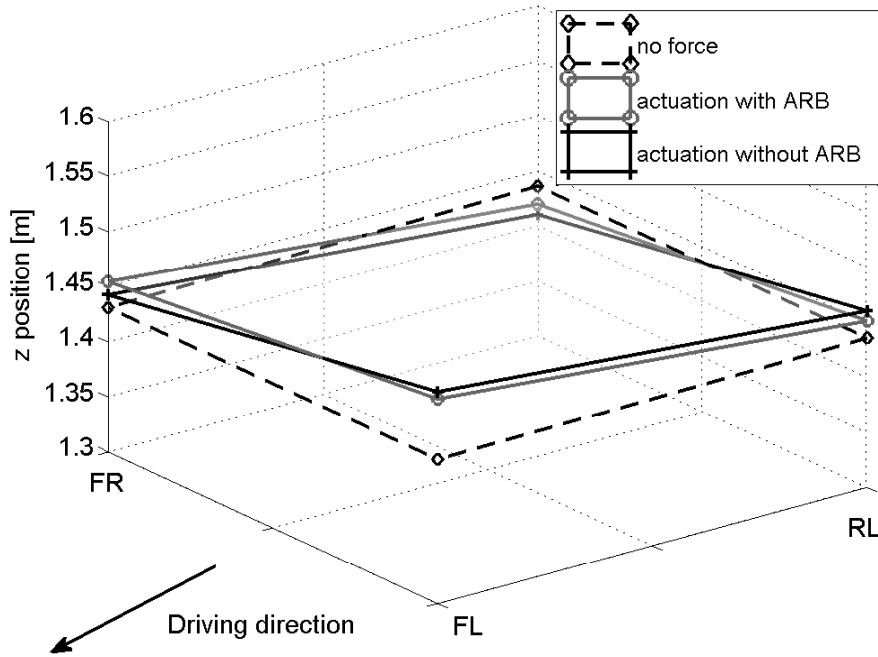


Figure 3.6: z-coordinate of chassis mount points and vehicle body roll-pitch-yaw movement on actuation $F_{ac_{FL}} = -2250$ N for input ($\delta_{sw} = 0^\circ$, $V_x = 0$ m/s).

The complex coupling between the individual suspension units and vehicle body can be seen in Figure 3.6. The compression of a single spring causes all the suspension modes to get activated which results in this convoluted motion of the sprung mass. The actuation of a single wheel causes the vehicle body to perform roll and pitch motion which causes an increase in the tire forces on the diagonally opposite end, see Figures 3.7 and 3.8. As a result to keep the net sum of vertical load to be constant the vertical tire force on the other two corners decreases. One can also observe the influence of the anti-roll bar on the force vertical tire forces and also the orientation of the vehicle body.

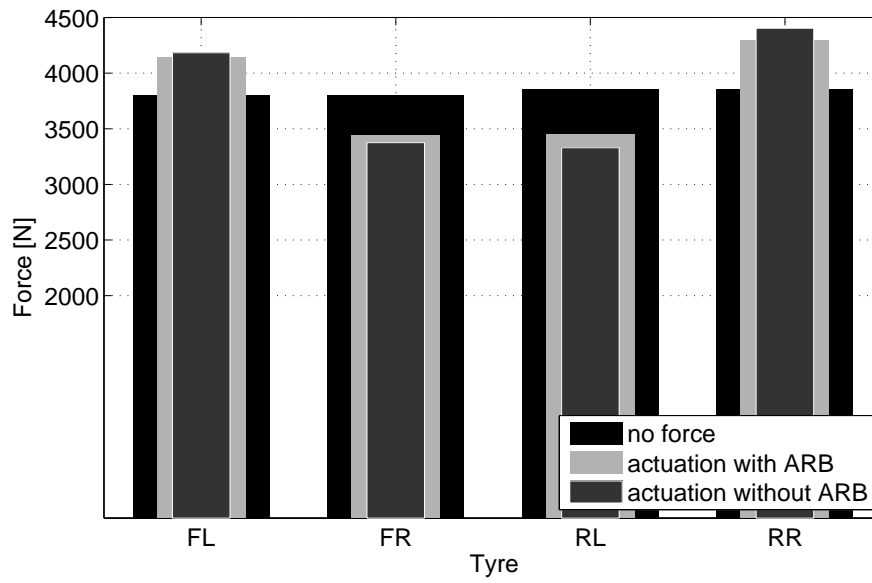


Figure 3.7: Redistribution of vertical tire force on actuation $F_{ac,FL} = -2250$ N for input ($\delta_{sw} = 0^\circ$, $V_x = 0$ m/s).

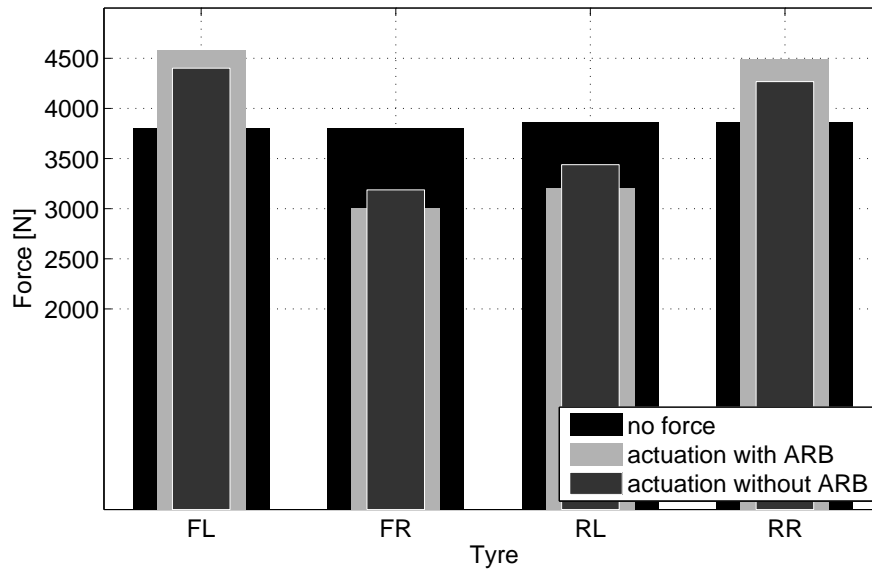


Figure 3.8: Redistribution of vertical tire force on actuation $F_{ac,RR} = -3750$ N for input ($\delta_{sw} = 0^\circ$, $V_x = 0$ m/s).

Key Takeaways

The deep coupling that exists between the four suspension units and the tires was discussed in Section 3.3.3. On the subject of vehicle handling and suspension actuation, a significant insight gained was the effect of actuating one suspension unit on the remaining units. Not only does the actuation cause a change in the vertical tire force of the corresponding tire but due to the coupled nature of the multi-body system the effect can be observed in the remaining tires. Another vital observation that can be made is that the sum total of the vertical tire forces remains constant and thus increasing the vertical force on a tire is bound to decrease the vertical force on some other tire in the suspension.

3.4 Dynamic Analysis

In this section, the multi-body vehicle model is simulated with various steady state cornering maneuvers in open-loop test conditions to gain insight of how an active suspension can change the lateral and yaw dynamics of the vehicle.

3.4.1 Exploring vehicle's stability limits

The importance of ensuring yaw-stability and lateral stability of the vehicle has been discussed in Chapter 2. In this thesis yaw-rate is used as the measure for yaw-stability and vehicle side-slip angle has been used to measure lateral stability. Step steer tests for different combinations of longitudinal speeds, V_x and steering wheel angle, δ_{sw} were simulated to quantify the yaw and lateral stability limits. At any given velocity the simulation was repeated by increasing the step size till the vehicle could no longer maintain the trajectory and experiences loss of yaw stability, lateral stability or both. The behavior of the unstable vehicle can be understood better by observing the yaw-rate vs. vehicle side-slip angle trajectories, see Figure 3.9.

The trajectory corresponding to Test 1 shows that the first instant of instability occurs in the yaw-rate of the vehicle due to the large steering wheel angle provided. One can observe the wobbles that exist in the yaw-rate which escalate into both the yaw-rate and the vehicle side-slip angle to rise out of control. The loss in yaw stability occurs due to the inability of the rear tires to generate the required side force causing the yaw angle of the vehicle to increase inordinately when compared to the steering wheel angle. The relation between yaw-rate and the side-slip angle was stated in (1.4) which explains the subsequent increase in the vehicle side-slip angle.

The trajectory for Test 2 and Test 3 show a different behavior when compared to Test 1. These two trajectories show that there are no oscillations in the yaw-rate of the vehicle instead the vehicle side-slip angle keeps on increasing. This can be visualized as the vehicle sliding away from the apex of the corner. The lateral load transfer during cornering causes the inner tires on the front and rear axle to saturate reducing the lateral force generated by them. This causes a drop in the effective lateral force generated by the axle thereby reducing the net centripetal force of the vehicle. In this way one can conclude that a decrease in the effective lateral force generated by each axle causes lateral instability in the vehicle during cornering.

Key Takeaways

The simulations from Section 3.4.1 show that the vehicle has the tendency to breach the yaw stability limits at low speeds and high steering wheel angle inputs. Conversely, the vehicle experiences a loss in lateral stability at high speeds before the yaw stability limits are approached. Both these phenomenon can be traced to unloading of the inner tires during cornering which causes a decrease in the lateral force developed at each corner of the vehicle. The unloading of the inner tires can be mitigated with an active suspension controller to provide an additional safety net during extreme cornering maneuvers.

The maximum yaw-rate and vehicle side-slip angle achieved during a complete step-steer simulation are cataloged in Table 3.1. These results were used to design the stable boundaries for the vehicle. The maximum yaw rate was set to $|r_{z,max}| = 35^\circ/\text{s}$ and the maximum vehicle side-slip angle was set to $|\beta_{max}| = 4^\circ$. An interesting observation can be made from the lateral acceleration values presented in Table 3.1. One can see that the maximum lateral acceleration that the vehicle can generate at the limit of yaw stability is the same as the maximum lateral acceleration that can be generated at the limit of lateral stability. The close coupling between the yaw-rate, vehicle side-slip angle and lateral acceleration as seen in (1.4) can be used to explain this phenomenon and if required lateral acceleration can be used as a measure to assess both lateral as well as yaw stability of the vehicle.

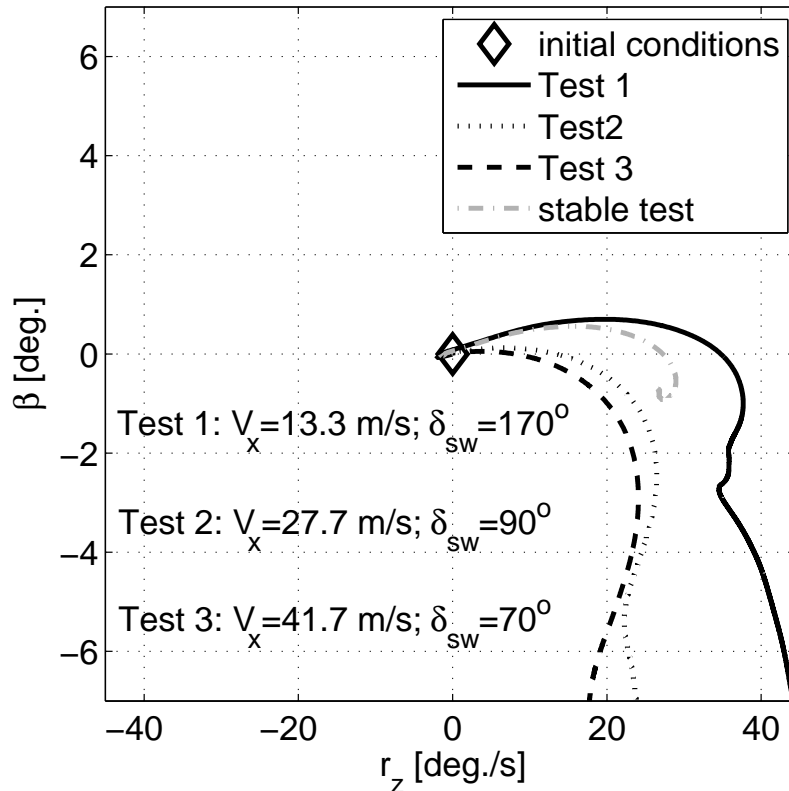


Figure 3.9: State trajectories of unstable vehicle

Table 3.1: Stability limits of BMW 318i: step-steer test

| V_x [m/s] | δ_{sw} [°] | r_z [°/s] | β [°] | a_y [m/s ²] |
|-------------|-------------------|-------------|-------------|---------------------------|
| 13.33 | 160 | 32.51 | -1.672 | 7.879 |
| 27.78 | 80 | 16.29 | -3.946 | 7.879 |
| 41.67 | 65 | 10.8 | -4.265 | 7.8 |

3.4.2 Lateral load transfer

The lateral load transfer occurring at each axle during cornering can be calculated as [34]:

$$\Delta F = \sigma_i m a_y \quad (3.1)$$

where,

$$\sigma_i = \frac{1}{2s_i} \left(\frac{c_{\phi_i} h'}{c_{\phi_1} + c_{\phi_2} - m g h'} + \frac{l - a_i}{l} h_i \right)$$

The validity of (3.1) is examined by plotting the vertical tire forces, $F_{z,i}$ as a function of the lateral acceleration, see Figure 3.10. The load transfer, ΔF can be observed to have a linear relationship with lateral acceleration and on performing a linear fit the coefficients obtained are in close agreement with the theoretical coefficients computed from the vehicle parameters. It is very important to realize that the change in vertical tire forces due to lateral load transfer is much larger in magnitude than what is achieved by suspension actuation. At high levels of lateral acceleration the load transfer is in excess of 2000 N and hence this behavior must be accounted for during the design of the active suspension controller.

3.4.3 Steady-state yaw-velocity gain

In this section simulations were performed to investigate the effect of loading a combination of two wheels during a steady-state corner and observing its effect on the steady-state yaw-velocity gain. The steering angle was chosen such that the reference vehicle does not spin out at any speed during the test and the actuator force, F_{ac} was chosen such that it does not cause any suspension spring to hit the bump-stop. The actuator force was introduced into the system at the upper and lower joints of the suspension springs. Furthermore, the actuator forces were applied on the vehicle once it had attained steady-state cornering condition and the final results obtained once steady state condition was reached once again. The results from the steady-state yaw-velocity gain test are enlisted below, see Figure 3.11:

Key Takeaways

- Like almost all passenger vehicle's the reference vehicle is designed to under-steer and the effect increases at higher lateral acceleration.
- Actuation of the front wheels has almost no effect on the steady-state yaw-velocity gain at low speeds but the understeering nature of the vehicle increases as the forward velocity increases. This is due to the increasing lateral load transfer taking place at the front axle which causes the inner tire to saturate. As a result the front axle is unable to develop lateral force which causes the yaw-rate to decrease.

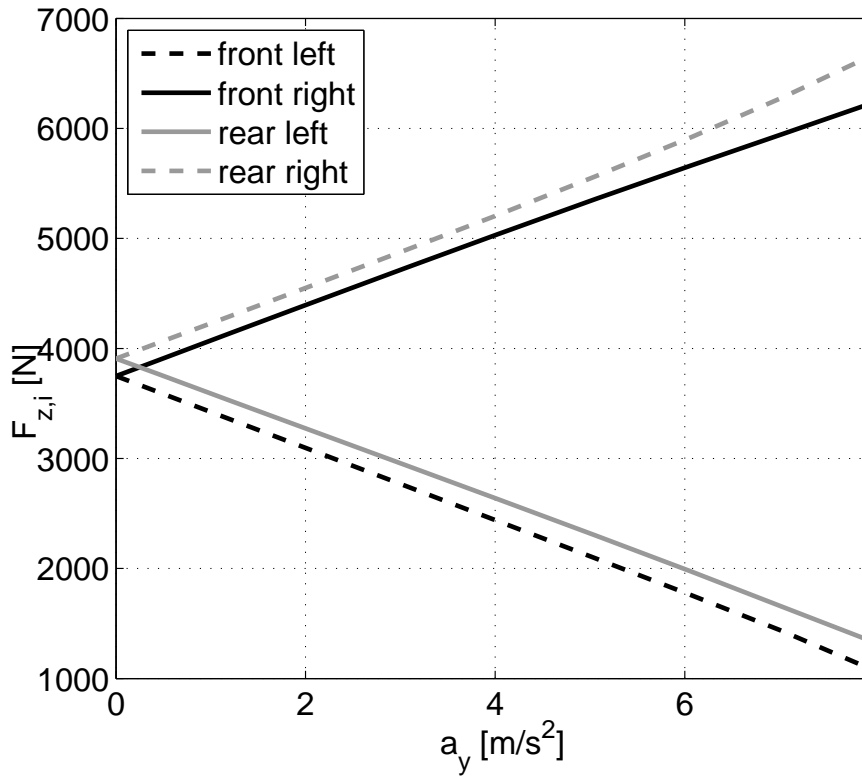


Figure 3.10: Lateral load transfer during cornering

- At velocities up to 25 m/s, actuating the outer wheels makes the vehicle understeer less as compared to the reference vehicle. However, beyond the speed of 25 m/s the actuated vehicle is unable to maintain a steady-state cornering condition. At these increased speeds the vertical force on the rear inner tire approaches zero which causes lift-off at the rear. Subsequently the rear outer tire has to bear with half of the vehicle's weight and thus saturates. This saturation causes the vehicle to lose yaw-stability as the yaw-rate increases beyond the stable limits exhibited in Section 3.4.1.
- The actuation of rear axle can make the vehicle understeer less at speeds up to 25 m/s. Though, beyond this speed the lateral acceleration of the vehicle increases beyond the stability limits as the tires are at the limit of adhesion. This results in the loss of yaw stability for the vehicle.
- Actuation of the inner wheels has the most progressive response as the vehicle under-steers more than the reference vehicle for all velocities, see Figure 3.11. However, as seen in Section 3.3.3 the actuation also has an effect on the cabin roll-pitch-yaw angles. Loading the inner wheels by actuation will be highly detrimental to the ride-comfort of the vehicle as it will also accrue roll movement in the vehicle cabin and cause it to tip even further away from the corner.
- Up to the forward velocity, V_x of about 25 m/s, loading the outer wheels will improve the steering response of the vehicle and also neutralize the inherent roll

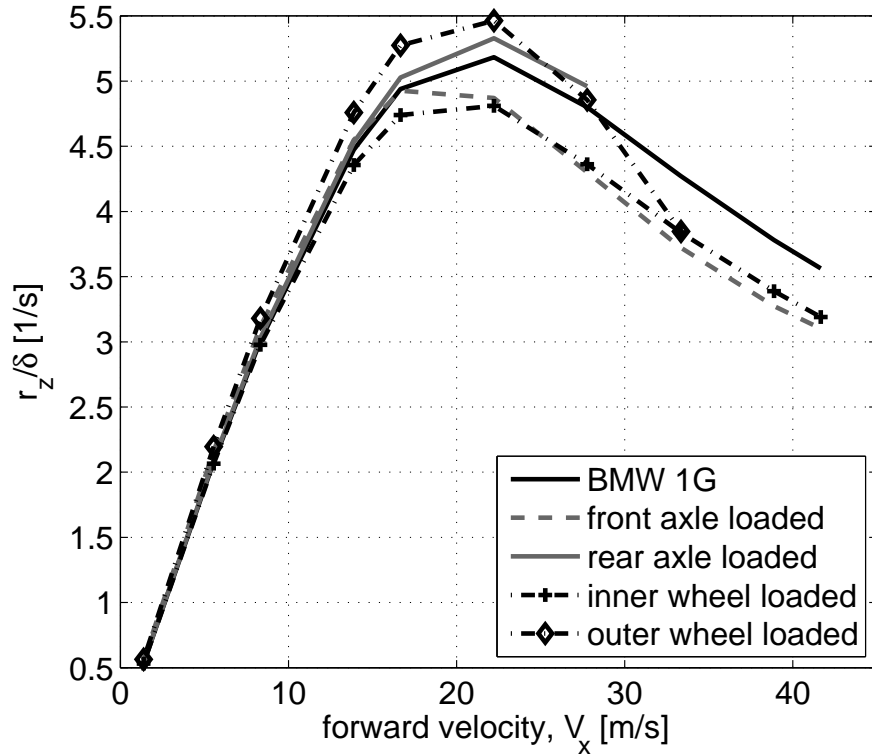


Figure 3.11: Steady-state yaw velocity gain for input ($\delta_{sw} = 55^\circ$, $V_x \in [5, 35]$ m/s).

movement of the vehicle body and seems to be a favorable way of influencing the handling characteristics of the vehicle. The loss in lateral stability at speeds higher than 25 m/s and steering wheel angle greater than 55° has already been demonstrated, see Section 3.4.1. Therefore, at elevated speeds the suspension actuation should attempt to decrease the understeer of the vehicle only within the yaw and lateral stability limits.

- To encapsulate it is fair to conclude that suspension actuation does influence the yaw-rate of the vehicle. A closed loop active suspension can successfully leverage this to alter the understeer/oversteer balance of the vehicle as well as ensure yaw-stability.

3.4.4 Handling diagram

If the side-slip angle of the front axle is more than the side-slip angle of the rear axle the vehicle is classified as an understeering vehicle and conversely if the side-slip angle of front axle is less than the side-slip angle of the rear axle the vehicle is classified as an oversteering vehicle. A handling diagram is used often as an aid to illustrate this handling balance of the vehicle. The results from the steady-state cornering simulation are used to plot the handling diagram of the vehicle under different loading conditions and the results are illustrated in Figure 3.12. Here, α_1 is the mean of the front left and front right tire side-slip angles and α_2 is the mean of the rear left and rear right tire side-slip angles. The observations of the handling diagram in Figure 3.12 are listed below

and can be correlated with the earlier observations from the steady-state yaw-velocity gain plot in Figure 3.11.

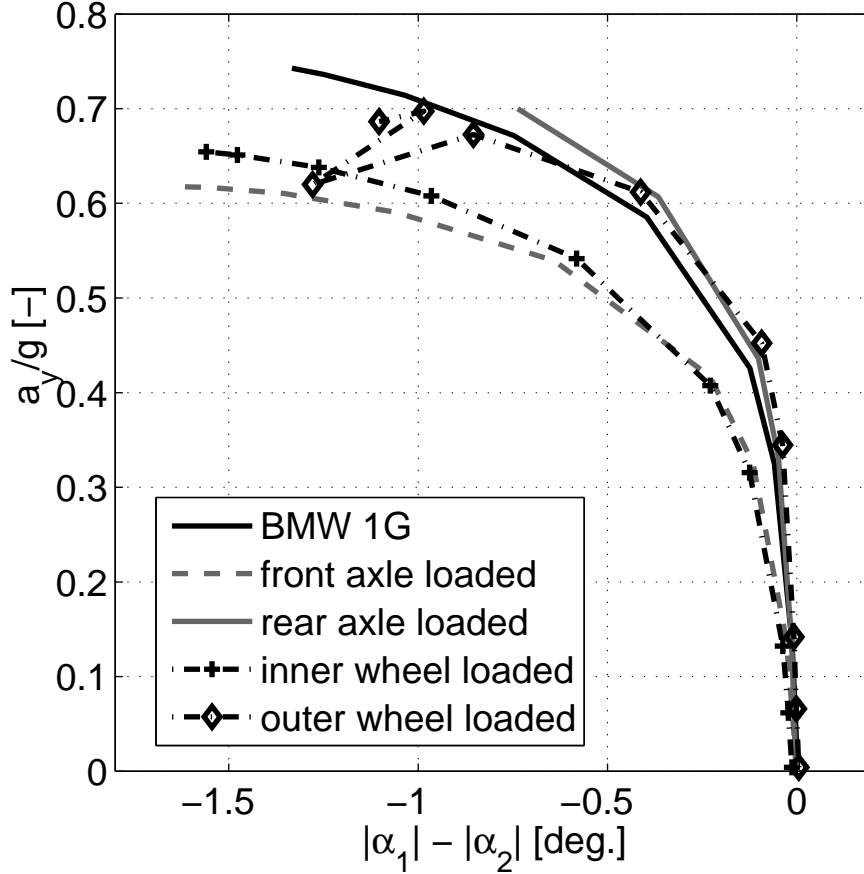


Figure 3.12: Handling diagram for input ($\delta_{sw} = 55^\circ$, $V_x \in [5, 35]$ m/s).

Key Takeaways

- From the simulation inputs one can observe that the vehicle is turning towards the left. Therefore, based on ISO8855 [4] the two axles will develop a negative side-slip angle. Observing the plot-lines in Figure 3.12 one can verify that the front axle generate a larger slip-angle than the rear axle thereby confirming the understeering nature of the vehicle.
- Loading the front axle or the inner wheels causes the vehicle to persistently under-steer more than the reference vehicle.
- Loading outer wheels makes the vehicle under-steer less when compared to the reference vehicle. However this effect is seen only till a lateral acceleration of approximately 0.65g beyond which the vehicle loses yaw stability which gives rise to data that cannot be utilized to study the handling balance of the vehicle.

- Loading the rear axle allows the vehicle to under-steer less than the reference vehicle till $0.7g$ beyond which the lateral forces in the rear tires saturates and the vehicle over-steers out of control.
- These insights can be correlated with the earlier observations from Figure 3.11.
- Linking these observations it can be stated that the changing vertical tire forces has an impact on the handling balance of the vehicle during a cornering maneuver. The ability of the altering the handling balance of the vehicle is a crucial improvements that can be realized by implementing a closed loop active suspension system.

3.4.5 Vehicle side-slip angle

The mathematical equation that defines the relation between lateral acceleration, yaw-rate and vehicle side-slip angle is stated in (1.4). The stability limit results obtained in Table 3.1 also hint towards a coupling between the three signals. In this section the effect of suspension actuation on the relation between lateral acceleration and vehicle side-slip angle will be studied to assess the effect of tire loading and unloading on the lateral dynamics of the vehicle, see Figure 3.13.

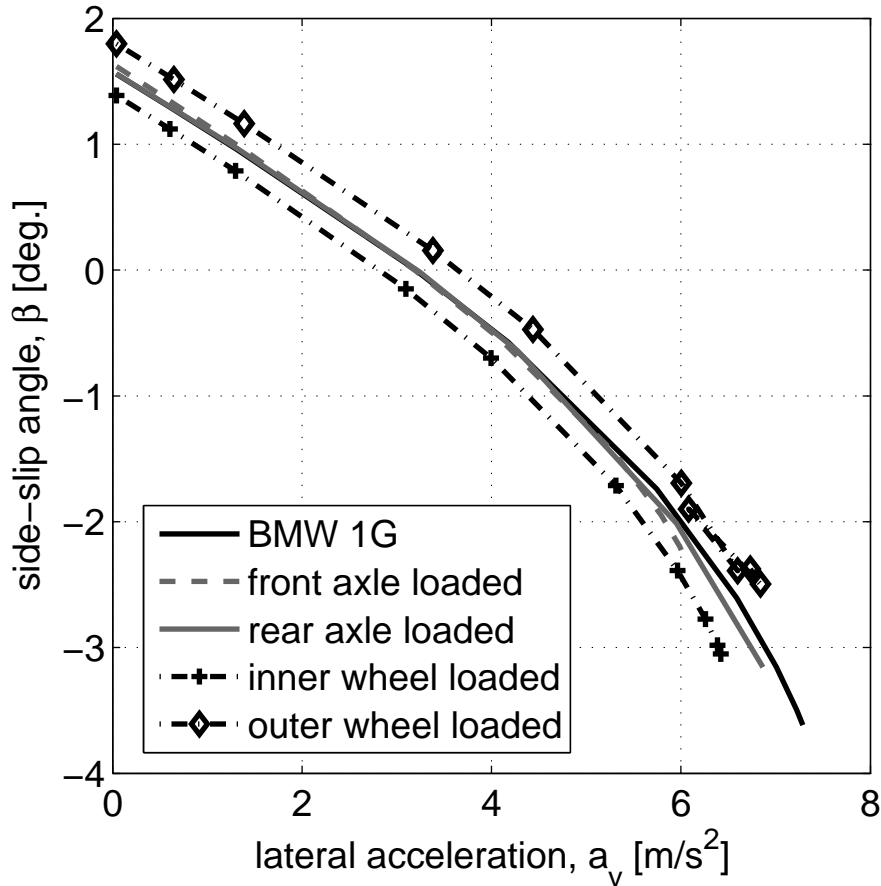


Figure 3.13: Development of vehicle side-slip angle, β as a function of lateral acceleration, a_y for input ($\delta_{sw} = 55^\circ$, $V_x \in [5, 35]$ m/s).

Key Takeaways

- Vehicle side-slip angle scales linearly with lateral acceleration up to approximately 0.4g. The linear relation between the two signals stays regardless of the loading/unloading of the tires.
- Loading the inner wheels consistently makes the vehicle slide more when compared to the reference vehicle. The loading of the inner tires decreases the detrimental effects due to lateral load transfer at each axle. As a result, the inner tires do not saturate allowing the vehicle to develop higher side-slip angle.
- The additional under-steer on loading the front axle was evident from Figure 3.12. This effect can also be confirmed by observing that the vehicle side-slip angle starts increasing compared to the reference vehicle after 0.4g.
- Loading the outer wheels decreases the vehicle side-slip angle up to a certain limit beyond which both the lateral acceleration and vehicle side-slip angle drop back to smaller values, see Figure 3.13. Thus, by combining this observation with the one made from Figure 3.11 one can state that the vehicle cannot achieve maximum yaw-rate and maximum side-slip angle simultaneously and the lateral stability limits of the vehicle are determined by the value of lateral acceleration, see Table 3.1. However, due to an almost linear relationship between lateral acceleration and vehicle side-slip angle one can safely use it to define the lateral stability limits for the vehicle.
- The influence of vertical tire actuation on the lateral dynamics of the vehicle can be corroborated from the observations in this section. It is appropriate to infer that an active suspension setup can aid in improving the yaw as well as lateral dynamics of a vehicle.

3.5 Conclusion

This chapter was dedicated on performing a thorough analysis of the system i.e. BMW 318i SimMechanics™ 1G multi-body model. The reference vehicle and the associated multi-body model were introduced in Section 3.2. The coupling and relation between the suspension components were discussed in Section 3.3. The results from this section helped in determining the limits of suspension actuators and also the efficiency of a suspension actuator at varying the tire force. The coupling between the four tires and suspension units were also studied to understand how actuating a single suspension units influences the vertical forces in the remaining tires. The yaw and lateral stability limits of the vehicle were investigated in Section 3.4.1. The limiting conditions that cause lateral and yaw stability of the vehicle were discussed and simulations were performed to calculate the stable boundary for the vehicle in the (r_z, β) plane. It was established in Section 3.4.3 that altering the tire vertical forces have an influence on the yaw-rate of the vehicle thereby verifying that an active suspension can indeed play a role in enhancing the steering response and yaw-stability of the vehicle. The handling balance of the vehicle can be influenced by altering the vertical tire forces and this was verified in Section 3.4.4. An active suspension systems potential to augment the lateral stability of the vehicle was studied and the simulations performed in Section 3.4.5 ratified this

assumption. The outcomes from the different sections can be combined to conclude that yaw-rate and vehicle side-slip angle provide sufficient insight into the lateral and yaw dynamics of a vehicle i.e. vehicle handling characteristics and that an active suspension setup has the potential to enhance the lateral and yaw dynamics of a vehicle.

CHAPTER 4

Vehicle Model

Less is more.

Ludwig Mies van der Rohe

4.1 Introduction

THE current chapter is dedicated on developing a simplified mathematical model for the BMW 318i. The simulations performed in the previous chapter established the clear link between suspension actuation and two key vehicle handling measures, yaw-rate and vehicle side-slip angle. However, the complex nature of the multi-body model poses a very big challenge for controller design. There is a need for a mathematical model that can accurately capture the tire, yaw and lateral dynamics of the vehicle. Furthermore, if the lateral and yaw dynamics of the vehicle can be expressed in state-space format, it can simplify the process of controller design. In this chapter such a model is derived to accurately capture the lateral and yaw dynamics of the vehicle along with accurate tire dynamics. This vehicle model is then validated against the reference BMW 318i SimMechanics™ 1G model by simulating steady state and dynamic driving maneuvers.

4.2 Proposed Vehicle Model

The literature review performed in Chapter 2 aided in reinforcing the need for an active suspension design for influencing the lateral and yaw dynamics of a vehicle. The ability of vertical tire force actuation to alter the yaw-rate and vehicle side-slip angle was proven in Chapter 3. In this section a mathematical model is proposed that captures the dynamics between tire vertical forces, $F_{z,i}$ tire lateral forces, $F_{y,i}$ tire side-slip angles, α_i along with the yaw and lateral dynamics due to lateral acceleration, vehicle side-slip angle and vehicle yaw-rate. A schematic representation of the top view of a vehicle in Figure 4.1 can be used to derive the model described in this section. A few assumptions and details of the model are enlisted below:

- The model complies to ISO:8855 [4] and all measurements follow this sign convention.

- The small angle approximation is taken for calculating the vehicle side-slip angle.

$$\beta = \tan^{-1} \left(\frac{V_y}{V_x} \right) \approx \frac{V_y}{V_x}.$$
- The vehicle roll axis is not considered in this model.
- This model does not consider the vertical, roll and pitch dynamics of the vehicle.
- The lateral load transfer is modeled however, longitudinal load transfer due to braking is neglected.
- The vertical dynamics of the tires, suspension and vehicle body are not considered in the model.
- The longitudinal tire forces, $F_{x,i}$ are neglected while calculating the yaw-rate and vehicle side-slip angle.
- This mathematical model is still in a nascent stage and hence does not factor in road disturbances. The simulations will be performed assuming the vehicle is running over a smooth and horizontal road surface.

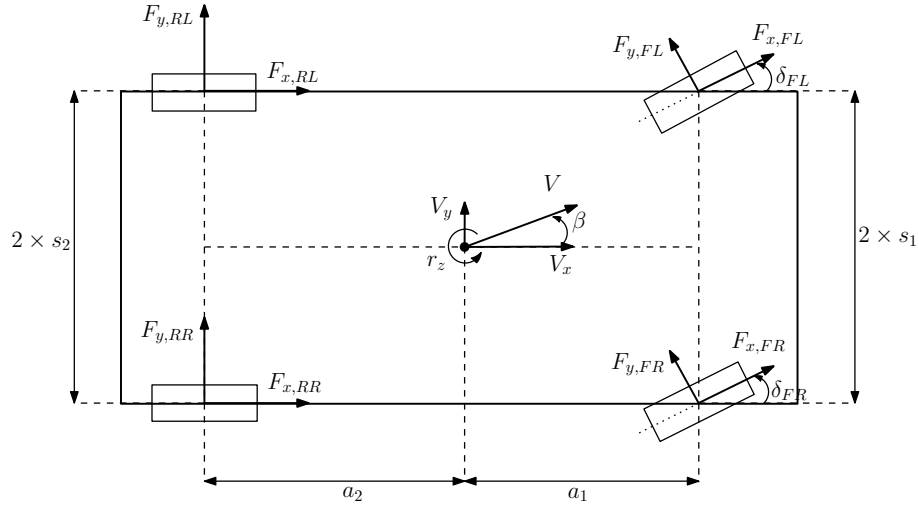


Figure 4.1: Proposed two-track vehicle model

4.2.1 Tire Modeling

The tires form the most complex and nonlinear part of this vehicle model. They are modeled using a simplified form of the TNO-Delft Magic Formula tire model. The Magic Formula function, MF used to model the tire takes the vertical tire force and tire side-slip angle as the input to compute the lateral tire force.

The MF function was validated by comparing it against the *.tir* property files mentioned in Section 3.2. The outcome of this validation test can be observed in Figure 4.2. The inputs provided to both the MF function and the *.tir* property file were: array of side-slip angles in the range $[0, 20]^\circ$ and the static vertical tire force ≈ 3800 N. The

plot show that the *MF* function captures the relation between the vertical tire force and tire side-slip angle accurately. The inclusion of *MF* function to model tire dynamics improves the model accuracy at high lateral acceleration maneuvers.

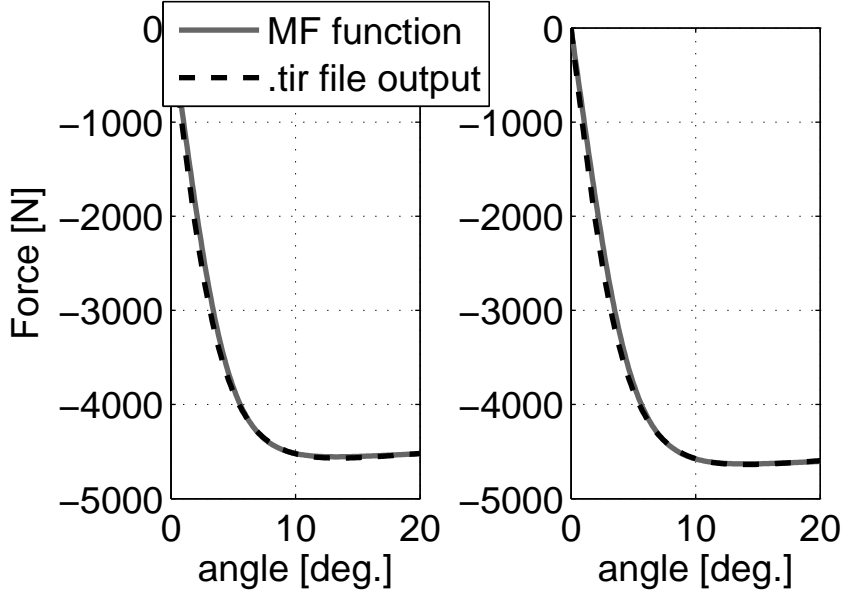


Figure 4.2: Comparison of output from *MF* function and *.tir* property file. front tire (left), rear tire (right)

Wheel slip calculation

The first part of Section 4.2.1 introduced the *MF* formula that will be used to model the tires in the proposed two-track model. In this section the equations used to calculate the individual tire side-slip angle will be stated. The complete mathematical derivation of these equations has been treated in [34] and the final result is stated below.

$$\alpha_{FL} = \tan^{-1} \left(\frac{-(V \sin \beta - r_z s_1) \sin \delta + r_z a_1 \cos \delta}{(V \cos \beta - r_z s_1) \cos \delta - r_z a_1 \sin \delta} \right) \quad (4.1)$$

$$\alpha_{FR} = \tan^{-1} \left(\frac{-(V \sin \beta + r_z s_1) \sin \delta + r_z a_1 \cos \delta}{(V \cos \beta + r_z s_1) \cos \delta - r_z a_1 \sin \delta} \right) \quad (4.2)$$

$$\alpha_{RL} = \tan^{-1} \left(\frac{V \sin \beta - r_z a_2}{V \cos \beta - r_z s_2} \right) \quad (4.3)$$

$$\alpha_{RR} = \tan^{-1} \left(\frac{V \sin \beta - r_z a_2}{V \cos \beta + r_z s_2} \right) \quad (4.4)$$

Vertical tire force

The vertical force on the tire contains a static and a dynamic component. The static component is equal to one half of the weight on the respective axle and the dynamic

component depends on lateral acceleration, suspension actuation etc. The vertical tire force incorporating the load transfer due to lateral acceleration can be stated as:

$$\begin{aligned} F_{z,FL} &= F_{z1,static} - \Delta F_{z,front} \\ F_{z,FR} &= F_{z2,static} + \Delta F_{z,front} \\ F_{z,RL} &= F_{z3,static} - \Delta F_{z,rear} \\ F_{z,RR} &= F_{z4,static} + \Delta F_{z,rear} \end{aligned} \quad (4.5)$$

where,

$$\Delta F = \sigma_i m a_y \quad (4.6)$$

$$\sigma_i = \frac{1}{2s_i} \left(\frac{c_{\phi_i} h'}{c_{\phi_1} + c_{\phi_2} - m g h'} + \frac{l - a_i}{l} h_i \right)$$

Lateral tire force

The two inputs to the MF function were described in the previous sections. These inputs can be plugged into the MF function to calculate the lateral force generate by each tire. This nonlinear relation between vertical tire force, tire side-slip angle and lateral tire force can be expressed as:

$$\begin{aligned} F_{y,FL} &= MF(\alpha_{FL}, F_{z,FL}) \\ F_{y,FR} &= MF(\alpha_{FR}, F_{z,FR}) \\ F_{y,RL} &= MF(\alpha_{RL}, F_{z,RL}) \\ F_{y,RR} &= MF(\alpha_{RR}, F_{z,RR}) \end{aligned} \quad (4.7)$$

Lateral chassis force

The lateral tire forces, $F_{y,i}$ are transmitted to the chassis through the various suspension linkages. If one assumes that the lateral tire forces are transmitted to the vehicle body completely, the chassis forces can be derived as:

$$\begin{aligned} F_{y1} &= F_{y,FL} \cos(\delta_{FL}) \\ F_{y2} &= F_{y,FR} \cos(\delta_{FR}) \\ F_{y3} &= F_{y,RL} \\ F_{y4} &= F_{y,RR} \end{aligned} \quad (4.8)$$

4.2.2 Vehicle body dynamics

The lateral forces acting on the vehicle body can be used to derive the yaw-rate and side-slip angle in a linear state-space representation. The equations of motion are provided below.

$$\begin{aligned} \dot{r}_z &= \frac{1}{I_{zz}} [a_1 (F_{y1} + F_{y2}) - a_2 (F_{y3} + F_{y4})] \\ \dot{\beta} &= \frac{1}{m V_x} [F_{y1} + F_{y2} + F_{y3} + F_{y4}] - r_z \end{aligned} \quad (4.9)$$

Thus, using (4.1) to (4.5) and (4.7) to (4.9) a relationship has been established between the vertical tire force and handling dynamics of the vehicle. The entire model can be laid out with a schematic representation as Figure 4.3. One key observation from Figure 4.3 is that the the entire model can be partitioned into linear and non-linear subparts. The vertical tire-load, tire contact patch velocities and *MF* function block form the nonlinear portion of the model whereas as seen in (4.9) the sprung mass dynamics constitute the linear portion of the system.

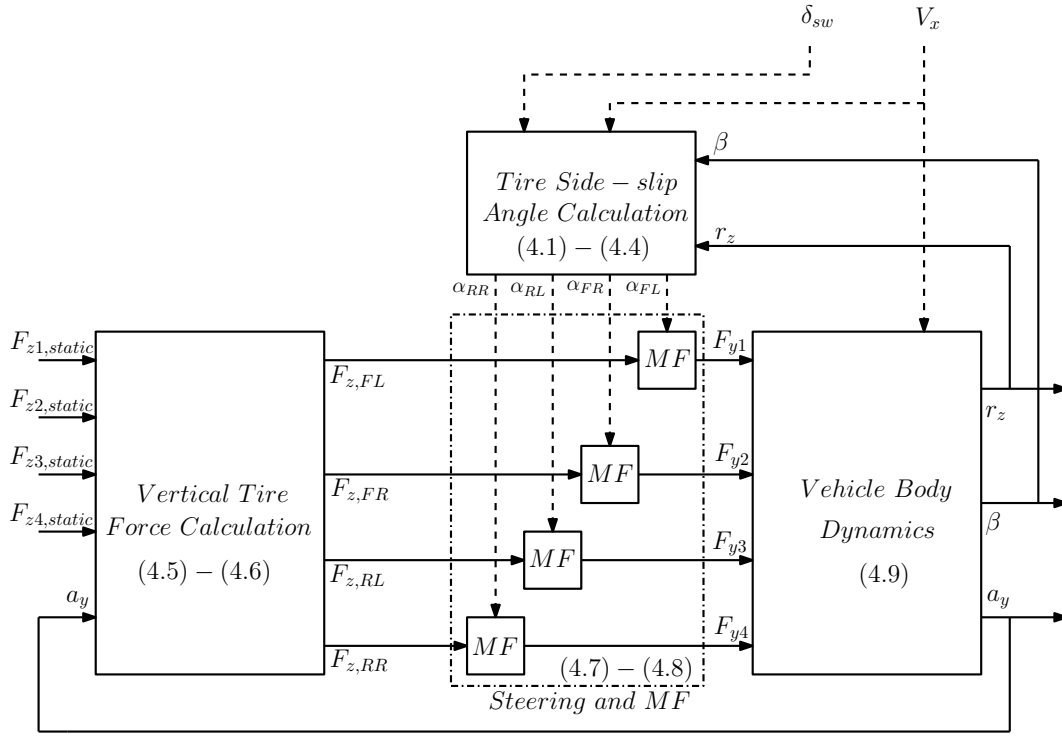


Figure 4.3: Schematic diagram of proposed two track vehicle model

Salient Features

In this section, some noteworthy points regarding the two-track model will be listed down.

- The two track model allows for a mathematical formulation from the vertical tire forces to lateral and yaw dynamics of a vehicle. The inclusion of a Magic Formula based tire model allows for highly accurate behavior a wider range of driving maneuvers at the expense of highly nonlinear mathematical formulation.
- It is possible to segregate the nonlinear and linear dynamics of the two-track model and implementing the scheme in a computational environment.
- Due to its relative simplicity compared to a multi-body model, the computation times are faster by an order of 100.
- The steering wheel angle, longitudinal velocity and the static tire forces form the open-loop inputs to the model.

- The implementation of the model in a software environment has been carried out in such a way that active suspension actuator forces can be introduced in the system as closed-loop inputs.
- The two-track vehicle model does not model the various suspension coupling modes. Hence, a change in vertical force on a tire due to suspension actuation does not cause the remaining three tires to redistribute their vertical forces.

4.3 Model Validation

The first step that is taken after designing or proposing any new model is to validate it against a real world vehicle or another benchmark model. The multi-body vehicle model introduced in Chapter 3 has been validated extensively with a real world vehicle and thus will serve as a reference for all future comparisons. The two-track model is validated for steady state as well as dynamic maneuvers to assess its performance under different driving conditions. The focus of this exercise will be to ascertain that lateral chassis forces which are the output of the nonlinear portion of the model match the signals obtained from the reference multi-body model. Furthermore, the vehicle body dynamics of the two-track model and the reference model will be studied for discrepancies.

4.3.1 Ramp-steer maneuver at $V_x = 13.3$ m/s

One of the key outcomes from the simulations in Sections 3.4.1 and 3.4.3 was that yaw-rate is a very important aspect of vehicle handling at speeds below 25 m/s and that an active suspension has the potential to influence this measure. Since, the two track vehicle model will be the basis for designing the active suspension controller, it is very important that it accurately captures the lateral and yaw dynamics of the vehicle at speeds below 25 m/s.

A ramp-steer driving maneuver is used to test the accuracy of the model at moderate velocities. Both the inputs to the system are provided in open loop conditions to assess performance of the proposed model, see Figures 4.4 and 4.5.

Key Observations

- The simulation input is designed such that both the transient as well as steady-state behavior of the model can be judged.
- The transient as well as steady-state yaw-rate behavior of the two-track model matches the reference model very well, Figure 4.4. Close examination of the plot shows that the proposed model cannot simulate the overshoot in the yaw-rate occurring just after 1 s in the simulation. The transfer function of the two-track model is of order 1 as a result of which it cannot reproduce the overshoot.

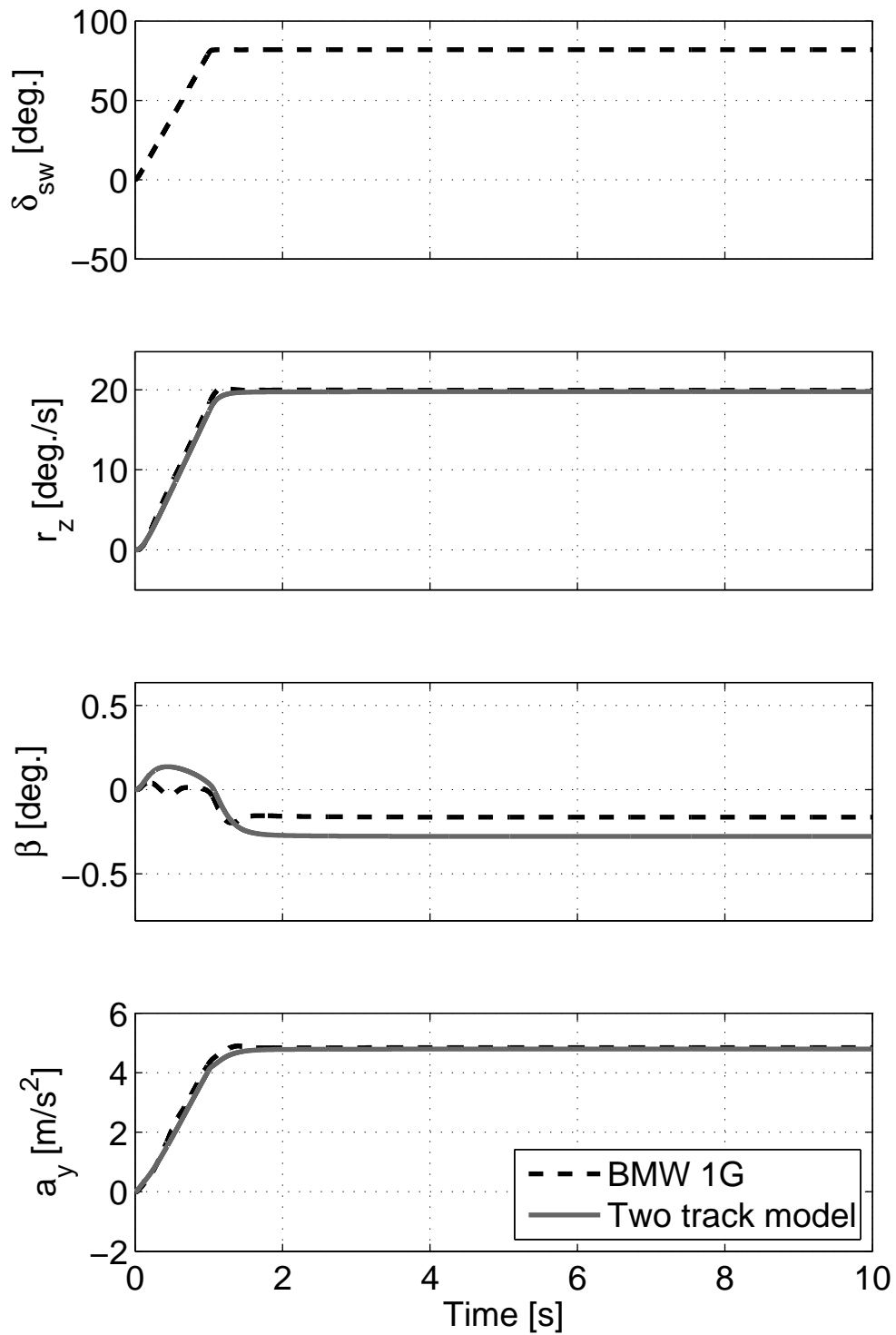


Figure 4.4: Yaw-rate, side-slip angle and lateral acceleration for ramp steer maneuver, ($\delta_{sw} = 85^\circ$, $V_x = 13.3$ m/s).

- The vehicle side-slip angle measurement does not compare appreciably with the reference model. The model shows a larger initial overshoot as well as suffers from a constant steady state error during the steady-state conditions. Furthermore, the two track model fails completely in replicating the oscillations in the vehicle side-slip angle during the first second of the simulation.
- Just like the yaw-rate measurement, the lateral acceleration matches quite well with the reference model during the steady state as well as the transient conditions.
- The output from the nonlinear portions of the two-track model i.e. lateral forces generated by the tire and steering system, match the reference model very well. The error in the inner front tire force can be attributed to the absence of longitudinal load transfer dynamics in the two-track model.

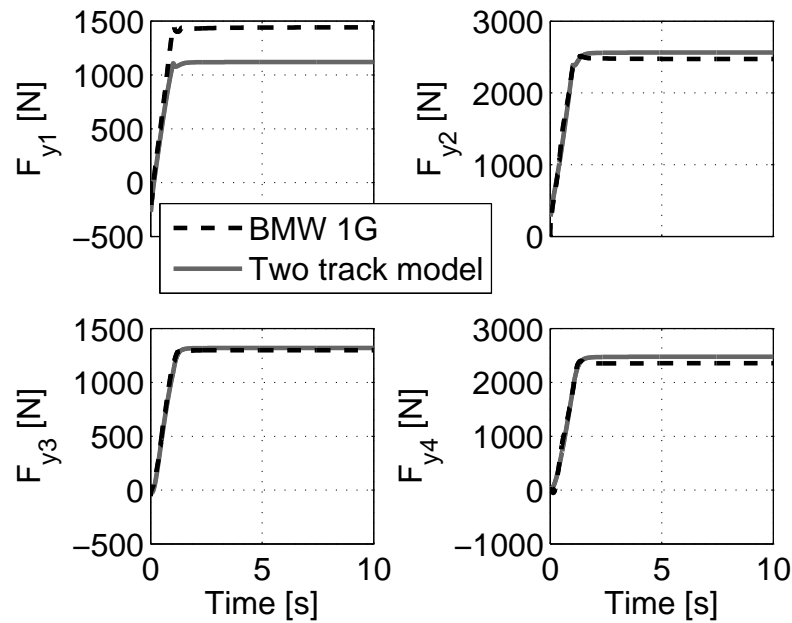


Figure 4.5: Lateral chassis forces for ramp steer maneuver, ($\delta_{sw} = 85^\circ$, $V_x = 13.3$ m/s).

4.3.2 Ramp-steer maneuver at $V_x = 27.7$ m/s

The ramp-steer simulation was repeated for a higher value of longitudinal velocity to critic the performance of the two track model for maneuvers that generate higher vehicle side-slip angles. The results of the simulation are presented in Figures 4.6 and 4.7 and the key observations are enlisted below.

Key Observations

- The transient performance of the model during this simulation is quite poor. All the signals show a large amount of mis-match with the reference model up to a time of 2 s.

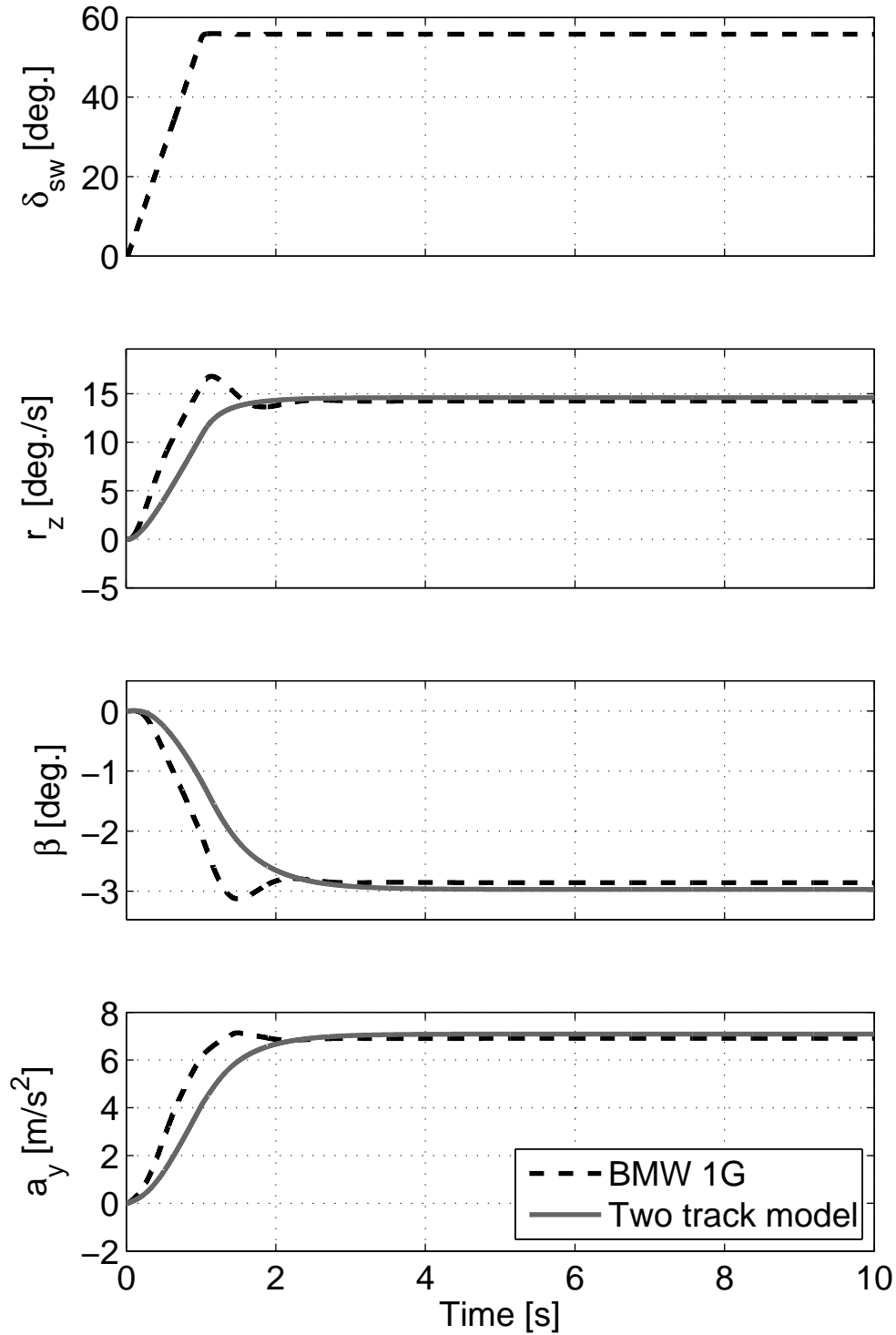


Figure 4.6: Yaw-rate, side-slip angle and lateral acceleration for ramp steer maneuver, ($\delta_{sw} = 55^\circ$, $V_x = 27.7$ m/s).

- The yaw-rate measurement once again fails to reproduce the overshoot at approximately 1 s. Moreover, the rate of increase is also not captured by the proposed model.
- The vehicle side-slip angle plot once again shows a mismatch during the transient part of the maneuver. An encouraging sign is the relatively tiny steady-state error once the transients settle down.
- The relative performance of the lateral acceleration can be judged in the same vein as the yaw-rate measurement. There is poor accuracy during the transient phase but excellent steady-state performance.
- The relative poor performance of the proposed model can also be observed from the lateral force plots, see Figure 4.7. As expected the front left tire forces do not match the references due to the reasons mentioned earlier. Furthermore, there exist small overshoots in the reference model which are not emulated by the proposed model at all. These errors can be attributed to the absence of dynamics that capture the coupling and compliance between the different steering, suspension and tires.

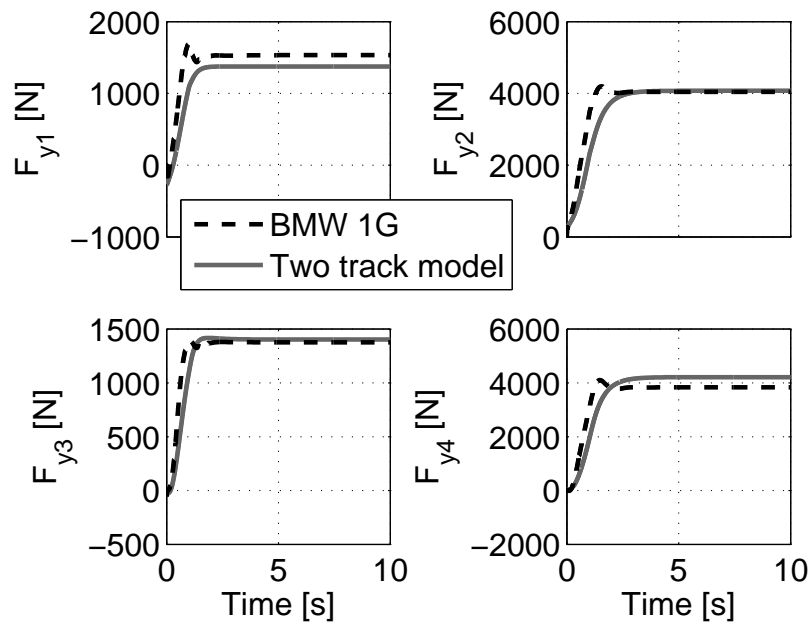


Figure 4.7: Lateral chassis forces for ramp steer maneuver, ($\delta_{sw} = 55^\circ$, $V_x = 27.7$ m/s).

4.3.3 Double step-steer

The driving maneuvers in Sections 4.3.1 and 4.3.2 helped in investigating the performance of the proposed two track model in a mixture of transient and steady-state conditions. On the other hand, the double step-steer maneuver is a completely dynamic test that can be used to evaluate the performance of a vehicle model in vigorous simulation conditions. The double step-steer test can be thought of as a simulation that imitates an

evasive maneuver performed by a driver. The results of the simulation test are presented in Figures 4.8 and 4.9.

Key Observations

- The proposed two track model once again achieves yaw-rate dynamics which match the reference model extremely well. The inability to produce the overshoot is evident once again. However, the remaining trajectory replicates the multi-body model to a very high degree.
- As expected, the vehicle side-slip angle generated by the two-track model is unable to match the reference model signal. The initial response at 1 s follows the reference model but the amplitude of this overshoot does not match the reference trajectory. Additionally, the proposed model fails to replicate the rebound and overshoot that is present in the multi-body model. Thus, it is safe to say that the vehicle side-slip angle measurement from the proposed model cannot be trusted during such dynamic maneuvers.
- Once again the two-track model accomplishes well with the lateral acceleration measurement. The simulation results show that the small kink just after 1 s is captured by the model but it is unable to account for the overshoot that occurs at the end of the step. Apart from failing to capture the overshoot, the proposed vehicle model matches the reference multi-body model extremely well.
- By observing the lateral forces in Figure 4.9 one can examine that the model once again performs well at capturing a majority of the dynamics from the multi-body model. However, the error in the inner front tire force and lack of overshoot are evident even in this simulation test.

4.3.4 Key takeaways

The performance of the proposed two-track model was scrutinized by simulating three driving maneuvers that provided a mixture of dynamic and steady-state conditions, see Sections 4.3.1 to 4.3.3. The results from the simulation were then validated against the benchmark multi-body model and the performance of the model was discussed in each section. The most important outcomes from the validation tests are listed below.

- The proposed two track model can capture most of the dynamic as well as steady state yaw-rate dynamics of the vehicle at speeds in the range of 13.3 m/s. Tests similar to Section 4.3.1 can be used study the steering response as well as yaw-stability of the vehicle whereas the simulation presented in Section 4.3.3 can be applied to study the steering response of the vehicle.
- The proposed vehicle model is unable to account for the transient dynamics during high speed maneuvers but provides excellent steady-state performance, see Section 4.3.2. Keeping in mind that the lateral stability is the limiting factor at such high speeds, the two-track model can be used to design active suspension controller that improves the lateral stability of the vehicle during steady-state conditions.

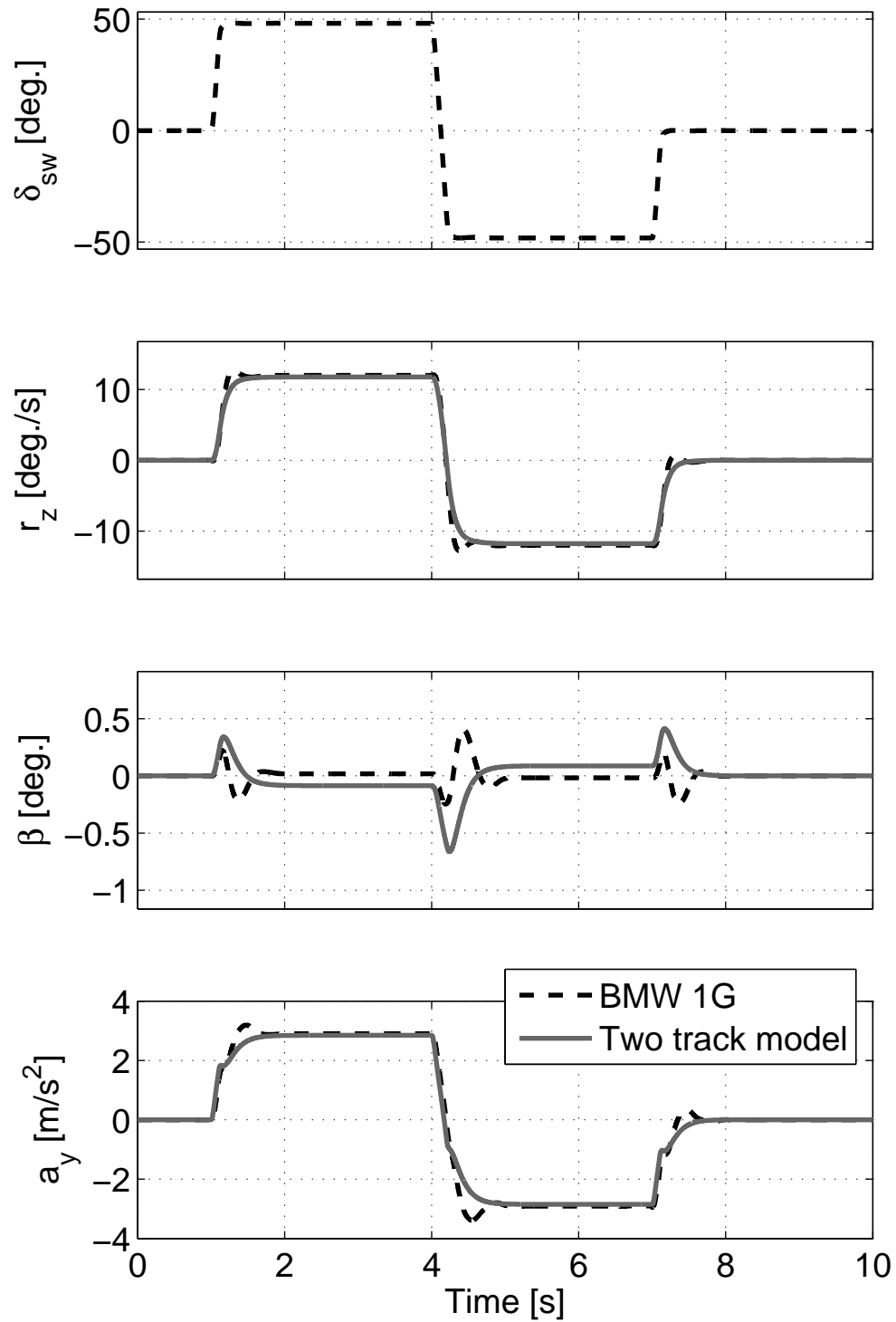


Figure 4.8: Yaw-rate, side-slip angle, lateral acceleration for double step steer, ($\delta_{sw} = 50^\circ$, $V_x = 13.3$ m/s).

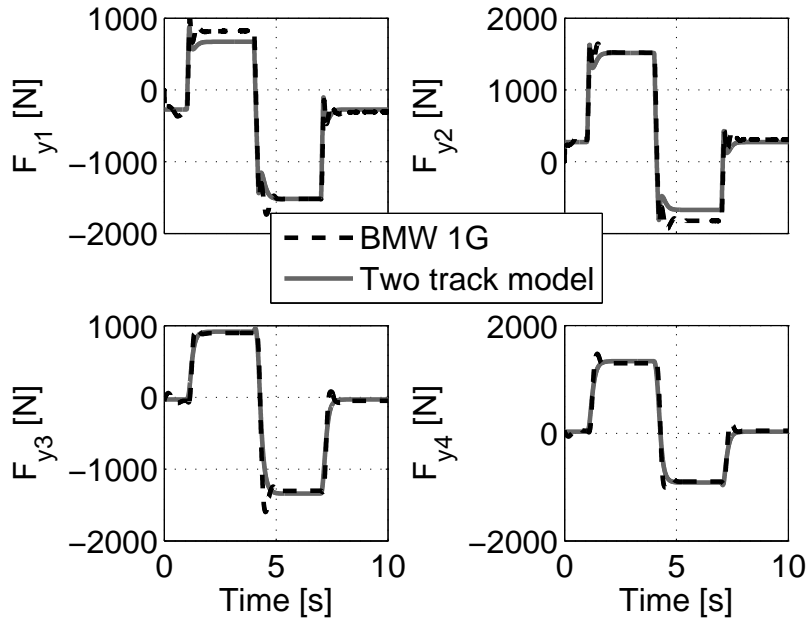


Figure 4.9: Lateral chassis forces for double step steer, ($\delta_{sw} = 50^\circ$, $V_x = 13.3$ m/s).

4.4 Conclusion

In this chapter a mathematical model that provides a relationship between the vertical tire forces and yaw and lateral dynamics of the vehicle was proposed and derived. The model incorporated a simplified form of magic formula tire model to improve the model behavior during extreme cornering maneuvers. A schematic representation of the proposed model was provided and also a convenient method of segregating it into linear and nonlinear subparts was illustrated. The proposed model was validated against the benchmark multi-body model and the obtained results were discussed in detail. An upshot was the realization that the model could be used for designing an active suspension controller and also that the simulation tests used in this chapter could also aid in performing handling assessments for transient as well as steady-state maneuvers.

CHAPTER 5

Controller Design

Design is a plan for arranging elements in such a way as best to accomplish a particular purpose.

Charles Eames

5.1 Introduction

THE ability of an active suspension system to alter the handling characteristics of a vehicle has been mentioned and illustrated multiple times during this thesis. There have also been open-loop simulations to corroborate the fact. As mentioned previously, active suspension systems can be classified into two broad categories; slow active suspensions and fully active suspensions, see Figure 1.1. In this chapter a low bandwidth slow active suspension controller and a high bandwidth fully active suspension controller will be designed using typical frequency domain based methods. The open-loop dynamics of the two systems will be studied in detail to gain a better understanding of expected behavior and estimate the closed loop performance.

Since, the controlles have to be designed for the lateral and yaw dynamics of the vehicle there is a need for a procedure to translate the requested lateral forces into appropriate suspension actuator forces. An algorithm that dynamically inverts the tire Magic Formula has been developed and proposed. The details for this algorithm have been shared and its implementation has been looked in further detail. The development of this algorithm also enabled the closed-loop implementation of the active suspension setup in a vehicle model this has been explained further by means of schematic illustrations. The slow active suspension and the fast active suspension system were then implemented in a closed-loop environment with a vehicle model to investigate their performance at enhancing the handling characteristics of a vehicle.

5.2 Vehicle Model

The linear dynamics of the vehicle derived in Section 4.2.2 are used for designing two active suspension controllers as explained in Section 5.1. To recall, the yaw and lateral

equations of motions are restated.

$$\begin{aligned}\dot{r}_z &= \frac{1}{I_{zz}} [a_1 (F_{y1} + F_{y2}) - a_2 (F_{y3} + F_{y4})] \\ \dot{\beta} &= \frac{1}{mV_x} [F_{y1} + F_{y2} + F_{y3} + F_{y4}] - r_z\end{aligned}\quad (5.1)$$

Defining $y_p = [r_z, \beta]^T$ as the output to the system, the system can be rewritten in a transfer function form as:

$$\begin{bmatrix} r_z \\ \beta \end{bmatrix} = G \begin{bmatrix} F_{y1} \\ F_{y2} \\ F_{y3} \\ F_{y4} \end{bmatrix}\quad (5.2)$$

where G represents the transfer function between the inputs, $[F_{y1}, F_{y2}, F_{y3}, F_{y4}]^T$ and outputs, $[r_z, \beta]^T$. The active suspension controllers will be designed to control the yaw-rate and the vehicle side-slip angle. The frequency domain realization of this four input two output, (4I2O) transfer function can be seen in Figure 5.1.

Note: (5.1) shows that the vehicle side-slip angle dynamics are a function of the longitudinal velocity of the vehicle. For simplicity and clarity the longitudinal velocity is assumed constant. $V_x = 27.7$ m/s for the remainder of this chapter.

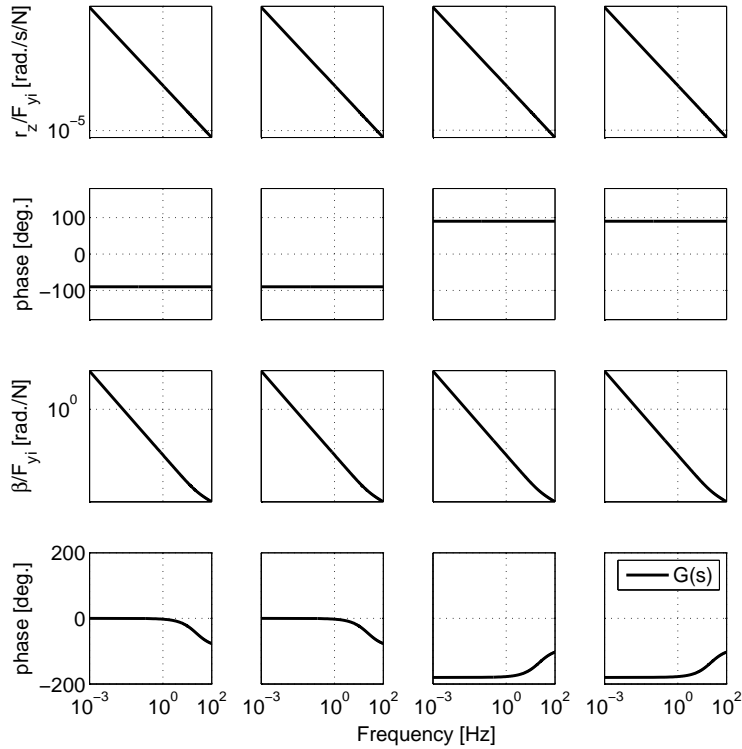


Figure 5.1: Frequency response function $G(s)$.

Key Takeaways

- The 4I2O transfer function description in (5.2) presents a resilient problem as the active suspension controller needs to be designed such that each actuator can influence both; the yaw-rate and the vehicle side-slip angle.
- A possible solution is to define two virtual inputs which are functions of the four lateral forces. Transforming the 4I2O system to a 2I2O system will provide the flexibility to form input output pairs which can be used to create decoupled controllers.
- The net lateral force on the front axle, $F_{y,axle1} = F_{y1} + F_{y2}$ and net lateral force on the rear axle, $F_{y,axle2} = F_{y3} + F_{y4}$ are a set of possible virtual inputs. However defining such inputs will necessitate that suspension actuators on one axle will be used to control yaw-rate and the suspension actuators on the remaining axle will be used to control the vehicle side-slip angle. From Figure 5.1 one can observe that the front axle and the rear axle contribute similarly towards the yaw-rate and a similar inference can be made regarding the contribution of lateral axle forces on the side-slip angle. Hence creating such input-output pairs is not advisable.
- Torque about z-axis, T_z and net lateral force, $F_{y,net}$ provide another set of possible virtual inputs. These virtual inputs can be expressed as a linear function of all the four lateral forces. Moreover, the notion of controlling yaw-rate with a torque input and side-slip with net force presents a natural and logical choice to simplify this MIMO control problem.

5.2.1 Input Transformation

As discussed above, two virtual inputs, torque about z-axis, T_z and net lateral force, $F_{y,net}$ are defined. The virtual inputs can be written as a linear combination of the four lateral forces and the equations are provided below.

$$T_z = a_1(F_{y1} + F_{y2}) - a_2(F_{y3} + F_{y4}) \quad (5.3)$$

$$F_{y,net} = F_{y1} + F_{y2} + F_{y3} + F_{y4} \quad (5.4)$$

(5.3) and (5.4) can also be represented in a matrix format as given below.

$$\begin{bmatrix} T_z \\ F_{y,net} \end{bmatrix} = \begin{bmatrix} a_1 & a_1 & -a_2 & -a_2 \\ 1 & 1 & 1 & 1 \end{bmatrix} \begin{bmatrix} F_{y1} \\ F_{y2} \\ F_{y3} \\ F_{y4} \end{bmatrix} \quad (5.5)$$

The matrix that maps the transformation between the virtual inputs and lateral forces is non-square and thus non-invertible. However, a Moore-Penrose pseudo inverse of this matrix can be calculated to define a static coupling matrix between the virtual inputs and the individual tire lateral forces. The static input decoupling matrix is represented as T_u and has dimensions $\mathbb{R}^{4 \times 2}$. The equation for the static coupling matrix T_u is provided below.

$$T_u = pinv \left(\begin{bmatrix} a_1 & a_1 & -a_2 & -a_2 \\ 1 & 1 & 1 & 1 \end{bmatrix} \right) \quad (5.6)$$

where, *pinv* stands for moore-penrose inverse

Overloading the $^{-1}$ operator to include the moore-penrose inverse one can simplify (5.5) to the equation given below.

$$\begin{bmatrix} T_z \\ F_{y,net} \end{bmatrix} = T_u^{-1} \begin{bmatrix} F_{y1} \\ F_{y2} \\ F_{y3} \\ F_{y4} \end{bmatrix} \quad (5.7)$$

Using the result from (5.7) in (5.2) the system can be expressed in the transfer function form stated below.

$$\begin{bmatrix} r_z \\ \beta \end{bmatrix} = GT_u \begin{bmatrix} T_z \\ F_{y,net} \end{bmatrix} \quad (5.8)$$

Using (5.8) to designate a new transfer function $G_{dc}(s)$ which is defined below.

$$G_{dc}(s) = G(s)T_u \quad (5.9)$$

Thus (5.8) and (5.9) can be used to arrive at a new 2I2O transfer function representation of the system described in (5.1). The transfer function between the outputs and virtual inputs can be stated as:

$$\begin{bmatrix} r_z \\ \beta \end{bmatrix} = G_{dc} \begin{bmatrix} T_z \\ F_{y,net} \end{bmatrix} \quad (5.10)$$

The frequency response plot for the transfer function presented above can be observed in Figure 5.2 and some of the important observations are stated below.

Key Takeaways

- The transfer function from T_z to r_z is very similar to a transfer function of a pure integrator. A similar observation can be made for the transfer function between $F_{y,net}$ and β .
- The virtual input $F_{y,net}$ is almost completely decoupled from the output r_z as can be seen from the extremely low magnitude gain. However, the input T_z has a considerable effect on the output β . Keeping this in mind, it is safe to expect the control input due to T_z to have a considerable effect on the vehicle side-slip angle.
- To sum up, a yaw-rate controller will be designed from the transfer function $G_{dc}(1,1)(s)$ and a side-slip controller will be designed from the transfer function $G_{dc}(2,2)(s)$.

5.3 Controller bandwidth selection

One of the primary goals of this thesis is to investigate the influence of control bandwidth on the effectiveness of an active suspension. Therefore, the decision to design a slow active suspension controller and a fully active suspension controller was made. In [1], it was shown that there exists a resonance at a frequency close to 1 Hz in the frequency response function from steering wheel angle, δ_{sw} to yaw-rate, r_z . This phenomenon was confirmed by obtaining the yaw-rate response to step-steer input

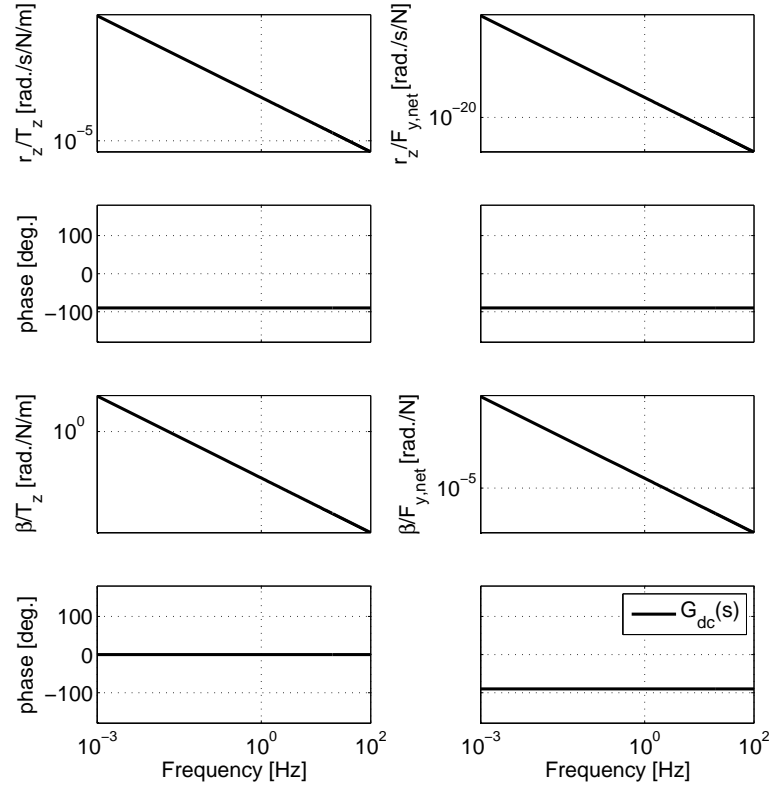


Figure 5.2: Bode plot of transfer function $G_{dc}(s)$.

across a range of longitudinal velocities. The results from this simulation are provided in Figure 5.3. The low frequency yaw-rate response to steering wheel input varies greatly with longitudinal velocity. Furthermore, biggest variation in the yaw-rate response is exists in the location and height of resonance peak. One can observe that the peak shifts upwards with increasing velocity and at the same time the location of the resonance shifts from 1.1 Hz to 0.8 Hz.

A significant portion of this thesis is related to improving vehicle handling by controlling the yaw-rate of the vehicle, it is imperative that the discussions above play a role in deciding the bandwidth of the slow-active suspension system. The open-loop bandwidth of the slow active suspension controller is chosen to be 1 Hz. This control bandwidth will be used for both; yaw-rate control and side-slip control. This will allow for a study to realize the potential of an active suspension at controlling these resonance peaks in the yaw-rate response of the vehicle.

To perform a meaningful assessment of the influence of bandwidth on the performance of an active suspension setup it is necessary to design a high bandwidth system that can represent the potential benefits of such a system. The open-loop bandwidth of the fully active system is chosen to be 30 Hz.

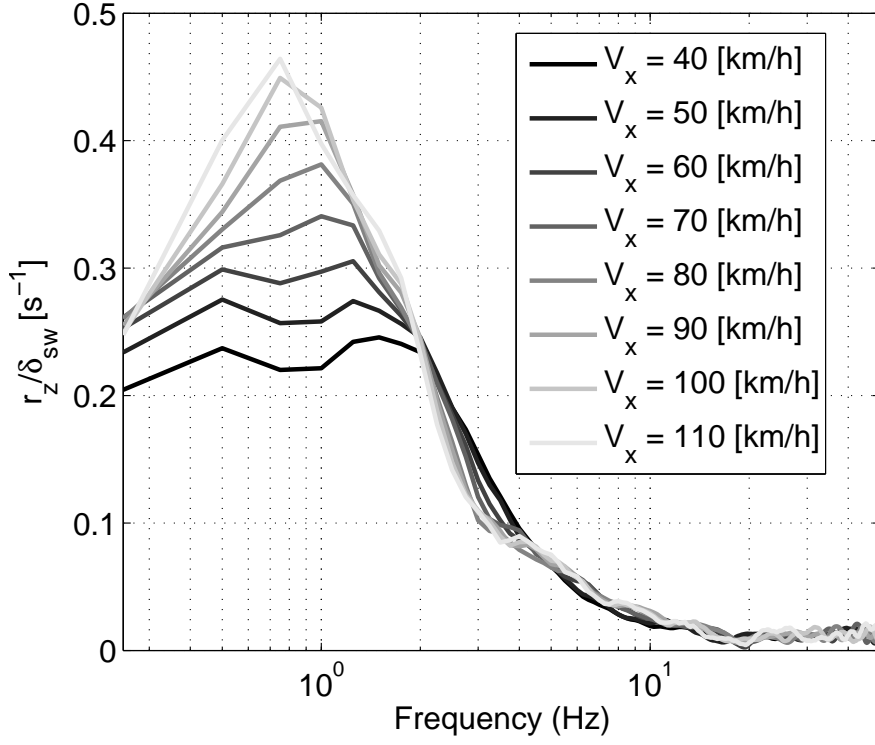


Figure 5.3: Yaw-rate, r_z response for step input on steering wheel, ($\delta_{sw} = 55^\circ$).

5.4 Slow active suspension control

The design of the low bandwidth slow active suspension will be discussed in the section. It can be observed that the transfer functions, $G_{dc}(1,1)(s)$ and $G_{dc}(2,2)(s)$ in Figure 5.2 resemble a pure integrators. The general equation for the controller that is designed for this transfer function can be stated as

$$K_{sa,i}(s) = (K_P + K_V s) F(s) \quad (5.11)$$

where,

$$F(s) = \frac{\omega^2}{s^2 + 2\omega\zeta s + \omega^2} \quad (5.12)$$

In (5.11), K_P and K_V are static controller specific gains whereas $F(s)$ is a second order low-pass filter. Here, the physical significance of the low-pass filter in (5.12) can be equated to the dynamics of a suspension actuator [35]. The actuators responsible for controlling the yaw-rate and the vehicle side-slip angle are the same and therefore the r_z controller and the β controller will incorporate the same actuator dynamics. The differences in the two controllers can be observed in the distinct static gains.

Yaw-rate (r_z) control

The arguments provided in the section above were used to design the r_z controller for a slow active suspension. The transfer function describing the controller is provided

below.

$$K_{sa,r_z}(s) = (K_{P,sa,r_z} + K_{V,sa,r_z} s) F_{sa}(s) \quad (5.13)$$

Side-slip (β) control

The transfer function describing the β controller of the slow active suspension is given below.

$$K_{sa,\beta}(s) = (K_{P,sa,\beta} + K_{V,sa,\beta} s) F_{sa}(s) \quad (5.14)$$

Note: One must observe that the control transfer functions in (5.13) and (5.14) incorporate identical actuator dynamics which can be stated as

$$F_{sa}(s) = \frac{\omega_{sa}^2}{s^2 + 2\omega_{sa}\zeta_{sa}s + \omega_{sa}^2} \quad (5.15)$$

5.5 Fully active suspension control

An approach similar to the one discussed in the section above is undertaken to design the fully active suspension controllers. The general structure provided in (5.11) is used to once again depict the controller and actuator dynamics.

Yaw-rate (r_z) control

The transfer function providing the structure of the r_z controller for the fully active suspension are given below.

$$K_{fa,r_z}(s) = (K_{P,fa,r_z} + K_{V,fa,r_z} s) F_{fa}(s) \quad (5.16)$$

Side-slip (β) control

The transfer function describing the β controller can be examined below.

$$K_{fa,\beta}(s) = (K_{P,fa,\beta} + K_{V,fa,\beta} s) F_{fa}(s) \quad (5.17)$$

Note: The actuator dynamics of the fully active suspension can be written as:

$$F_{fa}(s) = \frac{\omega_{fa}^2}{s^2 + 2\omega_{fa}\zeta_{fa}s + \omega_{fa}^2} \quad (5.18)$$

5.6 Key observations: open-loop dynamics

In this section the open-loop dynamics of the slow-active and the fully active suspensions will be compared to get a better understanding of their differences and similarities. The open-loop dynamics of the r_z controllers are illustrated in Figure 5.4 and the open-loop dynamics of the β controllers are illustrated in Figure 5.5. Some of the key takeaways are listed below.

- The open-loop bandwidth of the slow active r_z controller is 1 Hz and open-loop bandwidth of the fully active r_z controller is 30 Hz, see Figure 5.4.

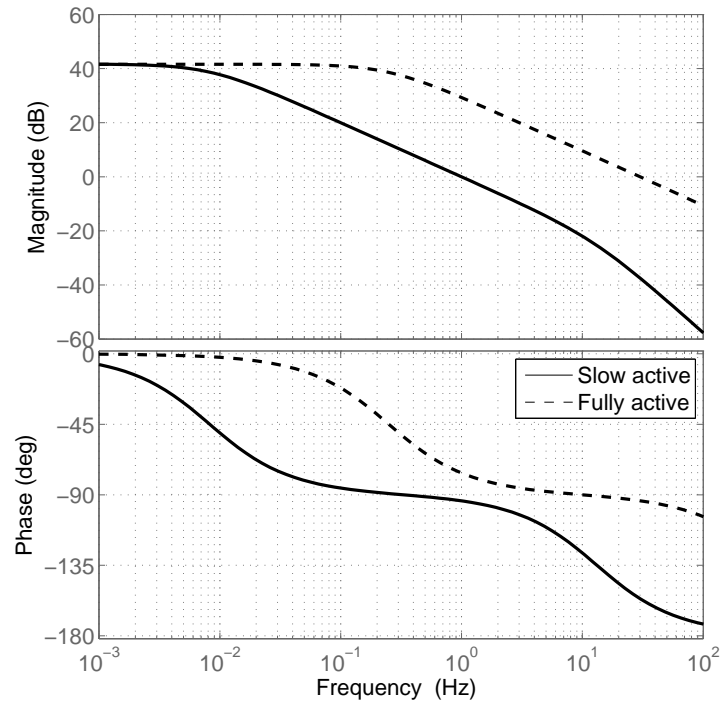


Figure 5.4: Transfer function, from input, $error_{r_z}$ to output, r_z ; $G_{dc}(1,1)(s)K_{i,r_z}(s)$.

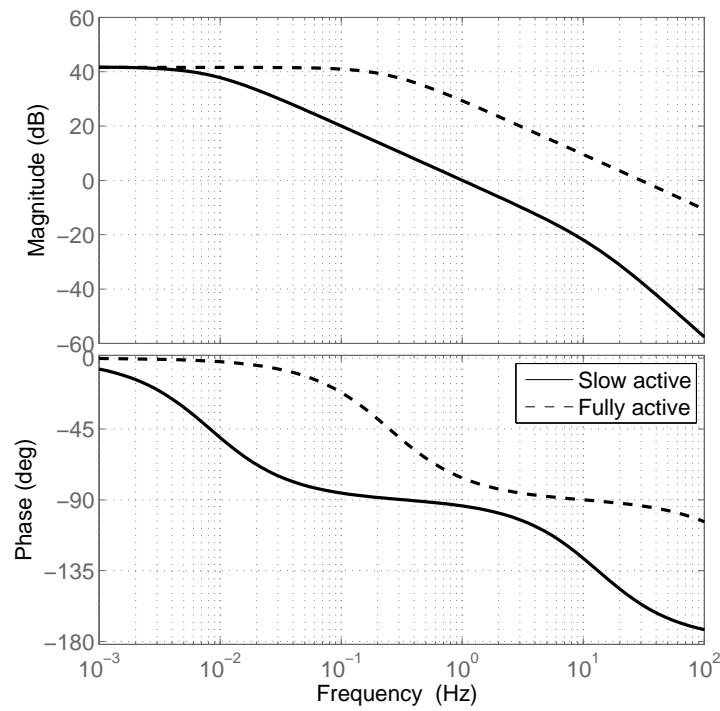


Figure 5.5: Transfer function, from input, $error_{\beta}$ to output, β ; $G_{dc}(2,2)(s)K_{i,\beta}(s)$.

- The slow active and fully active r_z controller open-loop dynamics exhibit identical low frequency behavior both in magnitude and phase. Thus the only differences between the controllers lie in their respective high frequency behavior. This helps in creating an environment where a comparison study between two controllers will highlight their distinct high frequency behavior.
- The open-loop bandwidth of the slow active β controller is 1 Hz and open-loop bandwidth of the fully active β controller is 30 Hz, see Figure 5.5.
- The behavior of the slow active and fully active β controller also conforms to the requirement of identical low frequency behavior with differences occurring at higher frequencies.
- The four controllers depict similar phase behavior in the vicinity of their respective bandwidths, see Figures 5.4 and 5.5. This means that one can expect similar behavior from each controller close to their respective bandwidths.
- Summing up one can say that the controllers designed meet the requirements of the slow active and fully active systems. Additionally, the incorporation of actuator dynamics that are consistent between the control loops will allow for a meaningful comparison study.

5.7 Closed-loop implementation of active suspension

A slow active controller and a fully active controller were designed in the sections above. However, before these controllers are implemented in a closed-loop environment there is a need to transform the control inputs into appropriate actuator forces. The r_z and β controllers will generate the required torque and lateral force signals respectively. These signals need to be converted to appropriate lateral forces generated by each tire. The suspension actuators cannot account for the lateral forces in the tires directly. These actuators can only vary the vertical forces in the tire. Hence, the requested lateral forces need to be translated into appropriate actuator forces. The solutions designed to tackle the issues explained above will be discussed in this section.

5.7.1 Closed-loop behavior

In this section the closed loop behavior of the r_z controller and β controller will be discussed. The closed loop transfer function can be stated as:

$$H_i(s) = \frac{G_{dc}(i,i)(s) K_i(s)}{1 + G_{dc}(i,i)(s) K_i(s)} \quad (5.19)$$

The respective closed-loop transfer functions were obtained and frequency responses are plotted in Figures 5.6 and 5.7. Some important observations made from the frequency response functions are listed below.

- The closed-loop behavior of the slow active r_z controller and the fully active r_z controller has almost identical behavior till 1 Hz. The magnitudes of the slow and the fast controller match each other till approximately 0.5 Hz whereas the phase behavior shows discrepancies after 0.1 Hz, see Figure 5.6.

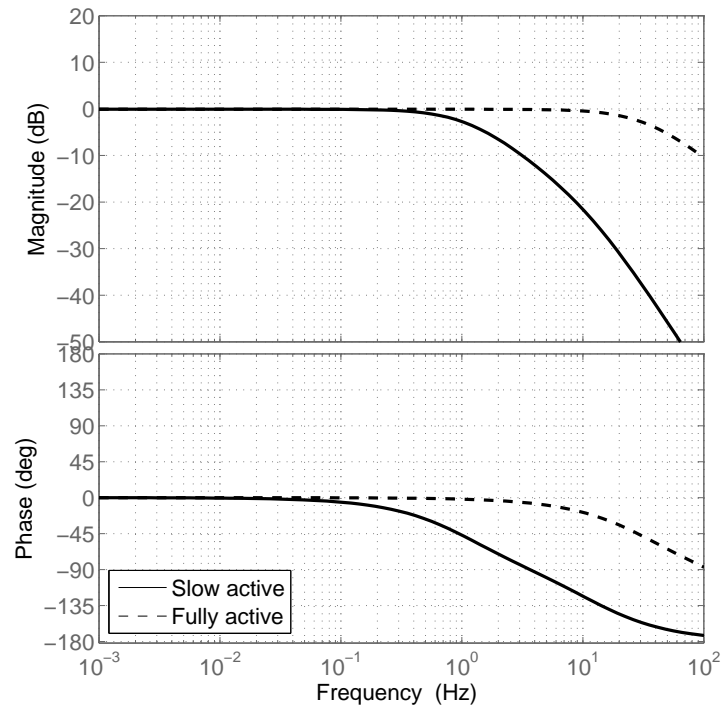


Figure 5.6: Closed-loop transfer function from input, $r_{z,ref}$ to output, r_z .

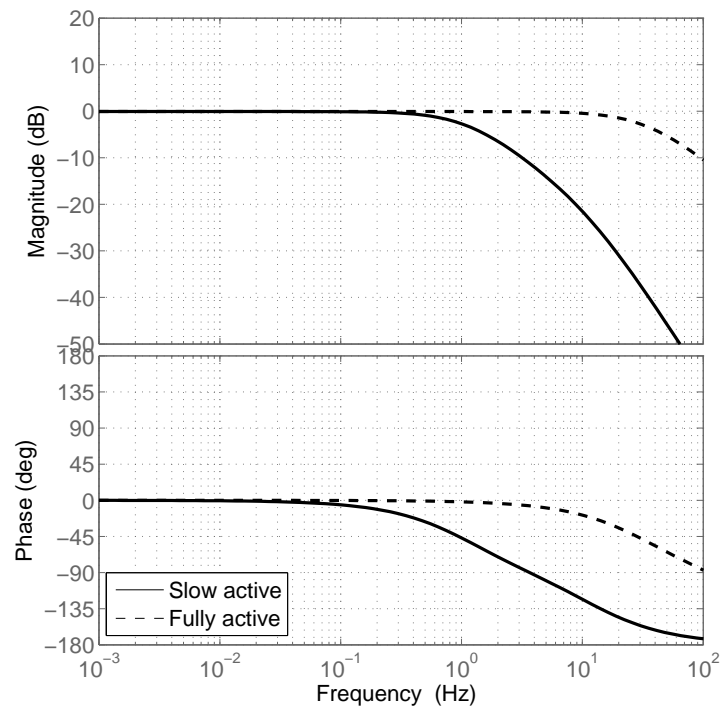


Figure 5.7: Closed-loop transfer function from input, β_{ref} to output, β_z .

- A similar observation can be made by observing the closed loop response of the β controller. Once again, drastic differences in magnitude occur only beyond the bandwidth of the slow active controller.
- Based on the observations from the open-loop as well as closed-loop frequency response plots, it can be concluded that the two systems should exhibit identical steady-state behavior thus allowing for an insightful study on the potential benefits from a high bandwidth system.

5.7.2 Calculate lateral tire force requirement

The controllers designed in section above were for a 2I2O system with T_z and $F_{y,net}$ as the two virtual inputs. These inputs need to be converted back to the individual lateral tire forces. A coupling matrix, T_u was defined in (5.6) to express the relation between virtual forces and the actual lateral tire forces. Using this equation the transformation from virtual inputs to tire forces can be stated as:

$$\begin{bmatrix} F_{y1} \\ F_{y2} \\ F_{y3} \\ F_{y4} \end{bmatrix} = T_u \begin{bmatrix} T_z \\ F_{y,net} \end{bmatrix} \quad (5.20)$$

Thus, using the transformation provided in (5.20) the requested torque and lateral force can be converted into individual tire forces.

Note: The transformation in (5.20) does not provide a unique solution since T_z and $F_{y,net}$ are created as a linear combination of the lateral tire forces. The linear co-efficients of the matrix T_u can be modified to arrive at a different solution. In the present implementation the matrix T_u assigns equal weight to the inside and outside wheels and thus the requested lateral axle forces are divided equally among the left and right tires. A dynamical transformation matrix that monitors each tire and optimizes the distribution of left and right lateral forces has the potential improve the system.

Dynamic inversion of nonlinearity

Using the transformation explained in the section above one can convert the required control signals into individual tire lateral forces. However, as explained in earlier sections the suspension actuators cannot influence the tire lateral forces directly. The nonlinear relation between the vertical tire force and lateral tire force was described in Section 4.2.1. One can recall, that this nonlinearity is dynamic and is a function of the vehicle states and tire forces. Thus it is not possible to arrive at an analytical expression that inverts the nonlinearity.

A custom algorithm was developed to solve this dynamic nonlinearity inversion problem. The elemental steps involved are provided in Algorithm 5.1. The algorithm uses the requested lateral tire forces, F_{yi} tire side-slip angles, α_i and vertical tire forces, $F_{z,i}$ as inputs. It then performs a search across the actuator limits to locate the actuator force which allows the tire to generate the appropriate lateral force. If the requested lateral force is beyond the limits of actuation, the algorithm saturates the actuator force to the appropriate maximum or minimum value. The output of the algorithm are four actuator forces that can be introduced into a vehicle model as inputs.

Algorithm 5.1: Dynamic inversion of Magic Formula tire model**Precondition:** α_i and $F_{zi,passive}$ are available at every time step

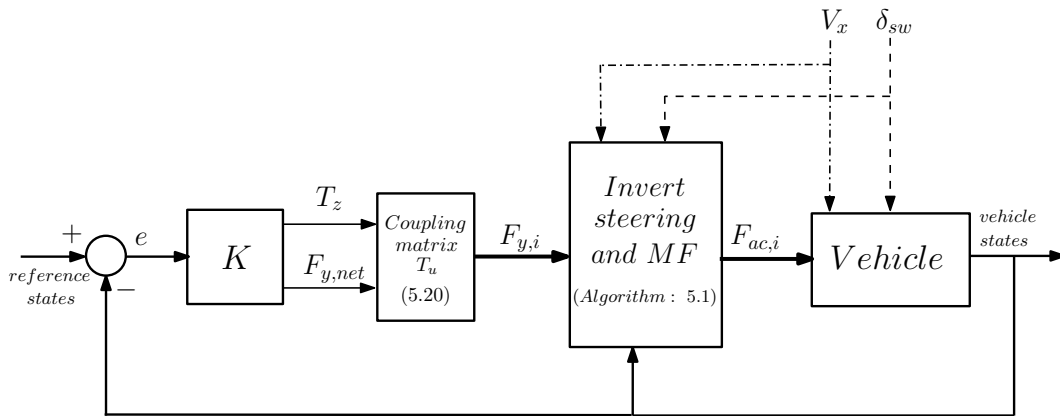
```

1 Inputs:
    $F_{ac,i} = invMF = (\alpha_i, F_{zi,passive}, F_{y,i})$ 
2 function INVMF( $\alpha_i, F_{zi,passive}, F_{y,i}$ )
3   Initialize:
    $F_{ac,i} \leftarrow 0$ 
    $F_{yi,min} \leftarrow 10^5$ 
    $F_{yi,temp} \leftarrow 0$ 
    $F_{zi,temp} \leftarrow F_{zi,passive} - \eta_i \times F_{ac,max} \cdots F_{zi,passive} \cdots F_{zi,passive} + \eta_i \times F_{ac,max}$ 
4   for  $ii \leftarrow 1$  to  $length(F_{zi,temp})$  do
5      $F_{yi,temp} \leftarrow MF(\alpha_i, F_{zi,temp}(ii))$ 
6      $jj \leftarrow |F_{yi,temp} - F_{y,i}|$ 
7     if  $jj < F_{yi,min}$  then
8        $F_{yi,min} \leftarrow jj$ 
9        $F_{ac,i} \leftarrow (F_{zi,temp}(ii) - F_{zi,passive}) / \eta_i$ 
10  return  $F_{ac,i}$ 

```

The methods explained above have been incorporated to convert the requested torque and lateral force first into appropriate tire lateral forces and then into suspension actuator forces. These procedures were followed to create a closed-loop active suspension setup. A schematic diagram explaining the environment is provided in Figure 5.8. The requirements for the closed-loop behavior have been listed below.

- The maximum permissible yaw-rate, $|r_{z,max}|$ has been set to $35^\circ/s$. Beyond these yaw-stability limits the r_z controller will saturate the reference yaw-rate, $r_{z,ref} = |r_{z,max}|$.
- The β controller is to enhance the lateral stability of the vehicle. Therefore, it will activate only if the vehicle attempts to exceed the side-slip stability limit of $|\beta_{max}| = 4^\circ$.

**Figure 5.8:** Closed-loop active suspension controller layout

5.8 Conclusion

The task of designing control schemes for yaw-rate control and side-slip control was undertaken in this chapter. The first challenge was to arrive at a system representation such that all the actuator inputs could be coupled to the yaw-rate and the vehicle side-slip measurement. This problem was tackled by defining two virtual inputs, T_z and $F_{y,net}$ such that a decoupled system could be realized for designing individual yaw-rate and side-slip controllers. The yaw-rate response of the vehicle to steering wheel inputs was used to decide the bandwidths of the slow active and the fully active controllers. Since one of the major goals of this thesis is to compare the performance of a slow active suspension and a fully active suspension, the controllers were designed such that they exhibit identical low frequency behavior. The open-loop and closed-loop frequency response measurements were studied to deduce expected behavior of the different suspension controllers. A custom methodology to transform the requested controller torques and forces to appropriate actuator forces was proposed and the implementation of the approach was looked in detail. Finally, the analysis performed in Section 3.4.1 was used to define the closed-loop system requirements and an schematic illustration of the closed-loop environment was provided.

CHAPTER 6

Results Analysis

The end of a melody is not its goal: but nonetheless, had the melody not reached its end it would not have reached its goal either. A parable.

Friedrich Nietzsche

6.1 Introduction

THE preceding chapters in this thesis have been devoted to conceiving an active suspension system to study the influence of such a system on the handling characteristics of a vehicle. A multi-body vehicle model was analyzed to gain insight on the potential of suspension actuation on the lateral and yaw dynamics of the vehicle. Subsequently, a model was proposed to describe the lateral and yaw dynamics of the vehicle and two active suspension controllers were designed for the vehicle model. In this chapter the results from simulations are investigated to understand the improvements in vehicle handling provided by an active suspension system. The yaw-rate along with vehicle side-slip angle are used to evaluate the yaw and lateral dynamics respectively. In addition to inspecting the dynamics of the vehicle, the relative performance of the slow active system and the fully active system is compared by observing the outputs of the suspension actuators.

6.2 Simulation Environment

The simulation environment used for closed-loop simulations is discussed briefly in this section. This short explanation is meant to provide a rationale for the analysis undertaken during the remainder of this chapter. The closed-loop schematic can be seen in Figure 5.8.

Vehicle model inputs

This section gives a short explanation on the origin and nature of the vehicle inputs.

- **Longitudinal velocity, V_x :** The longitudinal velocity is one of the open-loop inputs to the vehicle model.

- **Steering wheel angle, δ_{sw} :** The steering wheel angle is the second open-loop input to the model. The steering wheel angle signal is factored by the steering ratio and applied as steering angle to the front tires of the vehicle. The two open-loop inputs are explained in further detail in Section 3.2.1.
- **Actuator forces, $F_{ac,i}$:** The four actuator forces for the closed-loop inputs to the vehicle model. These inputs are calculated via the procedure explained in the previous chapter and represent the actuator forces generated by the active suspension actuator. These signals will be studied during the course of this chapter to compare the slow active and fully active suspension systems.

Vehicle model outputs

Similarly the output signals generated in this closed-loop environment are explained below.

- **Yaw-rate, r_z :** This output signal is used to study handling characteristics such as yaw stability and steering response. The actuator forces influence the yaw-rate of the vehicle and thus it is important to study how these handling characteristics can be improved.
- **Vehicle side-slip angle, β :** The second simulation output is used to assess the lateral stability of the system. Once again, the simulations performed in previous chapters have demonstrated how suspension actuation can be used to alter the lateral dynamics of the vehicle and thus observing the side-slip angle presents the opportunity to study another facet of vehicle handling.

6.3 Extreme Maneuvers

The importance of lateral and yaw stability of a vehicle was documented in Chapters 1 and 2 and the stable boundaries of the vehicle were defined in Section 3.4.1. In this section the unstable extreme maneuvers from Figure 3.9 are simulated to observe if an active suspension setup can enhance the lateral and yaw stability of the vehicle.

6.3.1 Yaw stability test

The simulations performed in Section 3.4.1 had shown that the vehicle tends to get unstable when subjected to very large steering angles at speeds close to 13.3 m/s. The vehicle first loses yaw-stability and the resulting oscillations in yaw-rate cause the lateral stability limits to be crossed as well resulting in loss of control. In this section such an extreme maneuver is replicated to judge if the active suspension system can provide a safety net during such situations.

The velocity profile and steering wheel angle are provided as open-loop inputs to the system and a closed-loop simulation is performed once with the slow active system and then with the fully active system. The results of the simulation can be observed in Figures 6.1 and 6.2. Some of the key observations that can be made by analyzing the results are listed below.

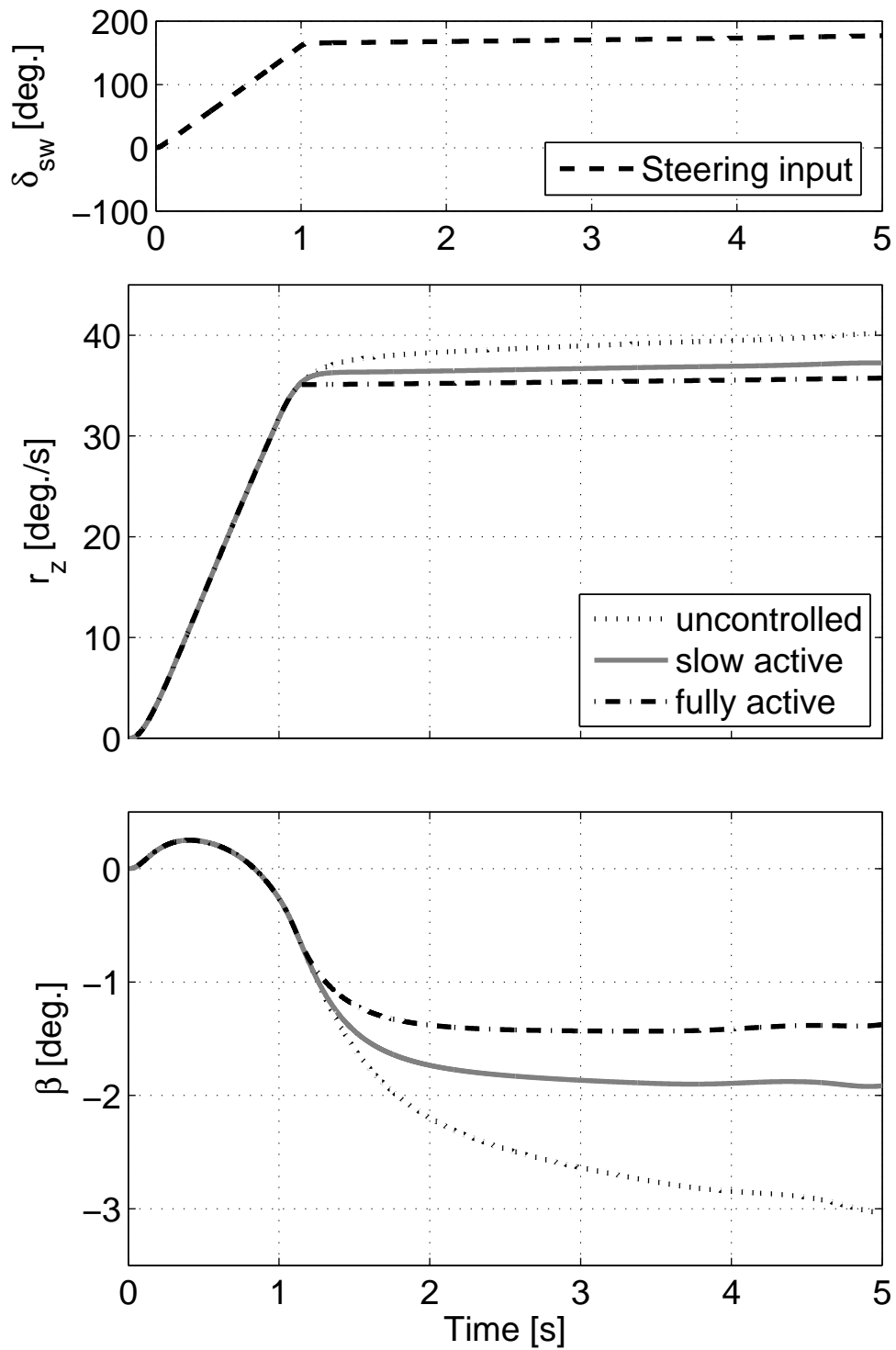


Figure 6.1: Steering wheel angle, yaw-rate, side-slip angle for extreme step steer maneuver, ($V_x = 13.3$ m/s).

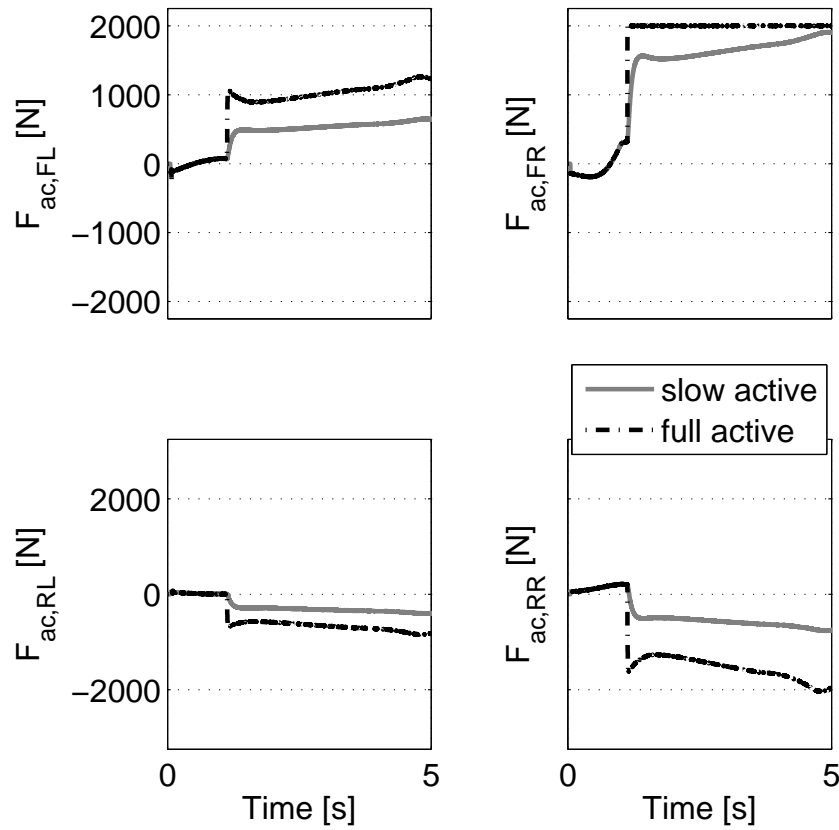


Figure 6.2: Actuator forces for extreme step steer maneuver, ($V_x = 13.3$ m/s).

Analysis of vehicle dynamics: yaw stability test

- As expected and observed earlier, such a large steering wheel input causes the uncontrolled vehicle to generate very high yaw-rate which result in the vehicle side-slip angle to increase rapidly as well, Figure 6.1.
- It can be observed that despite the large steering wheel angle input provided the two controlled vehicles are able prevent the instability.
- The vehicle with the fully active suspension is able to maintain the yaw-rate of the vehicle at exactly $r_{z,max}$ whereas, the vehicle with the slow active suspension does breach the yaw stability limits of the vehicle. However, it does not cause the yaw-rate to rise out of control but can maintain a constant value just beyond the stable boundary.
- The repercussions of ensuring yaw stability of the vehicle can be observed the vehicle side-slip angle. The side-slip angle in the uncontrolled vehicle is rising constantly and a longer simulation would have shown that it breaches the lateral stability limits as well. The yaw-rate and vehicle side-slip angle trajectories of the uncontrolled vehicle are consistent with what was observed in Figure 3.9.

- On the other hand, the two controlled vehicle are able to prevent the excessive and fast increase in the vehicle side-slip angle.

Analysis of actuator dynamics: yaw stability test

The differences in the lateral dynamics of the two controlled vehicles can be explained better by observing the actuator dynamics in Figure 6.2.

- One can observe that the fully active suspension generates larger actuator forces during the entire simulation. This allows the fully active suspension to control the yaw-rate of the vehicle to a larger extent when compared to the slow active suspension.
- The differences between the actuator forces can be explained by referring to Figure 5.4. The difference in the gains between 0.02 Hz and 1 Hz are mainly responsible for this behavior.

6.3.2 Lateral stability test

It has been mentioned in previous chapters that the lateral stability of the vehicle turns into a crucial factor stability criterion for cornering maneuvers performed speeds close to 27.7 m/s. The decrease in the effective lateral force generated by the front and rear axle is mainly responsible for the instability. In this section simulations with performed with an active suspension setup to assess if a controlled vehicle can demonstrate improved limit handling behavior.

A simulation test that depicts such a limit handling case was identified in Section 3.4.1 and Figure 3.9. Once again the steering wheel angle and longitudinal velocity were provided as open-loop inputs and this simulation was repeated with vehicles with an active suspension setup. The results from the simulation are provided in Figures 6.3 and 6.4.

Analysis of vehicle dynamics: lateral stability test

- One can observe that it is the vehicle side-slip angle that begins to exceed the stability limits during the course of this test, see Figure 6.3. The yaw-rate of the vehicle does not increase aggressively. Thus during such a maneuver the vehicle should maintain the yaw-rate without generating side-slip angles that are difficult to control for the driver.
- The improvements provided by vehicle with an active suspension system can be ratified from the yaw-rate and vehicle side-slip angle plots. The controlled vehicles match the required yaw-rate very closely but prevent the vehicle side-slip angle from exceeding the stability limits.
- On close observation it can also be seen that the vehicle with the fully active suspension adheres to the stability limits slightly better and can also generate marginally higher yaw-rates. However these effects are extremely minute and unlikely to be perceived by the driver.

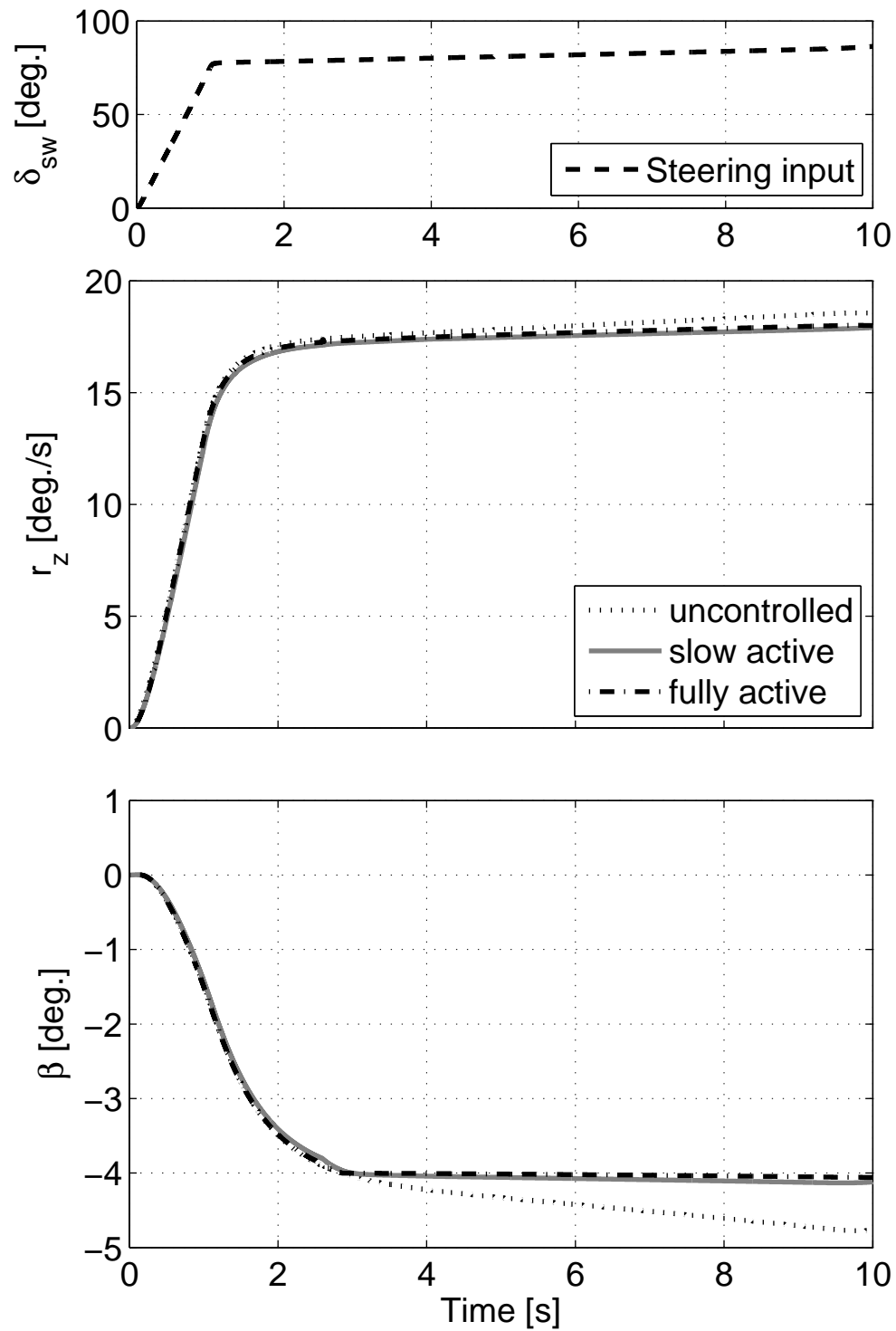


Figure 6.3: Steering wheel angle, yaw-rate, side-slip angle for extreme step steer maneuver, ($V_x = 27.7$ m/s).

Analysis of actuator dynamics: lateral stability test

The minute differences in vehicle dynamics as seen above can be explained by observing Figure 6.4.

- Beyond 2 s one can see that the steering wheel angle is increasing slowly. This generates a reference yaw-rate which the two controllers attempt to match. However, due to the lateral stability envelope the controllers are also forced to confine the vehicle side-slip angle to 4° .
- The higher bandwidth controller generates larger actuator forces to satisfy the two conditions which results in the imperceptibly improved performance. As explained in previous sections these difference in controller gains can again be traced to the difference in open-loop gains between 0.02 Hz and 1 Hz.

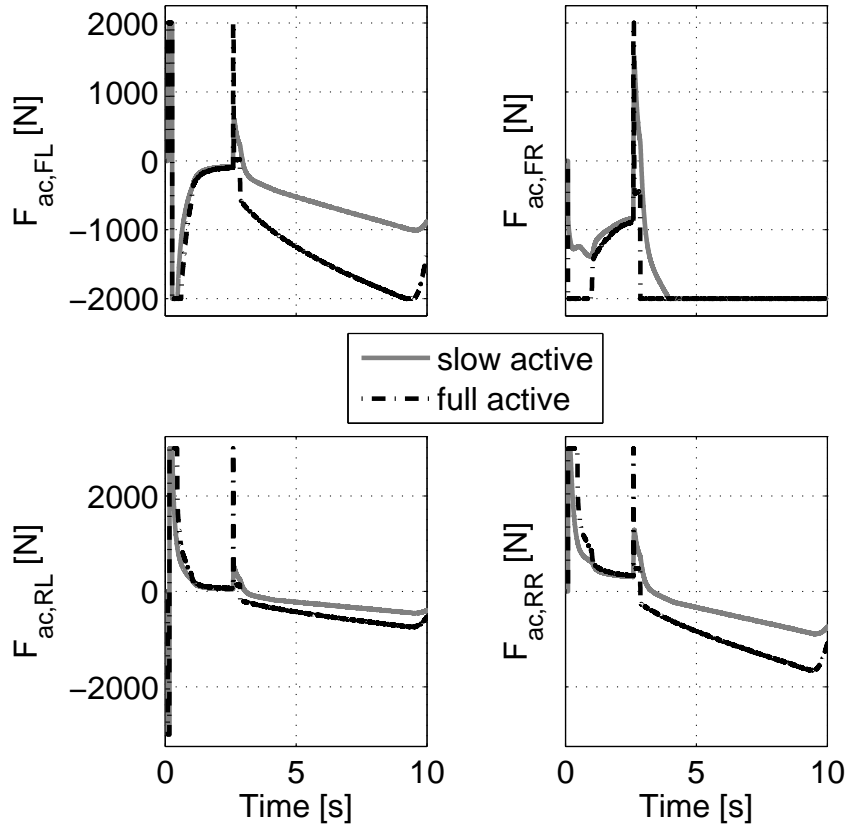


Figure 6.4: Actuator forces for extreme step steer maneuver, ($V_x = 27.7$ m/s).

6.3.3 Key takeaways: active suspension for improving vehicle safety

In this section the primary conclusions that can be drawn from the simulations results performed in the sections above are summarized.

- The simulation in Section 6.3.1 demonstrated the effectiveness of an active suspension system at improving the yaw stability of the vehicle. The vehicle with the fully active suspension was able to conform to the yaw stability limits much better than the vehicle with the slow active suspension. Furthermore, both the controller were successful in preventing the excessive rise in vehicle side-slip angle.
- The improved performance of the high bandwidth controller came at the expense of higher actuator forces. However, one must take note that higher actuator forces result in larger power losses. Taking this fact into consideration it can be seen that the slow active suspension provides ample improvements over an uncontrolled vehicle as it prevents excessive yaw-rate gain while limiting the vehicle side-slip angle and this is achieved with much smaller actuator forces.
- The diminishing gains in performance from the fully active suspension can also be observed from the simulations in Section 6.3.2. The fully active suspension generates much higher actuator forces but presents nominal performance gains.
- Both the simulations show that the performance gains of the fully active suspension cannot justify the larger actuator force requirements. The improvements provided by a slow active suspension over an uncontrolled vehicle are comparable to the improvements provided by a fully active suspension and are realized at much lower potential power requirements.

6.4 Enthusiastic Driving

The literature review in Chapter 2 showed that during corner entry the yaw-rate of the vehicle is perceived by drivers as a measure of the steering response of the vehicle. An enthusiastic driver prefers a vehicle that responds quickly to the steering inputs i.e has a faster yaw-rate increase.

A possible way to assess this behavior is to perform simulations for a transient cornering maneuver and observe if the vehicle with an active suspension can allow for a quicker yaw-rate gain compared to an uncontrolled vehicle. An open-loop steering input was provided as an input to mimic a cornering maneuver performed at 13.3 m/s. The results of the simulation can be observed in Figures 6.5 and 6.6.

Analysis of vehicle dynamics: enthusiastic driving test

- Both the controlled vehicle are able to increase the yaw-rate gain of the vehicle.
- One can observe that the fully active suspension can provide a much faster yaw-rate gain and also exhibits sharper transition to steady-state conditions. The vehicle with the active suspension controller can be seen to settle into the corner approximately 0.3 s quicker than the uncontrolled vehicle.
- On the other hand, the vehicle with the slow active suspension shows smaller increments over the uncontrolled vehicle and also exhibits much progressive behavior.

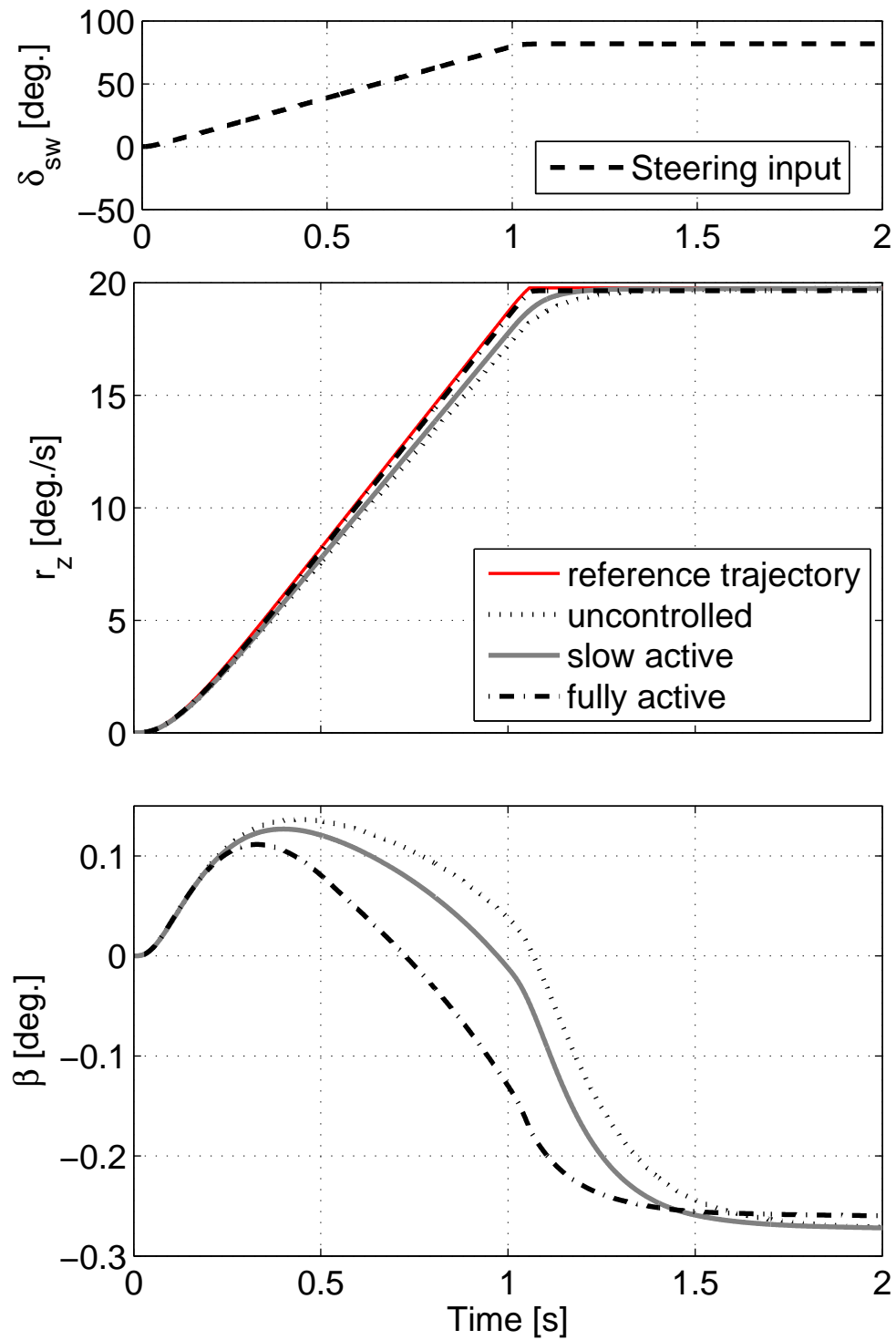


Figure 6.5: Steering wheel angle, yaw-rate, side-slip angle for ramp steer maneuver, ($V_x = 13.3$ m/s).

Analysis of actuator dynamics: enthusiastic driving test

The differences between the performance of the controllers during a transient and dynamic maneuver can be observed in Figure 6.6.

- The open-loop frequency domain plot in Figure 5.4 can once again be used to explain the differences between the actuator forces of the two suspension controllers. Compared to the earlier simulations, the test in this section generates a reference trajectory that has a larger component of higher frequency data. As a result the faster controller can provide much better responses due to the higher gains in the open-loop behavior.
- The fully active suspension controller appears to be working close to the limits of actuation to follow the quicker yaw-rate reference trajectory. One can see that it has loaded the front tires and unloaded the rear tires to increase the torque acting on the vehicle about the z-axis.
- The slow active suspension is unable to track the reference trajectory due to its inability to generate the higher actuator forces. However, one must reflect on the large actuator forces generated by the faster controller and the potential power requirements.

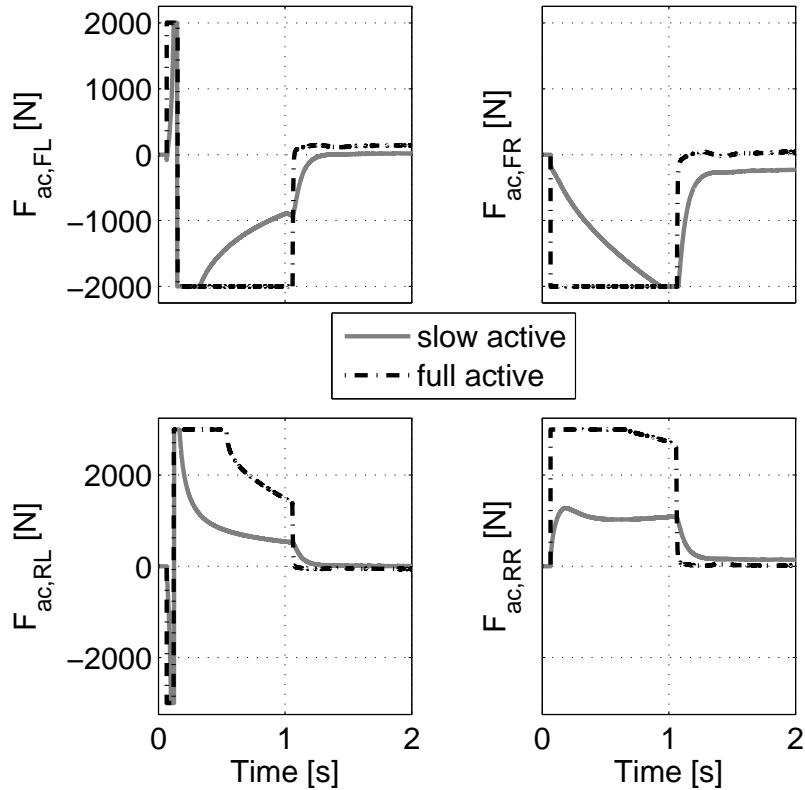


Figure 6.6: Actuator forces for extreme ramp steer maneuver, ($V_x = 13.3$ m/s).

6.5 Exploring actuator limits

The results discussed in the earlier sections have all dealt with the behavior of the vehicle and suspension actuator within the limits of actuation. In this section an attempt is made to understand how the closed-loop system behaves once the requested controller gains are beyond the actuator limits.

A double step-steer test akin to the one performed in Section 4.3.3 is repeated. Once again the steering wheel angle and longitudinal velocity are provided as open-loop inputs to the system. A reference trajectory 15% higher than the uncontrolled vehicle was provided as reference and the results were recorded for the two controlled vehicles. The results of the simulation can be observed in Figures 6.7 and 6.8.

Analysis of vehicle dynamics: actuator limits

- The marginally superior performance of the fully active suspension controller compared to the slow active suspension can be seen by observing the yaw-rate reference tracking behavior. However, it is also clear that none of the controller vehicles is able to match the reference trajectory during the transient or temporary steady-state conditions.
- The vehicle side-slip angle measurement from the uncontrolled as well as controlled vehicle should be ignored as this measurement failed the validation test in Section 4.3.3. Since, the vehicle side-slip angles during this test do not approach the limits, $|\beta_{max}|$ this measurement does not play a role in the actuator dynamics.

Analysis of actuator dynamics: actuator limits

The simulation performed in this section was performed to get a better understanding of the controller behavior when the requested forces fall outside the actuator limits. The actuator forces for this simulation can be observed in Figure 6.8.

- As mentioned earlier, the reference trajectory for this simulation is requests for a 15% higher yaw-rate generation during the driving maneuver. As a results the controller try to increase the torque about the z-axis acting on the vehicle.
- To fulfill this requirement one can observe that both the controller saturate the front actuators completely thus loading the front tires and a similar attempt is made to unload the rear tires.
- The two controllers exhibit similar behavior on the front tires but there exist some differences in the rear tire. This can be explained from the open-loop frequency measurements in Figure 5.4 and recollecting the low efficiency in translating the actuator force to vertical tire force, see Figure 3.5. Thus, a difference of 500 N in actuator force at its best results in only a change of approximately 100 N. This difference of approximately 100 N on the rear tires can explain the marginally higher yaw-rate achieved by the fully active suspension.

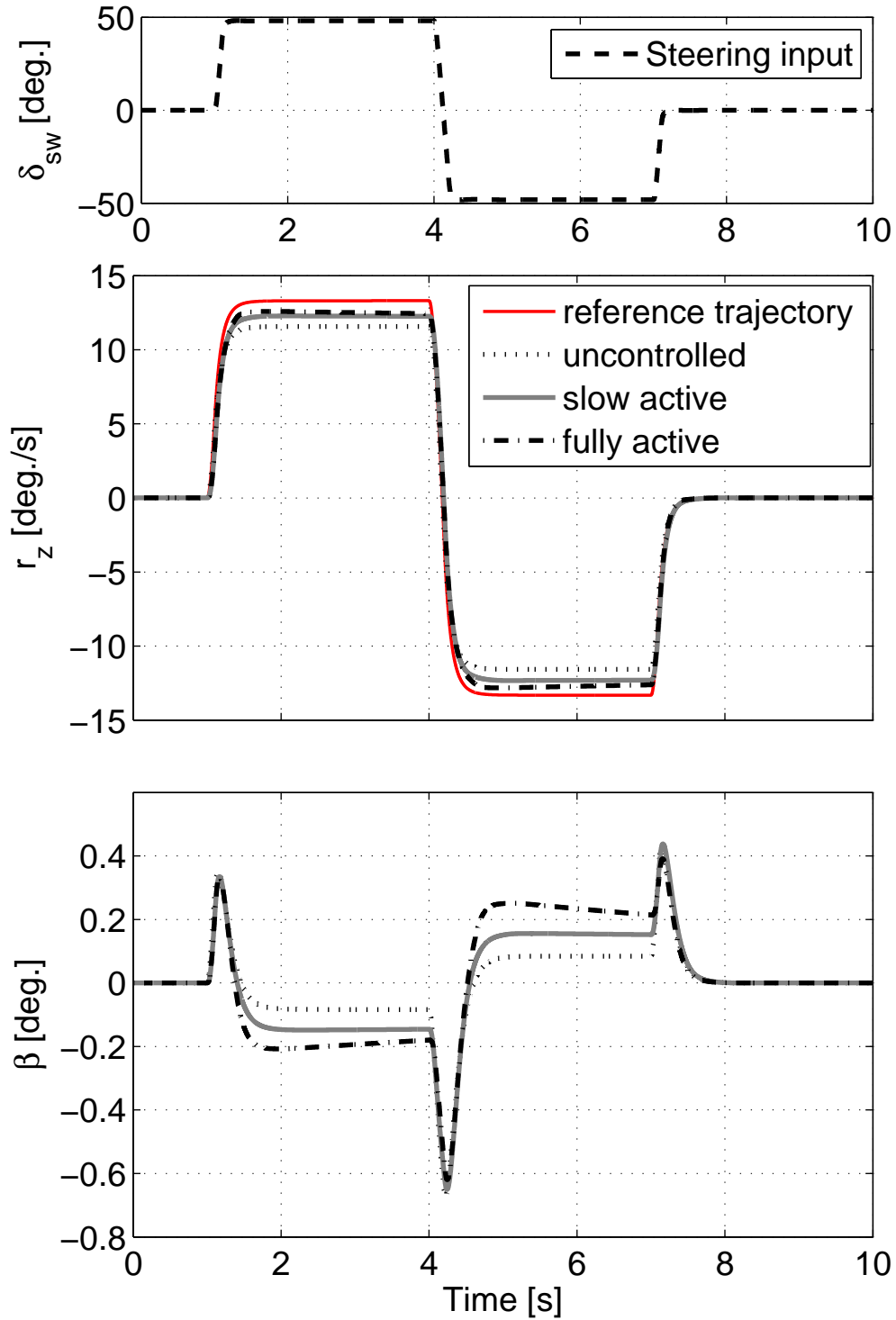


Figure 6.7: Steering wheel angle, yaw-rate, side-slip angle for double step steer, ($\delta_{sw} = 50^\circ$, $V_x = 13.3$ m/s).

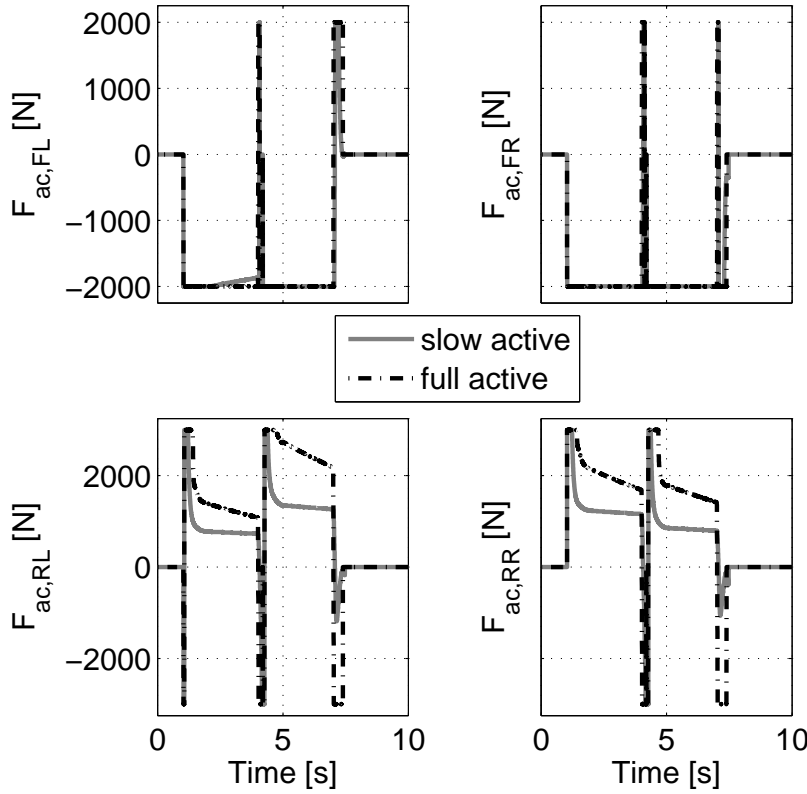


Figure 6.8: Actuator forces for double step steer, ($\delta_{sw} = 50^\circ$, $V_x = 13.3$ m/s).

6.6 Slow active control versus fully active control

The simulations performed in the earlier sections of this chapter have provided an apt opportunity for comparing the performance of a slow active suspension and the fully active suspension. Some of the most significant conclusions that can be drawn from the simulations are discussed below.

- Based on the closed-loop requirement described in Section 5.7.1, the β controller should not get activated unless the value of the vehicle side-slip angle exceeds $|\beta_{max}|$. An interesting observation made in all simulations is that yaw-rate tracking also influences the vehicle side-slip angle. This can be explained by the direct dynamical relation between the two quantities as seen in (1.4) and also the strong coupling between T_z and β as seen in the transfer function illustrated in Figure 5.2.
- A closed-loop active suspension has been shown to improve the yaw stability of the vehicle. Both the slow active suspension system and the fully active suspension system were able to limit the aggressive rise in yaw-rate and side-slip angle of a vehicle during an extreme handling maneuver, see Section 6.3. The closed-loop performance of the fully active suspension system was better than the slow active

suspension at both controlling the yaw-rate as well as vehicle side-slip angle. Nonetheless, the minuscule gains in performance were achieved at the expense of much higher actuator forces thereby at much higher power requirements. The simulations depict that the improvements provided by the slow active suspension are enough to prevent instability and provide ample time for the driver to take corrective or evasive measures via steering wheel or brake pedal thus annulling the case for the requirement of a high bandwidth suspension controller.

- The performance of an active suspension at influencing the transient handling behavior of the vehicle was studied in Section 6.4. The simulations performed demonstrated that the fully active suspension has the potential to alter the transient handling of the vehicle. The high bandwidth system allowed for a faster yaw-rate gain which could provide a quicker response to vehicle steering inputs. An ability to alter the transient handling characteristics is a desirable property for vehicles designed with sporty intentions. Despite the bigger performance advantage over the slow active setup the reasons for incorporating a fully active suspension are not conclusive as the high bandwidth system generated significantly higher actuator forces during the simulation which translates to large power requests in real life. One can argue that a slow active suspension used in an integrated chassis control setup could provide equal or better improvements in transient vehicle handling.
- The behavior of both the controllers was found to be very similar in simulations performed to understand the behavior of the system is operated beyond the limits of actuation. The nature of Algorithm 5.1 ensures that both the controllers operate very similarly when the requested forces are beyond the actuation limits.
- The simulations performed in this chapter present a strong case for developing active suspension systems to improve vehicle handling especially improvements in lateral and yaw safety of the vehicle. The controllers developed in this thesis were able to demonstrate that it is possible to influence the steady-state as well as transient handling of the vehicle. Furthermore, the results from the simulations and arguments presented above do not advocate development of high bandwidth systems. The relative gains from the high bandwidth systems were seen to be marginal and at the expense of substantially larger actuator forces. A more plausible implementation for an active system will be to develop an integrated steering, axle differential and suspension control system such that the individual drawbacks of each system can be mitigated. The potential benefits of such a system has been discussed in [1][36].

6.7 Summary

The goal of this thesis is to compare the performance of active suspension systems on improving vehicle handling. The slow active and fully active suspension controller designed in earlier chapters were implemented and their performance was studied in a closed-loop simulation environment. Through simulated extreme driving maneuvers it was shown that the controlled vehicles provided a safety mechanism to the vehicle by improving the yaw stability and the lateral stability of the vehicles. A transient driving maneuver was simulated to understand if an active suspension system could

aid in improving the transient handling of a vehicle. It was found that the fully active suspension was able to provide a faster yaw-rate gain during cornering whereas the gains due to a slow active suspension were much lower. The dynamics of the system and actuator were also studied to understand how the vehicle handling when subjected to inputs that are beyond the actuator limits. The results and observation from these simulation studies were combined to compare the performance of the slow active and the fully active controllers. The vehicle dynamics performance and corresponding actuator dynamics indicated that the the tiny performance gains from the fully active suspension were not worth the additional actuator forces. The primary conclusion derived from the chapter was that an active suspension can indeed improve the handling of the vehicle but a low bandwidth controller provides sufficient performance gains to negate the need for a fully active system.

CHAPTER 7

Conclusion and Future Work

Problems worthy of attack prove their worth by hitting back.

Piet Hein

7.1 Summary

THE fundamental research question investigated through this thesis can be stated as:

Design a slow active suspension controller and a fully active suspension controller to improve a vehicle's handling characteristics and investigate the relation between control bandwidth and achievable handling enhancements.

To present a cogent argument for the design of active suspension for improving vehicle handling the main research question has been divided into smaller objectives.

- Perform a thorough literature survey on past research in the field of semi-active and active suspension setup and its impact on the ride and handling behavior of a vehicle. Based on the findings from the review process provide substantiated arguments for the research work.
- Develop a vehicle model that can accurately capture and replicate the required dynamics of a vehicle and validate the designed model with the BMW SimMechanics™ 1G model.
- Design a slow active suspension and a full active suspension controller to influence the handling behavior of the vehicle model.
- Implement the active suspension controllers on a validated vehicle model and investigate the capability of the active suspension at improving the transient and steady-state handling of the vehicle model.
- Compare the performance of the two different active suspension controllers to determine the relation between controller bandwidth and achieved handling improvements.

7.2 Conclusions

A literature survey of existing research on vehicle handling and active suspension systems is performed in Chapter 2. It was shown that a majority of active suspension design problems define vehicle handling as dynamic tire compression and document improvements in vehicle handling based on this measurement. A review of studies based on pure vehicle handling studies presented that vehicle handling consists of multiple measures and lateral and yaw dynamics constitute a major portion of vehicle handling. The decision to utilize yaw-rate and vehicle side-slip angle as indicators of yaw and lateral dynamics of a vehicle were taken based on the results from the review process. The literature on active suspension control revealed that it was a prevalent practice to use single track vehicle models with linear tire models to depict the yaw and lateral dynamics of the vehicle. However, since such models cannot account for substantial vehicle dynamics during cornering it was decided to design a vehicle model that captured the yaw and lateral dynamics of the vehicle better and also used better tire models.

A multi-body vehicle model that accurately represents a vehicle was used to analyze the cornering behavior of a vehicle and understand how suspension actuation influenced it. As a first step, simulations were performed to determine the actuator limits which were found to be 2000 N and 3000 N for the front and rear suspension respectively. Additionally, the efficiency of the actuators at altering the vertical tire forces was found. Simulations were performed to determine the lateral and yaw stability limits of the vehicle and it was found that at low speeds and high steering wheel angle, yaw-stability is the limiting boundary whereas at high speeds vehicle side-slip angle is the limiting stable boundary. Additional simulations were performed in open-loop steady-state conditions to understand how suspension actuation influenced vehicle handling. It was found that actuation of suspension could alter both the yaw-rate and the vehicle side-slip angle. Furthermore, it was found that the actuation of the suspension also altered the handling balance of the vehicle thereby providing substantive arguments for pursuing this thesis.

It was found that the multi-body model was unsuitable for designing controllers due to a lack of state-space or transfer functions describing the dynamics of the vehicle. Consequently, a two-track vehicle model was proposed in Chapter 4 such that it provided clear dynamical equations depicting relations between the vertical tire forces and the lateral and yaw dynamics of the vehicle. The proposed vehicle model used a simplified Magic Formula representation and included the lateral load transfer dynamics. This model was validated against the reference multi-body vehicle model and it was found that it showed high accuracy in yaw-rate measurements for longitudinal velocities ranging from 13.3 m/s to 27.7 m/s. The model was found to show poor accuracy in vehicle side-slip angle measurements for dynamic measurements but depicted reasonably accurate steady-state behavior.

The two-track vehicle model was then used to design the active suspension controllers. The nonlinear two-track was subdivided into a dynamic nonlinear part and a linear part. The linear portion was stated in transfer function forms to obtain a 4I2O transfer function model. This 4I2O transfer function was then transformed into a 2I2O

form by performing certain static input transformations. It was then decided to use the 2I2O transfer function to create a yaw-rate control loop and a side-slip angle control loop. A slow active suspension controller with a bandwidth of 1 Hz and a fully active suspension controller with bandwidth 30 Hz were designed. The low frequency open-loop transfer functions of the different controllers were designed to be identical such that a meaningful performance comparison can be made. These controllers were then implemented in a MIMO setup. To solve the closed-loop implementation problem, the outputs from the controller were once again transformed to obtain the initial four inputs. A custom algorithm that dynamically inverted the Magic Formula tire model was then designed that converted these four input signal into appropriate actuator inputs. Hence by the end of Chapter 5 a two closed-loop active suspension setups were realized that used longitudinal velocity and steering wheel angle as open-loop inputs to simulate driving maneuvers and the four suspension actuator forces as closed-loop inputs to improve vehicle handling.

In Chapter 6 simulations were performed to determine the improvements in handling due to an active suspension setup and also a performance comparison between the slow active suspension and the fully active suspension controller was made. The closed-loop simulations showed that both the active suspension controllers were able to improve the yaw and lateral stability of the vehicle. It was observed that the fully active setup provided marginally better performance but in turn required much larger actuator forces to attain the performance. Simulations were performed to study if the active suspensions could help in improving the transient handling of the vehicle and it was seen that the full active suspension once again was able to provide bigger gains in vehicle response. However, once again the tiny improvements in performance did not justify the substantially larger actuator forces required.

The individual findings from this thesis can be amalgamated to answer the main research question. An active suspension is successfully able to improve vehicle handling by influencing yaw stability as well as lateral stability of the vehicle. The improvements in the lateral and yaw stability can be assumed to be largely independent of control bandwidth as shown by simulations of the slow active and the fully active system. Additionally it was also shown that the fully active suspension can also perceptibly alter the transient handling response of the vehicle. However, the observing the actuator forces and estimating the additional power requirements of the fully active system it was found that the gains in vehicle handling on increasing control bandwidth were not justified by the substantial increase in the actuator forces. To sum up, it can be said that the performance gain from substantially lower actuator forces make a slow active suspension an ideal design for improving vehicle handling.

7.3 Recommendations

Throughout this research, certain simplifications and assumptions were made to engineer possible solutions around problems. Future recommendations to further the scope of active suspension control and vehicle handling are enlisted below:

- This research focuses primarily on the handling characteristics of the vehicle by studying yaw-rate and vehicle side-slip angle. However these two measures

do not form the exhaustive set of parameters used to describe vehicle handling. Additional measures such as vertical tire forces, tire side-slip angles and slip angular velocity, $\dot{\beta}$ can be included for a more comprehensive study.

- The two-track vehicle model derived does not incorporate the vertical dynamics the road, unsprung masses or the vehicle body. This model can be expanded further to account for road imperfections and vertical positions of the tire, unsprung masses and sprung mass. This expanded vehicle model will aid in design of controllers with a multiple ride-comfort and vehicle handling based objectives. Furthermore, the accuracy of the model at high speed dynamic maneuvers needs to be improved as the current model is unable to match the transient behavior of the multi-body reference model.
- The two track model derived neglects the coupling between the actuators and the four suspension modes. The multi-body vehicle model can be studied in greater depth to obtain mathematical formulations for the actuator coupling and suspension excitation modes.
- The vehicle model derived simplifies the multi-body vehicle model and hence is orders of magnitude faster in simulation environment. However, some of this advantage is eroded with the closed-loop setup. This is due to the computation time of the inverse MF and steering function. The algorithm can be optimized further such that the control strategy can become suitable for real time implementation.
- The coupling matrix, T_u is designed as a static coupling matrix. Thus it does not differentiate between the inner and out tires during a corner and requests equal force from both of them. A smarter implementation will be a coupling matrix that is a function of the vehicle steering wheel angle, yaw-rate and lateral acceleration. Such a dynamic coupling matrix will allow for differential loading on both inner and outer tires which can aid in studying chassis warp effects.

Vehicle Parameters

THE vehicle parameters used in this thesis are compiled in Table A.1.

Table A.1: Vehicle Parameters

| Name | Parameter | Value | Unit |
|-------------------------------------|-----------|--------|------------------|
| Mass, vehicle | m | 1561 | kg |
| Moment of inertia around z-axis | I_{zz} | 2550.1 | kgm ² |
| Track width front | s_1 | 1.471 | m |
| Track width rear | s_2 | 1.478 | m |
| Distance from COG to front axle | a_1 | 1.3834 | m |
| Distance from COG to rear axle | a_2 | 1.3416 | m |
| Steering wheel to front wheel ratio | i_s | 18 | rad/rad |

APPENDIX B

Multi-body Model Layout

A schematic layout of the multi-body model of the BMW 318i can be viewed in Figure B.1.

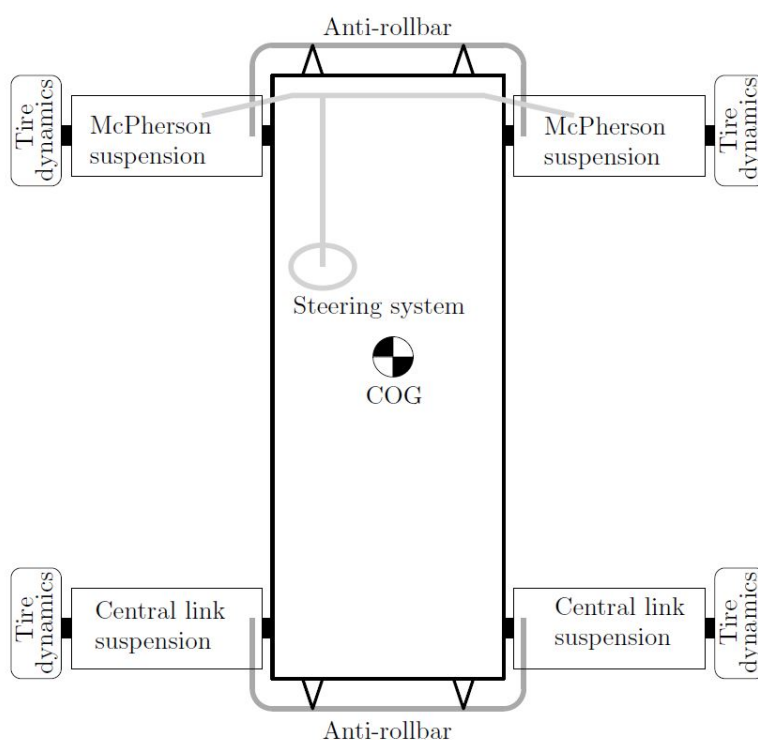


Figure B.1: Schematic layout of multi-body BMW vehicle model [1,32]

APPENDIX C

Suspension travel and bump-stops

BUMP stops are designed to improve the ride quality of a vehicle while protecting your vehicle's suspension. Bump stops mark the transition the designed spring stiffness and the spring stiffness at the extreme end of suspension travel. The presence of bump stops gives rise to a nonlinearity in the suspension spring stiffness due to the non smooth relation between suspension stiffness and spring travel, see Figure C.1.

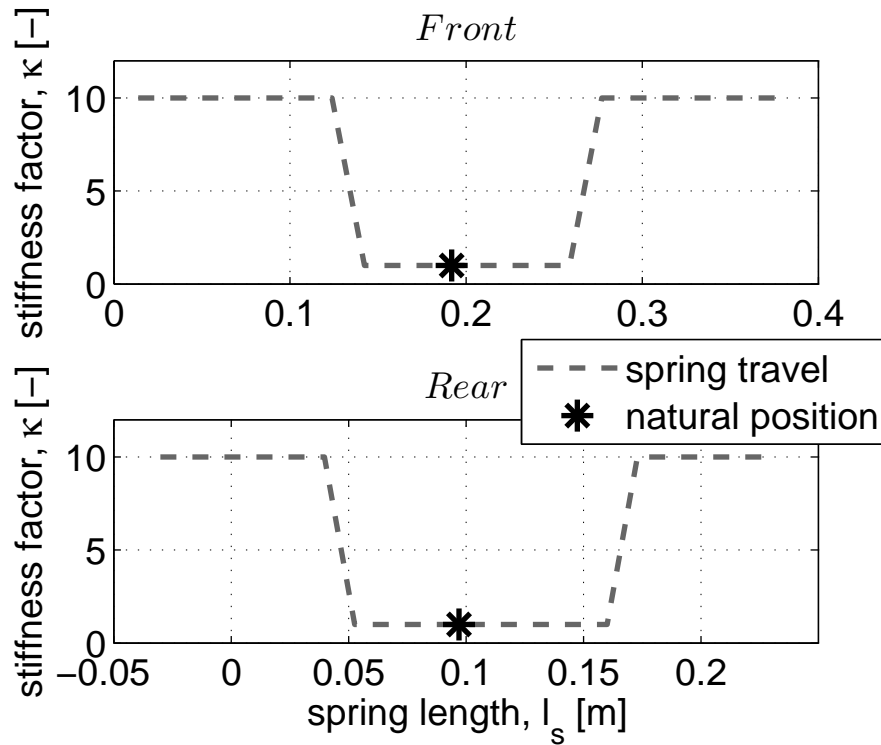


Figure C.1: Location of bump stops; front suspension (top), rear suspension (bottom)

The presence of the bump stops necessitates a design choice in the actuator force, $F_{ac,i}$ for the active suspension. The actuator force, $F_{ac,i}$ is constrained to limit the suspension spring travel in the linear region or design for higher actuator force, $F_{ac,i}$ by including the full nonlinear model of the suspension springs.

APPENDIX D

Suspension Modes

THE suspension and vehicle cabin displacement can be categorized into four primary motions.

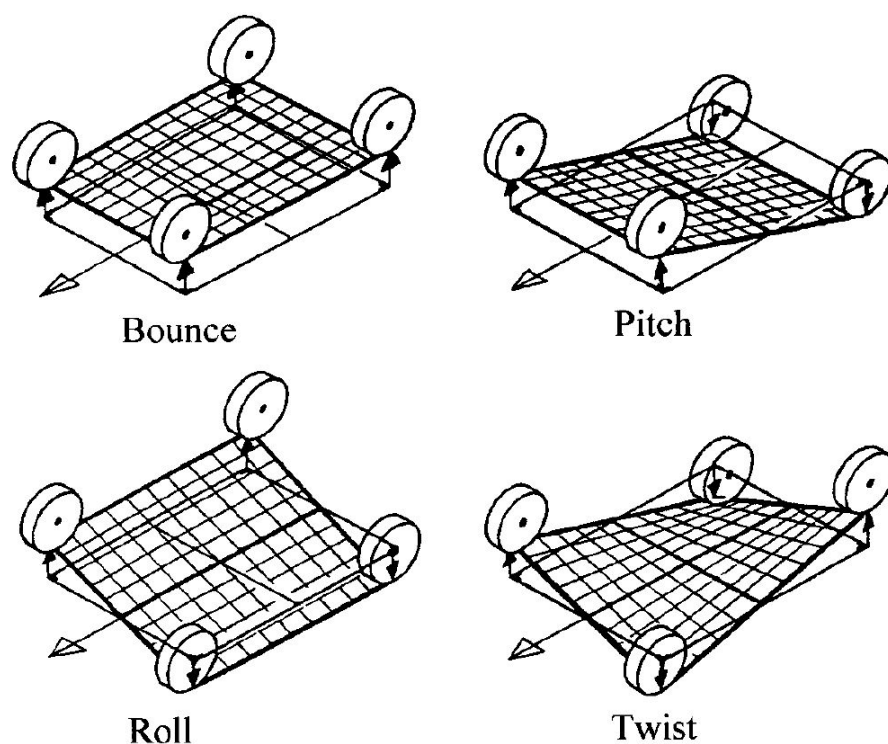


Figure D.1: Suspension modes: bounce (heave), pitch, roll and twist (warp) [37]

Bibliography

- [1] T. Sande. *Control of semi-active suspension and steer-by-wire for comfort and handling*. TU Eindhoven, Eindhoven University of Technology, 2015.
- [2] Vehicle dynamics lecture. Lecture Notes, Lotus Engineering, 2009.
- [3] S. Savaresi, C. Poussot-Vassal, C. Spelta, O. Sename, and L. Dugard. *Semi-active suspension control design for vehicles*. Elsevier, 2010.
- [4] International Organization for Standardization. *Road vehicles – Vehicle dynamics and road-holding ability, ISO 8855:2011*. The Organization, 2011.
- [5] M. Anderson. Vehicle Dynamics at Lotus. Lotus Engineering.
- [6] International Organization for Standardization. *Mechanical vibration and shock-Evaluation of human exposure to whole-body vibration-Part 1: General requirements, ISO 2631-1*. The Organization, 1997.
- [7] British Standards Institution. *British standard guide to measurement and evaluation of human exposure to whole body mechanical vibration and repeated shock, BS 6841*. BSI, 1987.
- [8] G. Hohl. Ride comfort of off-road vehicles. Technical report, DTIC Document, 1984.
- [9] F. Pradko and R. Lee. Vibration comfort criteria. sae technical paper 660139. *Society of Automotive Engineers, Warrendale*, 1966.
- [10] D. Hrovat. Survey of advanced suspension developments and related optimal control applications. *Automatica*, 33(10):1781–1817, 1997.
- [11] D. Hrovat. Optimal active suspension structures for quarter-car vehicle models. *Automatica*, 26(5):845–860, 1990.
- [12] D. Chen and D. Crolla. Subjective and objective measures of vehicle handling: drivers & experiments. *Vehicle System Dynamics*, 29(S1):576–597, 1998.
- [13] W. Manning and D. Crolla. A review of yaw rate and sideslip controllers for passenger vehicles. *Transactions of the Institute of Measurement and Control*, 29(2):117–135, 2007.
- [14] C. Bobier. *A Phase Portrait Approach to Vehicle Stabilization and Envelope Control*. PhD thesis, Stanford University, 2012.
- [15] S. Horiuchi, N. Yuhara, and H. Takeda. Identification of driver vehicle multiloop properties for handling quality evaluation. *VEHICLE SYSTEM DYNAMICS*, 18:285–297, 1989.

- [16] I. Badiru. Customer focus in eps steering feel development. *SAE International Journal of Passenger Cars-Mechanical Systems*, 7(2014-01-0148):1009–1015, 2014.
- [17] E. Ono, S. Hosoe, H. Tuan, et al. Bifurcation in vehicle dynamics and robust front wheel steering control. *Control Systems Technology, IEEE Transactions on*, 6(3):412–420, 1998.
- [18] R. Hoffman, J. Stein, L. Louca, and K. Huh. Using the milliken moment method and dynamic simulation to evaluate vehicle stability and controllability. In *ASME 2004 International Mechanical Engineering Congress and Exposition*, pages 173–180. American Society of Mechanical Engineers, 2004.
- [19] W. Milliken and D. Milliken. *Race car vehicle dynamics*, volume 400. Society of Automotive Engineers Warrendale, 1995.
- [20] D. Williams and W. Haddad. Nonlinear control of roll moment distribution to influence vehicle yaw characteristics. *Control Systems Technology, IEEE Transactions on*, 3(1):110–116, 1995.
- [21] F. Rossa, G. Mastinu, and C. Piccardi. Bifurcation analysis of an automobile model negotiating a curve. *Vehicle System Dynamics*, 50(10):1539–1562, 2012.
- [22] G. Koch, O. Fritsch, and B. Lohmann. Potential of low bandwidth active suspension control with continuously variable damper. *Control Engineering Practice*, 18(11):1251–1262, 2010.
- [23] J. Wang, D. Wilson, W. Xu, D. Crolla, et al. Active suspension control to improve vehicle ride and steady-state handling. In *Decision and Control, 2005 and 2005 European Control Conference. CDC-ECC'05. 44th IEEE Conference on*, pages 1982–1987. IEEE, 2005.
- [24] S. Ikenaga, F. Lewis, J. Campos, and L. Davis. Active suspension control of ground vehicle based on a full-vehicle model. In *American Control Conference, 2000. Proceedings of the 2000*, volume 6, pages 4019–4024. IEEE, 2000.
- [25] H. Chen and C. Scherer. An lmi based model predictive control scheme with guaranteed \mathcal{H}_∞ performance and its application to active suspension. In *American Control Conference, 2004. Proceedings of the 2004*, volume 2, pages 1487–1492. IEEE, 2004.
- [26] M. Yamashita, K. Fujimori, K. Hayakawa, and H. Kimura. Application of \mathcal{H}_∞ control to active suspension systems. *Automatica*, 30(11):1717–1729, 1994.
- [27] M. Bodie and A. Hac. Closed loop yaw control of vehicles using magneto-rheological dampers. Technical report, SAE Technical Paper, 2000.
- [28] D. Williams and W. Haddad. Nonlinear control of roll moment distribution to influence vehicle yaw characteristics. *Control Systems Technology, IEEE Transactions on*, 3(1):110–116, 1995.
- [29] Ferrari Side Slip Control 2 (SSC2). http://auto.ferrari.com/en_US/news-events/news/ferrari-488-gtb-extreme-power-extreme-driving-thrills/, 2015. [Online; accessed 19-June-2015].

- [30] Mercedes-Benz Active Body Control ABC. <http://techcenter.mercedes-benz.com/en/abc/detail.html>, 2013. [Online; accessed 19-June-2015].
- [31] Mercedes-Benz Active Body Control - fully active suspension technology. <https://www.youtube.com/watch?v=Df2mM5jP1W0>, 2012. [Online; accessed 19-June-2015].
- [32] A. Verkerk. Development and validation of ride & handling models for a bmw 318i (e46). Master's thesis, Eindhoven University of Technology, the Netherlands, 2014.
- [33] H. Pacejka. *Tire and vehicle dynamics*. Elsevier, 2005.
- [34] I. Besselink. Vehicle Dynamics 4L150. Lecture Notes, TU/e.
- [35] Jürgen Ackermann and Tilman Bünte. Actuator rate limits in robust car steering control. In *Decision and Control, 1997., Proceedings of the 36th IEEE Conference on*, volume 5, pages 4726–4731. IEEE, 1997.
- [36] H. Smakman. *Functional integration of slip control with active suspension for improved lateral vehicle dynamics*. TU Delft, Delft University of Technology, 2000.
- [37] E. Zapletal. Balanced suspension. Technical report, SAE Technical Paper, 2000.
- [38] D. Bastow, G. Howard, and J. Whitehead. *Car suspension and handling*. SAE international Warrendale, 2004.
- [39] I. Besselink. Advanced Vehicle Dynamics 4J570. Lecture Notes, TU/e.
- [40] A. Verkerk. Development and validation of ride & handling models for a bmw 318i (e46).
- [41] P. Els, N. Theron, P. Uys, and M. Thoreson. The ride comfort vs. handling compromise for off-road vehicles. *Journal of Terramechanics*, 44(4):303–317, 2007.
- [42] P. Holdmann and M. Holle. Possibilities to improve the ride and handling performance of delivery trucks by modern mechatronic systems. *JSAE review*, 20(4):505–510, 1999.
- [43] S. Choi, H. Lee, and E. Chang. Field test results of a semi-active er suspension system associated with skyhook controller. *Mechatronics*, 11(3):345–353, 2001.
- [44] K. Hong, D. Jeon, W. Yoo, H. Sunwoo, S. Shin, C. Kim, and B. Park. A new model and an optimal pole-placement control of the macpherson suspension system. Technical report, SAE Technical Paper, 1999.
- [45] J. Lin and C. Huang. Nonlinear backstepping active suspension design applied to a half-car model. *Vehicle system dynamics*, 42(6):373–393, 2004.
- [46] R. Tchamna, E. Youn, and I. Youn. Combined control effects of brake and active suspension control on the global safety of a full-car nonlinear model. *Vehicle System Dynamics*, 52(sup1):69–91, 2014.
- [47] D. Liaw, H. Chiang, and T. Lee. Elucidating vehicle lateral dynamics using a bifurcation analysis. *Intelligent Transportation Systems, IEEE Transactions on*, 8(2):195–207, 2007.

- [48] H. Peng, R. Strathearn, et al. A novel active suspension design technique-simulation and experimental results. In *American Control Conference, 1997. Proceedings of the 1997*, volume 1, pages 709–713. IEEE, 1997.
- [49] M. Lakehal-Ayat, S. Diop, and E. Fenaux. An improved active suspension yaw rate control. In *American Control Conference, 2002. Proceedings of the 2002*, volume 2, pages 863–868. IEEE, 2002.
- [50] V. Nguyen. *Vehicle handling, stability, and bifurcation analysis for nonlinear vehicle models*. PhD thesis, 2005.
- [51] M. Smith and F. Wang. Controller parameterization for disturbance response decoupling: application to vehicle active suspension control. *Control Systems Technology, IEEE Transactions on*, 10(3):393–407, 2002.

Vita

Shilp Dixit was born in Rajasthan, India in 1989. He successfully completed his B.E in Information Technology from University of Mumbai, India in 2010. Subsequently he worked at Deloitte Consulting LLC. as a Business Analyst from 2010 to 2012. He then moved to the Engineering Research Center in Tata Motors where he worked on semi-active suspension controller.

In September 2013, Shilp began his MSc. in Automotive Technology at Eindhoven University of Technology under the supervision of Prof. H. Nijmeijer. He undertook his graduate internship at DAF Trucks and is currently pursuing his graduation thesis at the Automotive Engineering Sciences Lab at the department of Mechanical Engineering of Eindhoven University of Technology. This thesis is a compilation of the work done during the graduation thesis.